4-1990

Photochemistry of Nitrous Acid and Nitrite Ion

Christopher L. Exstrom '90
Illinois Wesleyan University

PHOTOCHEMISTRY OF NITROUS ACID AND NITRITE ION

by

Christopher L. Exstrom

Submitted in partial fulfillment of the requirements

for Research Honors

Department of Chemistry

ILLINOIS WESLEYAN UNIVERSITY

April, 1990

TABLE OF CONTENTS

section or subsection	page
TABLE OF FIGURES	ii
INDEX OF TABLES	v
ABSTRACT	vi
INTRODUCTION	1
Thermal Decomposition of HONO	1
The Photochemical Reaction of HONO	4
The Photochemical Reaction of Nitrite	6
OH Reaction With Scavenger Compounds	9
Hydrogen Peroxide as a Source of OH	14
Nitrosation of Phenol	15
EXPERIMENTAL	17
Commercially Available Chemicals	17
Apparatus and Instrumentation	17
Thermal Reactions	18
Photolysis of HONO and NO_2^-	19
Photolysis of Hydrogen Peroxide and Benzene	21
UV/vis Spectra of Reactants, Products, and Related Compounds	21
RESULTS	25
UV/vis Spectra of Reactants, Products, and Related Compounds	25
HONO Thermolysis Results	38
Results of HONO Photolysis in Absence of Scavenger	42
Results of HONO Photolysis in Presence of Benzene	46
Nitrite Photolysis in Presence of Benzene	47
HONO Photolysis in Presence of Toluene	53
Nitrite Photolysis in Presence of Toluene	53
HONO Photolysis in Presence of Benzoic Acid	56
HONO Photolysis in Presence of Terephthalic Acid	56
Thermal Reaction of HONO with m-Cresol and Mixed Cresols	59
Photolysis of H_2O_2 in Presence of Benzene	59
DISCUSSION	63
Other Suggestions For Further Work	73
REFERENCES	75

TABLE OF FIGURES

Figure	Title	Page
1*	0.0151 M HONO Before Photolysis	26
2*	0.05097 M $NaNO_2$	27
3*	4.26×10^{-3} M Benzene	28
4*	6.087×10^{-4} M Phenol	29
5*	2.5×10^{-5} M p-Nitrosophenol (at acidic pH)	30
6a*	1.04×10^{-3} M m-Cresol	31
6b*	8.1×10^{-4} M Toluene	31
7a*	1.74×10^{-3} M o-Cresol	32
7b*	1.06×10^{-3} M p-Cresol	32
8a*	9.59×10^{-4} M Benzoic Acid	33
8b*	9.41×10^{-5} M Salicylic Acid	33
9a*	9.35×10^{-5} M p-Hydroxybenzoic Acid	34
9b*	9.35×10^{-5} M m-Hydroxybenzoic Acid	34
10*	Saturated Terephthalic Acid (approx. 1×10^{-4} M)	35
11a*	9.90×10^{-4} M Catechol	36
11b*	1.05×10^{-3} M Resorcinol	36
12*	1.02×10^{-3} M Hydroquinone	37
13	[HONO] vs. Time for Thermolysis of 0.0566 M HONO	40
14	[HONO] vs. Time for Thermolysis of 0.0197 M HONO	40
15	[HONO] vs. Time for Thermolysis of 0.0101 M HONO	41
16	[HONO] vs. Time for Photolysis of 0.0145 M HONO in Absence of Scavenger	44
17	[HONO] vs. Time for Photolysis of 0.0494 M HONO in Absence of Scavenger	44

* indicates UV/vis absorption spectrum

TABLE OF FIGURES (cont'd)

Figure	Title	Page
18	[HONO] vs. Time for Photolysis of 0.0200 M HONO in Absence of Scavenger	45
19*	0.0148 M HONO and 4.62×10^{-4} M Benzene After 155 Minutes Photolysis	48
20	[HONO] vs. Time for Photolysis of 0.0103 M HONO in Presence of Benzene	49
21	[PNP] vs. Time for Photolysis of 0.0103 M HONO in Presence of Benzene	49
22	[HONO] vs. Time for Photolysis of 0.00998 M HONO in Presence of Benzene	50
23	[PNP] vs. Time for Photolysis of 0.00998 M HONO in Presence of Benzene	50
24	[HONO] vs. Time for Photolysis of 0.0148 M HONO in Presence of Benzene	51
25	[PNP] vs. Time for Photolysis of 0.0148 M HONO in Presence of Benzene	51
26*	0.02354 M NO_2^- and 0.04575 M Benzene Before Photolysis	52
27*	0.02354 M NO_2^- and 0.04575 M Benzene After 32 min., 20 s Photolysis	52
28*	0.0101 M HONO and 1.55×10^{-3} M Toluene Before Photolysis	54
29*	0.0101 M HONO and 1.55×10^{-3} M Toluene After 100 Minutes Photolysis	54
30*	0.0255 M NO_2^- and 2.6×10^{-3} M Toluene Before Photolysis	55
31*	0.0255 M NO_2^- and 2.6×10^{-3} M Toluene After 110 Minutes Photolysis	55
32*	0.0101 M HONO and 1.9×10^{-3} M Benzoic Acid After 30 Minutes Photolysis	57

* indicates UV/vis absorption spectrum

TABLE OF FIGURES (cont'd)

Figure	Title	Page
33*	0.0101 M HONO and 1.9×10^{-3} M Benzoic Acid Before Photolysis	57
34*	0.0151 M HONO and Saturated Terephthalic Acid Before Photolysis	58
35*	0.0151 M HONO and Saturated Terephthalic Acid After 8 Hours Photolysis	58
36*	0.0101 M HONO, 4.24×10^{-5} M p-Cresol, 4.16×10^{-5} M m-Cresol, 3.48×10^{-5} M o-Cresol After 235 Minutes Thermolysis (1 °C)	60
37*	0.0101 M HONO and 6.24×10^{-5} M m-Cresol After 220 Minutes Thermolysis (1 °C)	60
38*	9 M H_2O_2 and 0.07 M Benzene Before Photolysis	61
39*	9 M H_2O_2 and 0.07 M Benzene (pH = 3.0) After 10 Minutes Photolysis	61
40*	9 M H_2O_2 and 0.07 M Benzene (pH = 0.1) After 10 Minutes Photolysis	62
41*	9 M H_2O_2 and 0.07 M Benzene (pH = 8.9) After 10 Minutes Photolysis	62

* indicates UV/vis absorption spectrum

INDEX OF TABLES

Table	Title	Page
1	Reactant Amounts Used in Thermolyses	18
2	Reactant Amounts Used in HONO Photolyses	20
3	Reactant Amounts Used in Nitrite Photolyses	21
4	Molar Absorptivities of Reactants, Products, and Related Compounds	25
5	HONO Concentrations in Thermolysis of 0.0566 M HONO	38
6	HONO Concentrations in Thermolysis of 0.0197 M HONO	38
7	HONO Concentrations in Thermolysis of 0.0101 M HONO	39
8	HONO Thermolysis Kinetic Orders (Fractional-Life Method)	39
9	HONO Concentrations During Photolysis of 0.0145 M HONO in Absence of Scavenger	42
10	HONO Concentrations During Photolysis of 0.0494 M HONO in Absence of Scavenger	42
11	HONO Concentrations During Photolysis of 0.0200 M HONO in Absence of Scavenger	43
12	HONO and PNP Concentration Changes During 0.0103 M HONO Photolysis	46
13	HONO and PNP concentration Changes During 0.00998 M HONO Photolysis	46
14	HONO and PNP Concentration Changes During 0.0148 M HONO Photolysis	47
15	UV Spectra of HONO/Toluene Photolysis Mixture	53
16	UV Spectra of NO_2^-/Toluene Photolysis Mixture	53
17	UV Spectra of HONO/Benzoic Acid Photolysis Mixture	56
18	UV Spectra of HONO/Terephthalic Acid Photolysis Mixture .	56
19	UV Spectra of HONO/Cresols and HONO/Phenol Mixtures	59

ABSTRACT

Aqueous solutions of HONO (ranging from 0.010 M to 0.057 M) and NO_2^- (ranging from 0.025 M to 0.035 M) were each photolyzed with 365 nm ultraviolet (UV) light. In the presence of benzene scavenger, OH radical intermediate was indicated by formation of p-nitrosophenol (PNP). Ultraviolet/visible (UV/vis) absorption spectra of photolyzed aqueous HONO/benzene solutions showed the presence of PNP by its characteristic absorption at 298 nm. UV/vis absorption spectra of photolyzed aqueous NO_2^-/benzene solutions showed no evidence of PNP formation.

Other compounds used as scavengers were toluene, benzoic acid, and terephthalic acid. UV/vis spectra of photolyzed aqueous HONO/scavenger solutions showed an intense broad peak in the 295-310 nm range, indicating that the scavenger was hydroxylated by OH, formed from HONO photolytic dissociation, and subsequently nitrosated by reaction with excess HONO.

Hydrogen peroxide, a known OH producer, was photolyzed in the presence of benzene to verify the proposed OH-scavenging sequence under varying pH conditions. UV/vis spectra showed evidence of hydroxybenzene formation upon photolysis.

The thermal decomposition of HONO was studied and a kinetic order (with respect to HONO) of 0.5 $\pm$ 0.5 was determined. Quantitative data concerning the photochemical decomposition of HONO was too inconsistent to make reasonable comparisons to thermal decomposition data.

INTRODUCTION

The chemistry of nitrous acid (HONO) has been of interest in recent years because it is a potentially important source of atmospheric hydroxyl radical (OH) [1,2]. Influencing the pathway of oxidation of atomspheric species such as SO_2 and hydrocarbons, OH formation in the atmosphere is known to contribute to photochemical smog formation and ozone depletion [2,3]. While the gas phase reactions and kinetics of HONO and OH have been studied extensively, very little concerning decomposition of aqueous HONO, e.g. HONO in aerosols or oceans, has been reported. This work considers both the quantitative and qualitative aspects of thermal and photochemical decomposition of HONO, including the use of scavengers to trap OH and the validity of the proposed OH-scavenging mechanism.

Thermal Decomposition of HONO

In aqueous solution, HONO is known to undergo two well understood equilibria, acid dissociation (eq. 1) and dehydration (eq. 2):

$$HONO(aq) + H_2O = H_3O^+(aq) + NO_2^-(aq) \quad (1)$$

$$2\ HONO(aq) = N_2O_3(aq) + H_2O \quad (2)$$

While these two equilibria are quickly established in aqueous solution, a third equilibrium (eq. 3) has a half-life of about 14 hours at 0 °C [4]:

$$3\ HONO(aq) = 2\ NO(aq) + H_3O^+(aq) + NO_3^-(aq) \quad (3)$$

Montemartini was the first to establish the stoichiometry and the kinetic order of HONO thermal decomposition (with respect to HONO) [5]. At low concentrations, first order kinetics were observed, while 2.5-order kinetics were found at higher HONO concentrations.

Later reports of low HONO concentration kinetic order agreed with those of Montemartini [4,6]: Reported orders at higher HONO concentrations ranged from 2.5 to 3.5 [7] and 4 [8]. Studies of HONO thermal decomposition by Rettich [9] showed first order kinetics at HONO concentrations less than 0.10 M and 2.5 order at higher concentrations. In the most recent study of HONO thermal decomposition by Park and Lee [10], the reaction shown in eq.(2) was investigated, and a kinetic order of 2, with respect to HONO, was assumed.

Abel and coworkers were the first to propose two separate mechanisms for the higher order thermal decomposition, as shown in eqs.(4-5) and (6-9), respectively [8]:

$$4\ HONO(aq) = 2\ NO(aq) + 2\ H_2O + N_2O_4(aq) \quad (4)$$

$$N_2O_4(aq) + H_2O = HONO(aq) + H_3O^+(aq) + NO_3^-(aq) \quad (5)$$

and

$$2\ HONO(aq) = N_2O_3(aq) + H_2O \quad (6)$$

$$N_2O_3(aq) = NO(aq) + NO_2(aq) \quad (7)$$

$$2\ NO_2(aq) = N_2O_4(aq) \quad (8)$$

$$N_2O_4(aq) + H_2O = HONO(aq) + H_3O^+(aq) + NO_3^-(aq) \quad (9)$$

Twenty years later, Thie proposed another mechanism, which is given in eqs.(10-12) [11]:

$$2\ HONO(aq) = NO(aq) + NO_2(aq) + H_2O \quad (10)$$

$$2\ NO_2(aq) = N_2O_4(aq) \quad (11)$$

$$N_2O_4(aq) + H_2O = HONO(aq) + H_3O^+(aq) + NO_3^-(aq) \quad (12)$$

Studies by Usubillaga [7], Rettich [9], and Park and Lee [10] do not differentiate among the three mechanisms given in equations (4-5), (6-9), and (10-12), respectively.

The study of the thermal decomposition of HONO is important because the photochemical destruction of HONO is accompanied by a thermolysis, which must be accounted for in photochemical kinetic calculations. Because HONO efficiently absorbs ultraviolet (UV) radiation with characteristic absorptions between 300-400 nm [12], ultraviolet/visible (UV/vis) spectroscopy may be used to monitor HONO concentration levels during a photochemical or thermal reaction. Although the only other species in equations (4-12) that can be detected by UV/vis spectroscopy is NO_3^-, it should be feasible to determine the rate of decrease of HONO concentration during a thermal reaction and calculate the kinetic order with respect to HONO.

The Photochemical Reaction of HONO

While the first studies of HONO thermal decomposition began over 100 years ago, the first report of gaseous HONO photolysis was made by Cox and Atkins in 1973 [13]. In the gas phase, HONO rapidly establishes an equilibrium with nitric oxide and nitrogen dioxide, as illustrated in equation (13):

$$NO(g) + NO_2(g) + H_2O = 2\ HONO(g) \quad (13)$$

The following mechanism, equations (14-17), was proposed for photochemical decomposition of HONO irradiated with light at 330-380 nm [14]:

$$HONO(g) + h\nu = NO(g) + OH(g) \quad (14)$$

$$OH(g) + NO(g) + M = HONO(g) + M \quad (15)$$

$$OH(g) + NO_2(g) + M = HNO_3(g) + M \quad (16)$$

$$OH(g) + HONO(g) = H_2O + NO_2(g) \quad (17)$$

An alternative primary process (analogous to eq. 14) was also proposed:

$$HONO(g) + h\nu = H(g) + NO_2(g) \quad (18)$$

It was discovered that the primary quantum yield for eq.(14) was nearly twice that for eq.(18). Also, formation of NO and OH are favored on the basis of bond dissociation energies [15]. Nash considered only eq.(14) as the primary process and reported that HONO

decomposes photochemically in the following manner [16]:

$$HONO(g) + h\nu = OH(g) + NO(g) \quad (19)$$

$$OH(g) + HONO(g) = H_2O + NO_2(g) \quad (20)$$

Cox has reported that eq.(18) contributes no more than 10% of the total HONO photolysis, and he reported a primary quantum yield, with respect to HONO, for eq.(19) of 0.92 $\pm$ 0.16 [1]. Current photolysis studies of gaseous HONO photochemical decomposition have been concerned with reactions in the presence of atmospheric constituents, such as ozone and Ar [2], and excitation energies of the OH fragment [17,18]. No additional mechanisms have been proposed for HONO photochemical decomposition.

Murty and Dhar reported the first study of aqueous HONO photochemistry [19]. Quantum yields up to 15 were reported for wavelengths above 445 nm, a region in which HONO does not significantly absorb light. Rettich suggested that the observed disappearance of HONO was due to thermal decomposition, which was accelerated because of heating of the reaction solution by the light source [9].

Rettich extensively studied the photochemistry of aqueous HONO, and determined quantum yields of HONO disappearance as functions of the following parameters: ionic strength, pH, nitrite concentration, water source, light source, reaction vessel geometry, and HONO concentration [9]. The limiting quantum yield, which was reported to be 0.095, was suggested to correspond to the probability of escape from the solvent cage in the primary dissociation shown in equation

(21) [9]:

$$HONO(aq) + h\nu \longrightarrow \{HONO^*\} \longrightarrow \{OH + NO\} \longrightarrow OH(aq) + NO(aq) \quad (21)$$

where { } = solvent cage

* = indicates excited state

The overall quantum yield of HONO disappearance increased linearly from 0 to 0.14 as HONO concentration increased from 0 to 0.14 M. At HONO concentrations higher than 0.14 M, the quantum yield remained constant at 0.14. There have been no reports of aqueous photochemistry since the studies by Rettich.

The Photochemical Reaction of Nitrite

The photochemistry of nitrite (NO_2^-) is a topic of much confusion and debate. An early finding by Holmes [20] was that NO_2^- underwent no net photochemical reaction. In a study of the inorganic nitrogen cycle of the sea by Hamilton, NO_2^- was found to be unreactive to UV radiation in both seawater and distilled water [21].

Treinin and Hayon irradiated a sample of 0.27 mM NO_2^- with 228.8 nm light, using a Cd source, for 100 minutes, and reported a quantum yield of NO_2^- depletion of less than 0.001 [22], yet they reported that NO_2^- did undergo photolytic dissociation. The mechanism of this dissociation is given in eqs.(22-23) [22,23]:

$$NO_2^- + h\nu \longrightarrow NO + O^- \quad (22)$$

$$O^- + H_2O = OH + OH^- \quad (23)$$

Bromide (Br^-) and carbonate (CO_3^{2-}) react with OH to form transient radical anions of Br_2^- and CO_3^-, respectively, which can be detected by their transient absorption spectra [22]:

$$Br^- + OH \longrightarrow Br + OH^- \quad (24)$$

$$Br + Br^- = Br_2^- \quad (25)$$

$$CO_3^{2-} + OH \longrightarrow CO_3^- + OH^- \quad (26)$$

OH was also found to react with nitrite itself, yielding O_3^-, which was detected by its transient absorption spectrum [22]:

$$OH + NO_2^- \longrightarrow NO_2 + OH^- \quad (27)$$

$$O^- + NO_2^- + H_2O \longrightarrow NO_2 + 2\ OH^- \quad (28)$$

$$O^- + O_2 = O_3^- \quad (29)$$

The nitrogen oxides produced (see eqs. 22-29) undergo hydrolysis in aqueous solution to completely regenerate nitrite. The overall hydrolysis stoichiometry proposed by Treinin and Hayon [22] is given in equation (30), and the hydrolysis of NO at high concentrations proposed by Zafiriou [24] is given in equation (31):

$$NO_2 + NO + H_2O = 2\ NO_2^- + 2\ H^+ \quad (30)$$

$$4\ NO + O_2 + 2\ H_2O = 2\ H^+ + 4\ NO_2^- \quad (31)$$

Despite previous reports of the unreactivity of nitrite in seawater, Zafiriou and True reported net disappearance of nitrite in seawater upon photolysis. They reported that the primary

dissociation step occurred according to equation (32) [25]:

$$NO_2^- + H_2O + h\nu = NO + OH + OH^- \quad (32)$$

Nitrite losses were reported to range from 2 to 27 percent per day. Zafiriou proposed that these nitrite losses might be due to: 1) sensitized photolysis, with varying types and amounts of sensitizers; 2) direct photolysis with a quantum yield sensitive to pH, O_2 concentration, salinity, temperature, and wavelength; and 3) a variable extent of regeneration of nitrite by secondary reactions of NO (see eq. 31) [26].

In a recent flash-photolysis study of aqueous nitrite [26], Zafiriou reported quantum yields of OH-production ranging from 0.013 (pH=7.9, 371.1 nm, 49 °C) to 0.085 (pH=7.9, 298.5 nm, 23 °C). His proposed nitrite decomposition mechanism is given in equations (33-40) [26]:

$$NO_2^- + h\nu \rightarrow NO_2^{-*} \quad (33)$$

$$NO_2^{-*} \rightarrow NO_2^- + \text{heat} \quad (34)$$

$$NO_2^{-*} \rightarrow \{NO, O^-, n\ H_2O\} \quad (35)$$

$$\{NO, O^-, n\ H_2O\} \rightarrow NO + O^- + H_2O \quad (36)$$

$$\{NO, O^-, n\ H_2O\} \rightarrow NO_2^- \quad (37)$$

$$\{NO, O^-, H_2O\} \rightarrow \{NO, OH, OH^-, (n-1)\ H_2O\} \quad (38)$$

$$\{NO, OH, OH^-, (n-1)\ H_2O\} \rightarrow HONO + (n-1)H_2O + OH^- \quad (39)$$

$$\{NO, OH, OH^-, (n-1)\ H_2O\} \rightarrow NO + OH + OH^- + (n-1)H_2O \quad (40)$$

OH Reaction With Scavenger Compounds

While the presence and concentration of HONO in solution may be monitored by UV/vis spectroscopy, OH concentrations cannot because 1) OH is a transient species and not stable in aqueous solution, and 2) OH absorbs UV radiation only in the vacuum-UV region (below 200 nm). However, OH reacts with many aromatic and other unsaturated organic compounds, and these may be used to scavenge OH when it is formed upon HONO photolysis. In fact, OH has been considered the "vacuum cleaner" of the troposphere, as many organic pollutants scavenge OH and are subsequently removed from the troposphere [27].

As with HONO photochemistry, gas-phase OH chemistry has received much more attention than condensed-phase phenomena. Davis and coworkers first reported on the kinetics of the reaction between OH and benzene and toluene in the gas phase at 300 K [28]. While the disappearance of benzene or toluene was noted, no attempt at product separation and analysis were made.

A product study of the OH reaction with benzene, toluene, and 1,3,5-trimethylbenzene by Sloane [29] was conducted, and his summary of the scavenging reactions are shown in equations (41-44) [29]:

$$OH + C_6H_{6-n}(CH_3)_n \longrightarrow$$

$$C_6H_{6-n}(CH_3)_nOH \qquad n = 0,1,3 \qquad (41)$$

$$C_6H_{5-n}(CH_3)_nOH + H \qquad n = 0,1,3 \qquad (42)$$

$$C_6H_{5-n}(CH_3)_{n-1}OH + CH_3 \qquad n = 1,3 \qquad (43)$$

$$C_6H_{6-n}(CH_3)_{n-1}CH_2 + H_2O \qquad n = 1,3 \qquad (44)$$

Tully and coworkers studied the reactions between OH and benzene

and toluene [30]. Pseudo-first order decays of OH were observed in the temperature ranges of 296-325 K and 380-425 K, while rapid decrease in reactivity and nonexponential OH decay were observed in the temperature range of 325-380 K. This led to the proposal of a reversible scavenging mechanism [30,31]:

$$OH + C_6H_6 \longrightarrow C_6H_5 + H_2O \quad (45)$$

$$C_6H_5 + H_2O \longrightarrow \{C_6H_6OH\}^* \quad (46)$$

$$\{C_6H_6OH\}^* \longrightarrow C_6H_6 + OH \quad (47)$$

$$C_6H_6 + OH + M \longrightarrow \{C_6H_6OH\} \quad (48)$$

$$\{C_6H_6OH\} \longrightarrow C_6H_6 + OH \quad (49)$$

Studies by Shepson and coworkers [32] of irradiation of toluene and o-xylene in a MeONO/NO/air system led to proposals of numerous OH-substitution and ring-fragmentation mechanisms. OH radicals were proposed to be generated by the photolytic cleavage of methyl nitrite (MeONO) [32]:

$$MeONO + h\nu \longrightarrow MeO + NO \quad (50)$$

$$MeO + O_2 \longrightarrow H_2CO + HO_2 \quad (51)$$

$$HO_2 + NO \longrightarrow OH + NO_2 \quad (52)$$

All mechanisms proposed for the reaction of toluene or xylene with OH begin with OH attack on the aromatic ring instead of attack at the methyl group(s). In each scheme, OH attack is followed by the addition of O_2, a step unlikely to occur in the condensed phase because of solvent cage effects on the starting aromatic compound and

the dissociated nitrite compound (see ref. 32).

A study by Atkinson and coworkers [33] of OH radical reactions with biphenyl and naphthalene demonstrated that O_2 oxidized the hydroxycyclohexadienyl radical to a simple hydroxysubstituted aromatic compound, while NO_2 caused nitration of the same radical:

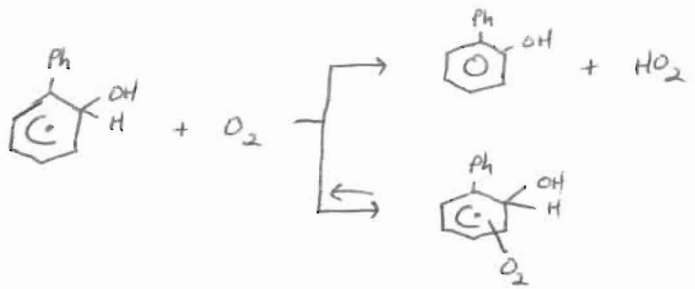

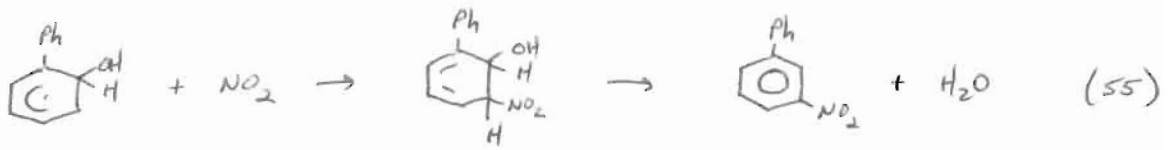

A number of unsaturated organic compounds have been known to scavenge OH in aqueous solution. Ethylene (C_2H_4) and benzene were used by Rettich [9] in his study of HONO photochemistry. Equations (56-60) show the sequence of reactions leading to the formation of glycolaldehyde ($HOCH_2CHO$) from scavenging of the OH radical by C_2H_4 [9,34-37]:

$$HONO(aq) + h\nu = OH(aq) + NO(aq) \quad (56)$$

$$OH(aq) + C_2H_4(aq) = HOCH_2CH_2(aq) \quad (57)$$

$$HOCH_2CH_2(aq) + NO(aq) = HOCH_2CH_2NO(aq) \quad (58)$$

$$HOCH_2CH_2NO(aq) = HOCH_2CHNOH(aq) \quad (59)$$

$$HOCH_2CHNOH(aq) + H_2O = HOCH_2CHO(aq) + NH_2OH(aq) \quad (60)$$

A mechanism for the reaction between OH and aqueous benzene was first proposed by Jacob and coworkers [35] (eqs. 61-64). Products formed in this reaction are phenol (eqs. 62-63), hydrogen peroxide (eq. 63), and alpha- and beta-hydroxymucondialdehyde (eq. 64) [9]:

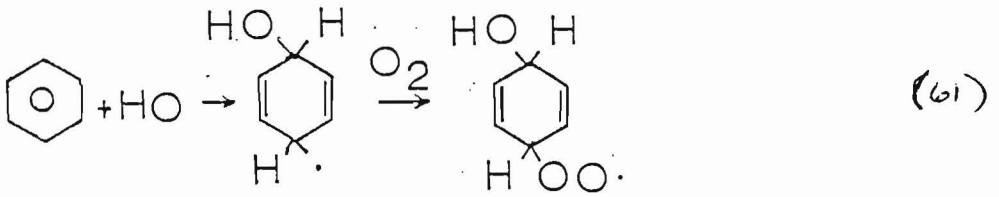

(61)

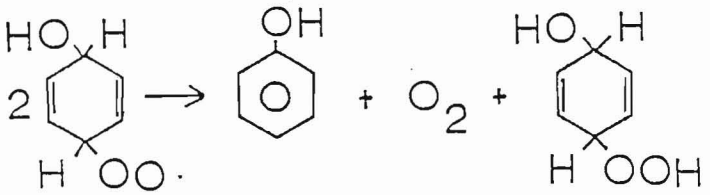

(62)

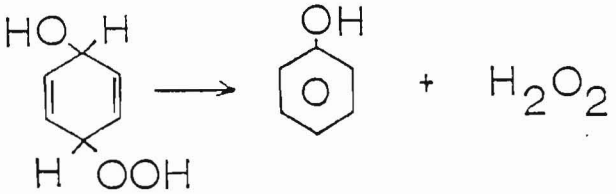

(63)

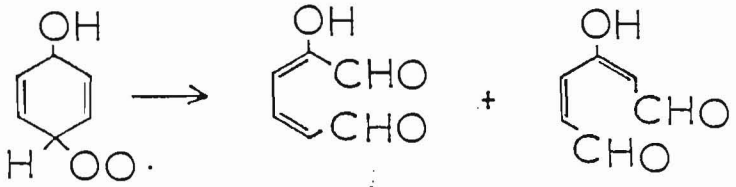

(64)

A similiar mechanism for aromatic hydroxylation was proposed by Eberhardt [38] (eqs. 65-68). Under acidic conditions, it was suggested that intermediate was a benzene radical cation:

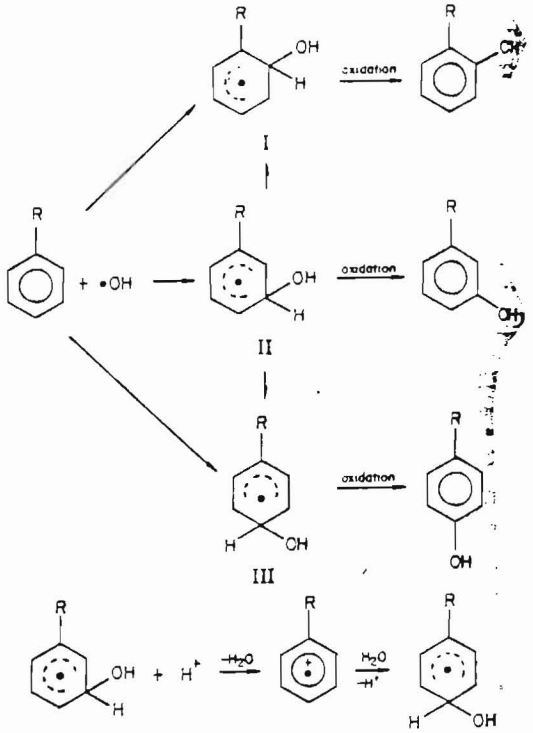

(65)

(66)

(67)

(68)

The only other aromatic hydrocarbon whose scavenging ability in aqueous solution has been studied is toluene [29]. When OH was generated by radiolysis (irradiation by gamma rays) of water, isomeric ratios of the ortho-, meta-, and para-cresol (cresol = hydroxytoluene) products were found to be 35.5%, 43%, and 21.5%, respectively. In toluene, there are 2 ortho- and 2 meta-sites, whereas there is only 1 para-site, thus it is statistically expected that the p-cresol yield would be noticeably lower than the o- and m-cresol yields. Aromatic ring substituents do not affect radical reactivity. Because the mechanism in equations (65-68) is a radical instead of an electrophilic substitution mechanism, electron withdrawing/releasing effects play a minor role in determining product isomeric ratios. In an electrophilic substitution mechanism,

one would expect the major product in equations (65-68) to be the para-cresol because hydrocarbon substituents slightly activate the ring and direct substitution toward the ortho- and para-sites. The reaction intermediate suggested was an aromatic ring radical because no phenylmethanol was reported to have formed.

Hydrogen Peroxide as a Source of OH

It is well known that hydrogen peroxide (H_2O_2) yields OH in both auto- and radiation-induced decomposition. Equation (69) shows the thermal decomposition reaction of H_2O_2 [40]:

$$2\ H_2O_2(aq) \quad = \quad 2\ H_2O \ + \ O_2(g) \qquad (69)$$

Equations (70-72) show a mechanism for equation (69) which was proposed by Abel [41]:

$$H_2O_2 \quad = \quad HO_2^- \ + \ H^+ \qquad (70)$$

$$HO_2^- \ + \ H_2O_2 \ \text{--->} \ HO_2 \ + \ OH^- \ + \ OH \qquad (71)$$

$$HO_2 \ + \ OH \ \text{--->} \ H_2O \ + \ O_2 \qquad (72)$$

In the photochemical dissociation of H_2O_2, two primary dissociation steps are hypothesized, and both include production of OH. These mechanisms for H_2O_2 decomposition were first proposed by Hunt and Taube [42]:

Scheme I

$$H_2O_2 + h\nu \longrightarrow 2\ OH \quad (73)$$

$$OH + H_2O_2 = HO_2 + H_2O \quad (74)$$

$$2\ HO_2 = H_2O_2 + O_2 \quad (75)$$

Scheme II

$$H_2O_2 + h\nu \longrightarrow H_2O + O \quad (76)$$

$$O + H_2O_2 = OH + HO_2 \quad (77)$$

$$OH + H_2O_2 = HO_2 + H_2O \quad (78)$$

$$2\ HO_2 = H_2O_2 + O_2 \quad (79)$$

While numerous studies of OH reaction with aromatic compounds in gaseous and aqueous solution have been conducted, there is only one report of H_2O_2 as the source of OH [43]. Ohta and Ohyama determined room temperature rate constants for reactions of aromatic hydrocarbons (in the gas phase) with OH (from photolysis of 90% H_2O_2). They reported that OH reacted with toluene four times faster than with benzene [43].

Nitrosation of Phenol

Challis and coworkers extensively studied the kinetics and mechanism of nitrosation of phenol and anisole by HONO [47,48]. In acidic solution HONO is in equilibrium with nitrosonium ion (NO^+), as illustrated in equation (80) [49]:

$$H^+ + HONO = H_2ONO^+ = NO^+ + H_2O \quad (80)$$

Either the nitrosonium ion or the hydrated nitrosonium ion (H_2ONO^+) may attack the activated aromatic ring, with electrophilic substitution occuring [48]. This proposed mechanism is shown in equation (81) [49]:

(81)

EXPERIMENTAL

Commercially Available Chemicals

Except where indicated, all chemicals were kept at room temperature and were used without further purification.

$NaNO_2$ (reagent grade), benzoic acid (reagent grade), salicylic acid (unknown) and benzene (spectral grade) were obtained from J.T. Baker. Hydrogen peroxide (30%) was obtained from Fisher Chemical Company and was stored at approximately 5 °C. Toluene (technical grade) was obtained from Fisher Chemical Company and was distilled prior to use. Hydroquinone (unknown grade) was obtained from Mallinckrodt Chemicals.

The following chemicals were obtained from Aldrich Chemical Company: p-nitrosophenol, phenol, terephthalic acid, o-cresol, m-cresol, p-cresol, m-hydroxybenzoic acid, p-hydroxybenzoic acid, catechol, and resorcinol. All of these chemicals were 98% reagent grade and were not further purified prior to use.

Apparatus and Instrumentation

Ultraviolet/visible absorbance spectra were measured on a Perkin-Elmer 559 UV-visible spectrophotometer with a slit width of 0.25 nm. Fisher 1.00 cm quartz cells were used for both reference and sample solutions. The sample chamber of the spectrophotometer was purged with dry nitrogen to prevent "fogging" of the quartz cells during measurements at 1 °C.

Reaction solutions were photolyzed with light from a G.W. Gates and Co. Hg arc broad spectrum lamp or a Blak-Ray B-100A low pressure

Hg lamp (Ultraviolet Products) with the Hg broad emission filtered at approximately 365 nm.

Thermal Reactions

General Reactions. In order to maintain reaction solutions at 1.0 ± 0.2 °C, the water bath was thermostated at 0.4 ± 0.1 °C and allowed to equilibrate for approximately 1 hour. A 100-mL pyrex beaker containing water or aqueous $NaNO_2$ was placed in the bath, and the temperature of the solution was measured periodically for several hours. This procedure was repeated during irradiation with the Blak-Ray lamp.

All reactant solutions, aqueous $NaNO_2$, HCl, and water, were initially at 1 °C. Amounts of each reactant used for each thermolysis are given in Table 1:

Table 1

Reactant Amounts Used in Thermolyses

$[NO_2^-]$, M	mL NO_2^- soln.	[HCl], M	mL HCl soln.	mL water
1.0143	3.000	0.1102	50.00	0.00
1.0143	1.000	0.1102	50.00	0.00
0.05097	10.00	0.1102	25.00	10.00

The nitrite solution was poured into the HCl and water solution. This solution was swirled and placed in the thermostated water bath. A 2-3 mL aliquot was removed periodically and its UV absorption spectrum between 200-440 nm was recorded.

Reaction of HONO and Phenol. Each reactant solution was cooled

to 1 °C before mixing. Into a 100 mL beaker were pipetted 10.00 mL of 0.05097 M $NaNO_2$, 25.00 mL of 0.1102 M HCl, 5.00 mL of 0.00673 M phenol, and 10.00 mL of water. The mixture was swirled briefly and placed in the thermostated water bath at 1 °C. A 2-3 mL aliquot was removed periodically, and its UV absorption spectrum between 200-440 nm was recorded.

Reaction of HONO and m-Cresol. Each reactant solution was cooled to 1 °C before mixing. Into a 100-mL beaker were pipetted 10.00 mL of 0.05097 M $NaNO_2$, 25.00 mL of 0.1102 M HCl, 5.00 mL of 0.0104 M m-cresol, and 10.00 mL water. The mixture was swirled briefly and placed in the thermostated water bath at 1 °C. A 2-3 mL aliquot was removed periodically, and its UV absorption spectrum between 200-440 nm was recorded.

Reaction of HONO and Mixed Cresols. Each reactant solution was cooled to 1 °C before mixing. Into a 100-mL beaker were pipetted 10.00 mL of 0.05097 M $NaNO_2$, 25.00 mL of 0.1102 M HCl, 2.000 mL of 0.0104 M m-cresol, 2.000 mL of 0.0174 M o-cresol, 1.000 mL of 0.0106 M p-cresol, and 10.00 mL of water. The mixture was swirled briefly and placed in the thermostated water bath at 1 °C. A 2-3 mL aliquot was removed periodically, and its UV absorption spectrum between 200-440 nm was recorded.

Photolysis of HONO and NO_2^-

Photolysis of HONO in Presence of Scavenger. Each reactant solution was cooled to 1 °C before mixing. Into a 100-mL beaker were pipetted specified volumes of 0.05097 M $NaNO_2$, 0.1102 M HCl, aqueous scavenger (benzene, toluene, benzoic acid, or terephthalic acid), and

water (used to bring the total reaction solution volume to 50.00 mL if necessary). This solution was swirled briefly and placed in the thermostated water bath at 1 °C. Amounts of reactants used in each photolysis are presented in Table 2:

Table 2

Reactant Amounts In HONO Photolyses

mL NO_2^- soln.	mL HCl soln.	[scavenger], M	mL scavenger
10.00	25.00	0.09031 M benzene	2.000
15.00	35.00	0.0120 M benzene	2.000
10.00	25.00	0.00516 M toluene	15.00
10.00	25.00	0.009589 M b. acid	10.00
15.00	35.00	terephthalic acid (solid)	

The mixture was irradiated with light at 365 nm. A 2-3 mL aliquot was periodically removed and its UV absorption spectrum between 200-440 nm was recorded.

Photolysis of NO_2^- in Presence of Scavenger. Each reactant solution was cooled to 1 °C before mixing. Into a 100-mL beaker were pipetted specified volumes of 0.05097 M $NaNO_2$, aqueous scavenger (benzene or toluene), and water. The mixture was swirled briefly and placed in the thermostated water bath at 1 °C. Amounts of reactants used are given in Table 3:

Table 3

Reactant Amounts in Nitrite Photolyses

mL NO_2^- soln.	[scavenger], M	mL scavenger	mL water
10.00	0.09031 M benzene	5.00	35.00
10.00	0.00516 M toluene	15.00	0.00

The mixture was irradiated with light at 365 nm. A 2-3 mL aliquot was periodically removed and its UV absorption spectrum between 200-440 nm was recorded.

Photolysis of Hydrogen Peroxide and Benzene

Samples of benzene (0.110 g, 0.114 g, and 0.116 g, for solutions 1, 2, and 3, respectively) were weighed into 100-mL beakers and into each beaker, 20.00 mL of 30% H_2O_2 was pipetted. Solution 1 was acidified with aqueous HCl, and aqueous NaOH was added to solution 2 so that the pH values for solutions 1, 2, and 3 were 0.1, 8.9, and 3.0, respectively. Each solution was photolyzed at room temperature with radiation from a Hg arc broad spectrum lamp for approximately 10 minutes. Approximately 30 mL of concentrated HCl was added. After allowing the solutions to stand for an additional 48 hours, the UV spectrum of each was recorded at 200 to 300 nm.

UV/vis Spectra of Reactants, Products, and Related Compounds

HONO. Into a 100-mL beaker was pipetted 1.000 mL of 1.0143 M $NaNO_2$ and 50.00 mL of 0.1102 M HCl. This mixture was swirled briefly, and a 2-3 aliquot was immediately removed. The UV absorption spectrum of this aliquot was recorded between 260-440 nm.

NO_2^-. A 1.7584 g sample of $NaNO_2$ was dissolved in approximately 400 mL of water and diluted to 500.0 mL of solution in a volumetric flask. A 2-3 mL aliquot of this solution was removed, and its UV absorption spectrum was recorded between 250-500 nm.

Benzene. A 0.39 g sample of benzene was weighed into a 500.0 mL volumetric flask and diluted to volume with water. Approximately a week later, a 2-3 mL aliquot of this solution was removed and its UV absorption spectrum between was recorded between 220-300 nm.

Toluene. A 7.5 mg sample of toluene was transferred via syringe to a 10.00 mL volumetric flask. This sample was diluted to volume with water. A 2-3 mL aliquot was removed and its UV absorption spectrum was recorded between 220-300 nm.

p-Cresol. A 11.5 mg sample of p-cresol was transferred via syringe to a 10.00 mL volumetric flask. This sample was diluted to volume with water. A 2-3 mL aliquot was removed and its UV absorption spectrum was recorded between 220-340 nm.

m-Cresol. A 11.2 mg sample of m-cresol was transferred via syringe to a 10.00 mL volumetric flask. This sample was diluted to volume with water. A 2-3 mL aliquot was removed and its UV absorption spectrum was recorded between 220-340 nm.

o-Cresol. A 18.8 mg sample of o-cresol was transferred via syringe to a 10.00 mL volumetric flask. This sample was diluted to volume with water. A 2-3 mL aliquot was removed and its UV absorption spectrum was recorded between 220-340 nm.

Benzoic Acid. A 0.1171 g sample of benzoic acid was weighed out into a 150-mL beaker, dissolved in approximately 90 mL of water and diluted to 100.00 mL in a volumetric flask. A 1.000 mL aliquot was

pipetted into a 10.00 mL volumetric flask and diluted to volume with water. A 2-3 mL aliquot of this solution was removed and its UV absorption spectrum was recorded between 250-400 nm.

Salicylic Acid. A 0.1300 g sample of salicylic acid was weighed out into a 150-mL beaker, dissolved in approximately 90 mL of water and diluted to 100.00 mL in a volumetric flask. A 1.000 mL aliquot was pipetted into a 10.00 mL volumetric flask and diluted to volume with water. A 1.000 mL aliquot of this solution was pipetted into a 10.00 mL volumetric flask and diluted to volume with water. A 2-3 mL aliquot of this solution was removed, and its UV absorption spectrum between was recorded between 240-400 nm.

Phenol. A 0.5729 g sample of phenol was weighed out into a 150-mL beaker, dissolved in approximately 90 mL of water, and diluted to 100.00 mL in a volumetric flask. This solution was diluted by one-hundredth (by one-tenth twice successively), pipetting 1.000 mL aliquots and diluting to 10.00 mL using volumetric flasks. A 2-3 mL aliquot of the final dilution was removed, and its UV absorption spectrum was recorded between 200-300 nm.

p-Hydroxybenzoic Acid. A 0.1292 g sample of p-hydroxybenzoic acid was weighed out into a 150-mL beaker, dissolved in approximately 90 mL of water, and diluted to 100.00 mL in a volumetric flask. This solution was diluted by one-tenth twice successively, pipetting 1.000 mL aliquots and diluting to 10.00 mL using volumetric flasks. A 2-3 mL aliquot of the final dilution was removed, and its UV absorption spectrum was recorded between 240-360 nm.

m-Hydroxybenzoic Acid. The procedure for p-hyroxybenzoic acid was followed exactly, replacing 0.1292 g of p-hydroxybenzoic acid

with 0.1291 g m-hydroxybenzoic acid.

Catechol. A 0.0109 g sample of catechol was weighed out into a 150-mL beaker, dissolved in approximately 90 mL water, and diluted to 100.00 mL in a volumetric flask. A 2-3 mL aliquot of this solution was removed and its UV absorption spectrum was recorded between 240-360 nm.

Resorcinol. The procedure for catechol was followed exactly, replacing the catechol sample with 0.0116 g of resorcinol.

Hydroquinone. The procedure for catechol was followed exactly, replacing the catechol sample with 0.0112 g of hydroquinone.

RESULTS

UV/Vis Spectra of Reactants, Products, and Related Compounds

Ultraviolet/visible spectra of the following compounds in aqueous solution are shown in Figures (1-12), respectively: 0.0151 M HONO, 0.05097 M NO_2^-, 4.26 mM benzene, 0.6087 mM phenol, 0.025 mM PNP (at acidic pH), 8.1 mM toluene, 1.06 mM p-cresol, 1.04 mM m-cresol, 1.74 mM o-cresol, 0.9589 mM benzoic acid, 0.09412 mM salicylic acid, 0.09347 mM m-hydroxybenzoic acid, 0.09354 mM p-hydroxybenzoic acid, saturated terephthalic acid, 1.05 mM resorcinol, 0.990 mM catechol, and 1.02 mM hydroquinone. Molar absorptivities were determined for each of these compounds and are given in Table 4:

Table 4

Molar Absorptivities of Reactants, Products, and Related Compounds

Fig.	Compound	Conc.	λ (max)	Abs.	ϵ
1	HONO	0.0151 M	371	0.818	54.2
2	NO_2^-	0.05097 M	352	1.158	22.7
3	benzene	4.26	254	0.612	144
4	phenol	0.6087	269	0.848	1390
5	p-nitrosophenol	0.025	296-300	0.261	10400
6a	toluene	8.14	261	1.485	182
6b	o-cresol	1.74	270	2.53	1450
7a	p-cresol	1.06	277	1.63	1540
7b	m-cresol	1.04	271	1.36	1310
8a	benzoic acid	0.959	272	0.780	813
8b	salicylic acid	0.0941	296	0.322	3420
9a	p-hydroxybenzoic	0.0935	248	1.17	12500
9b	m-hydroxybenzoic	0.0935	288	0.203	2170
10	catechol	0.990	275	2.20	2220
11	resorcinol	1.05	273	1.92	1830
12	hydroquinone	1.02	289	2.62	2570

(NOTE: all wavelengths are in nm; all concentrations are in mM except where indicated; all molar absorptivities are in M^{-1} cm^{-1})

FIGURE 1

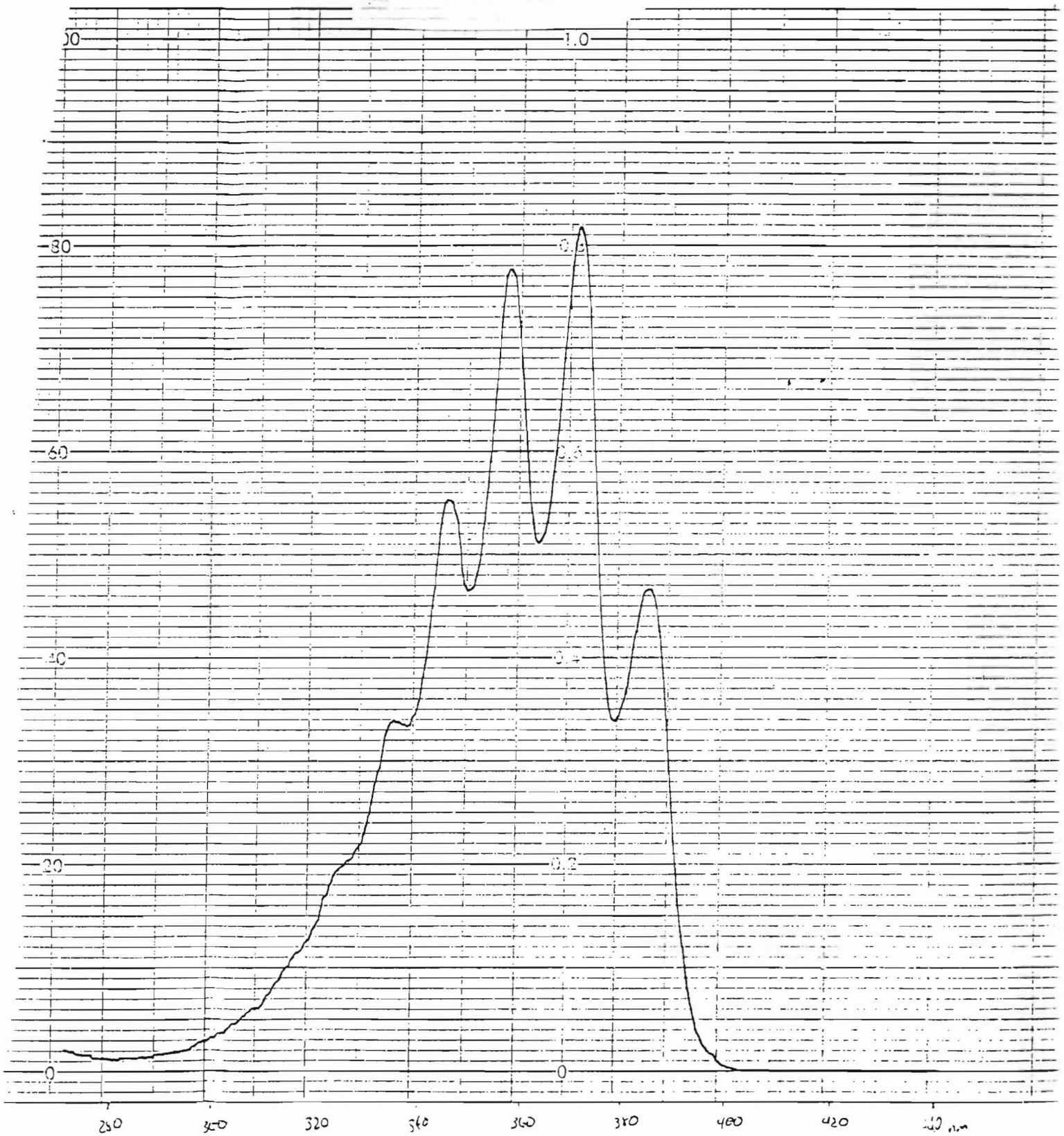

0.0151 M HONO before photolysis

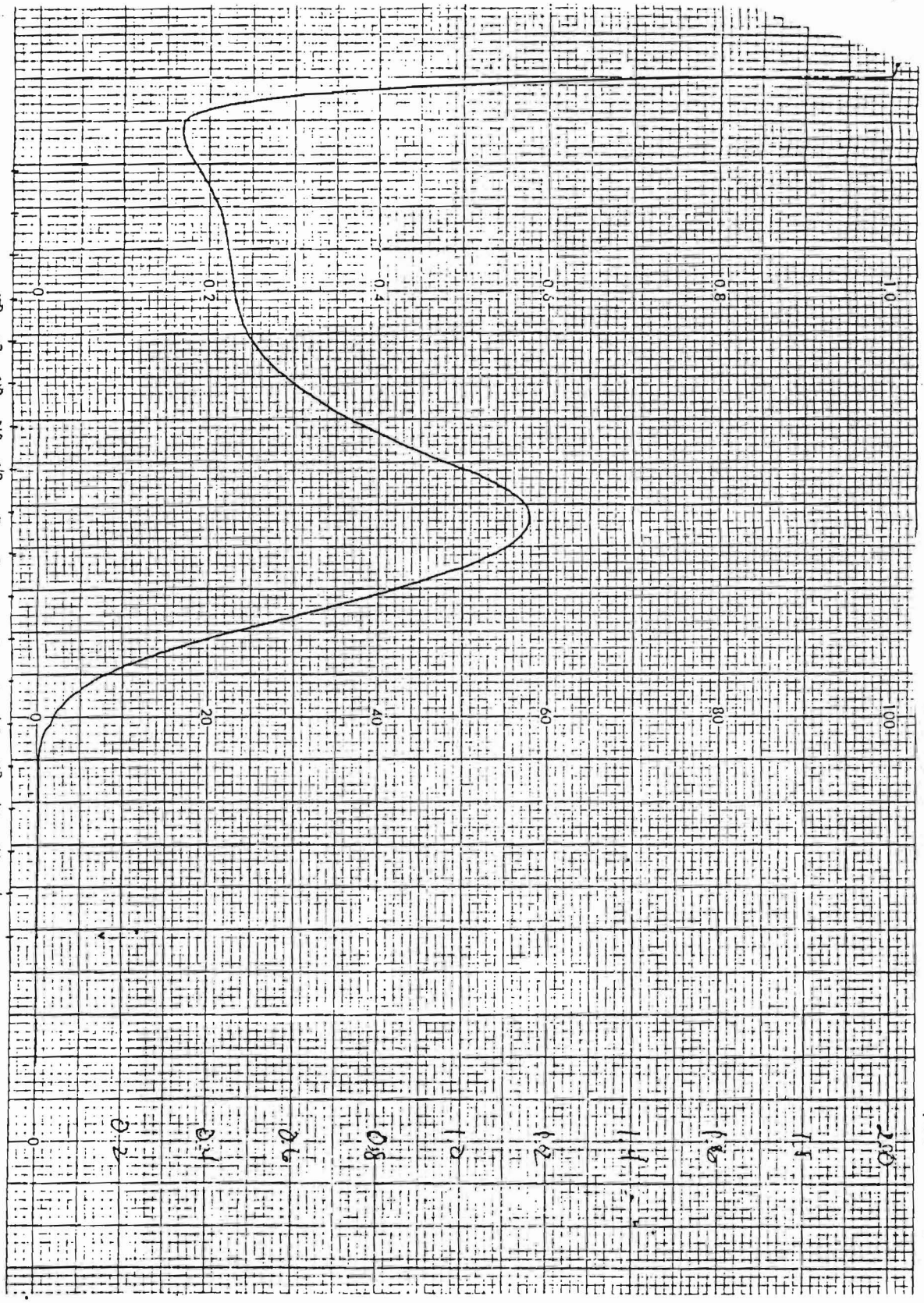

FIGURE 2

FIGURE 3

4.26×10^{-3} M benzene

FIGURE 4

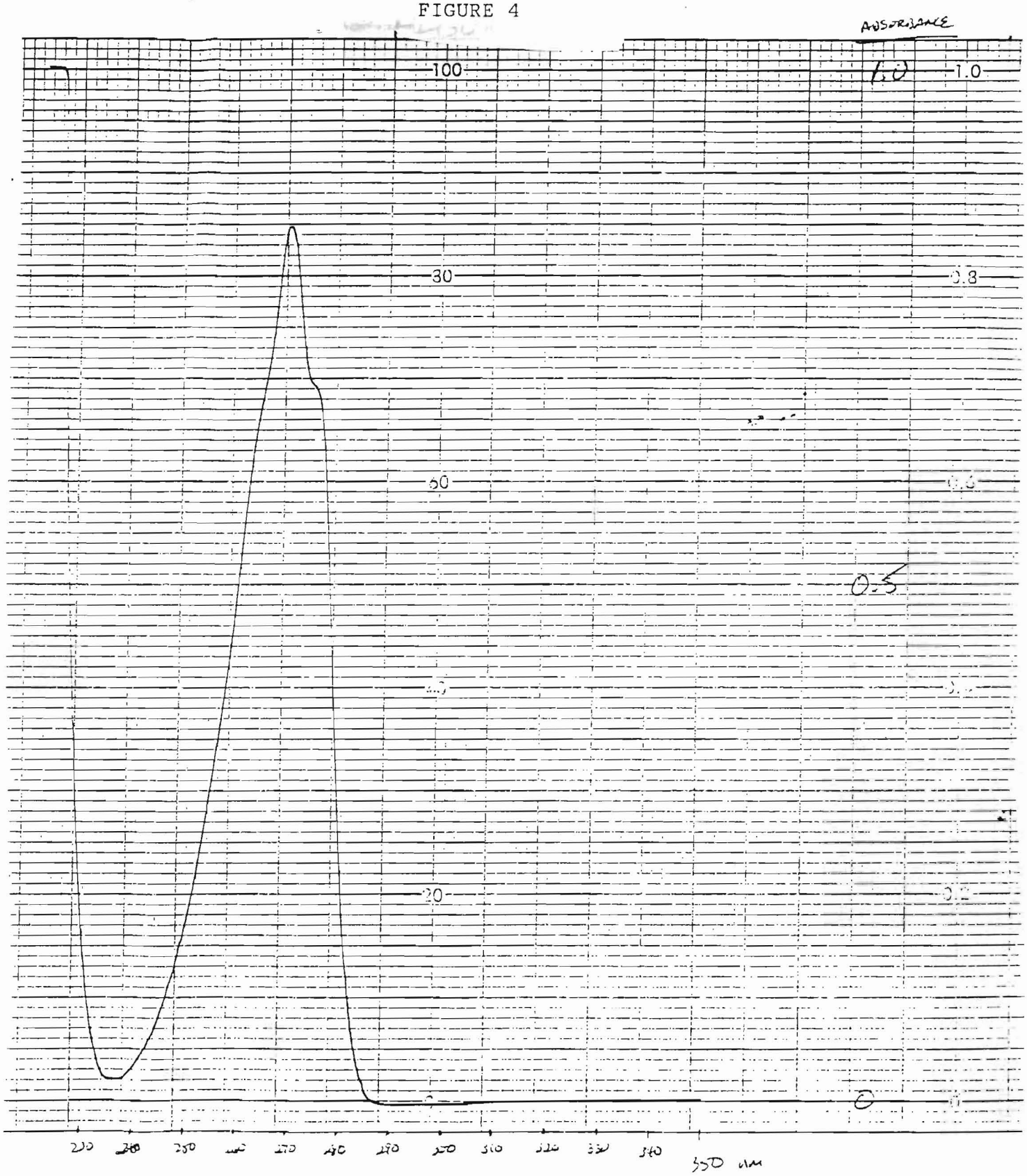

6.087×10^{-4} M phenol

FIGURE 5

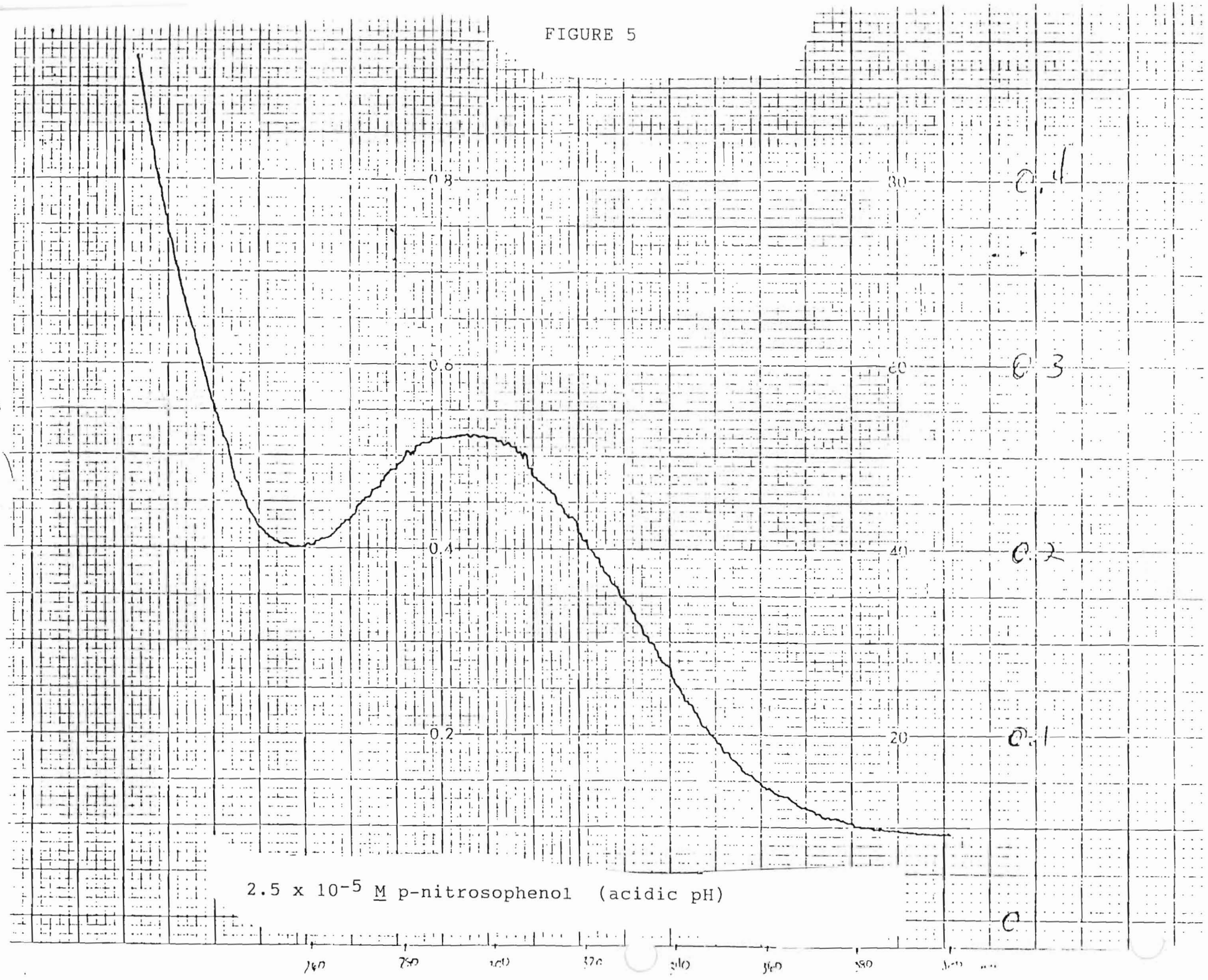

FIGURE 6a

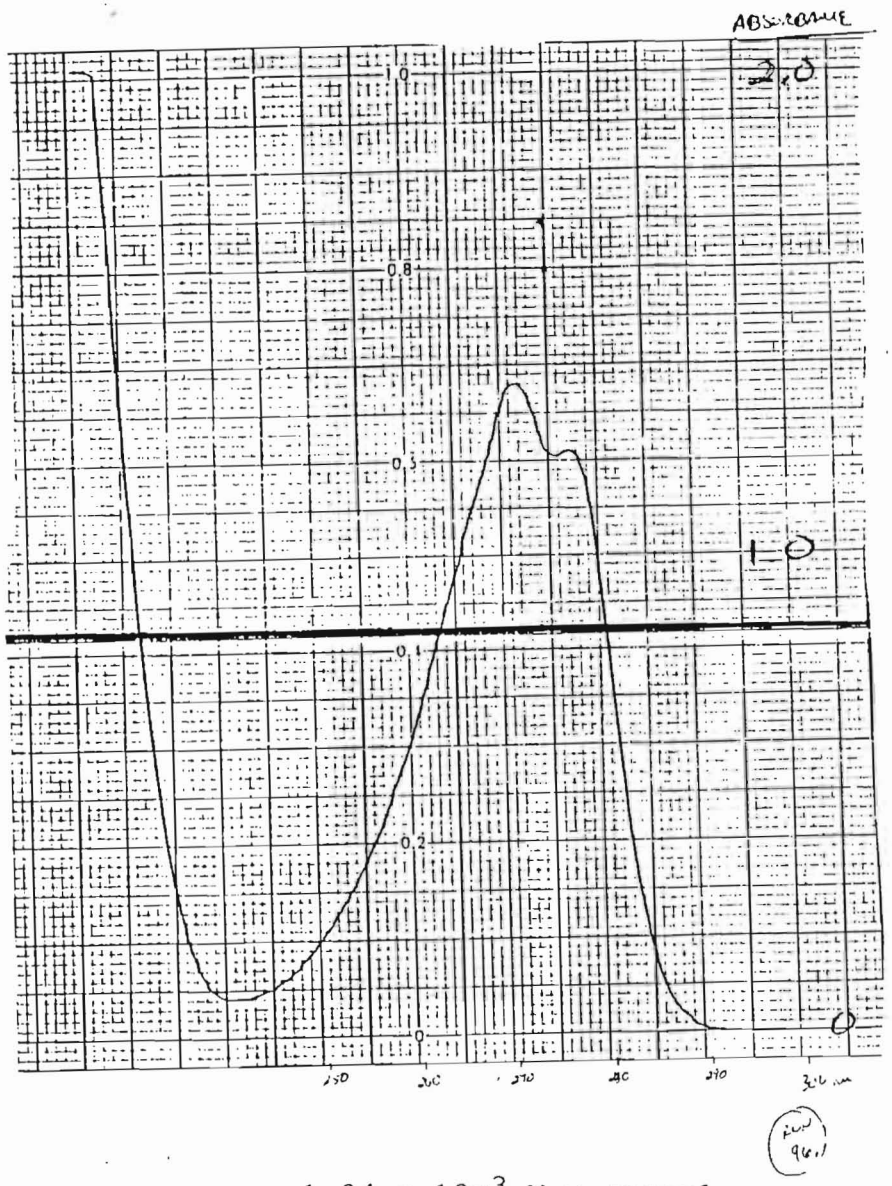

1.04 x 10^{-3} M m-cresol

FIGURE 6b

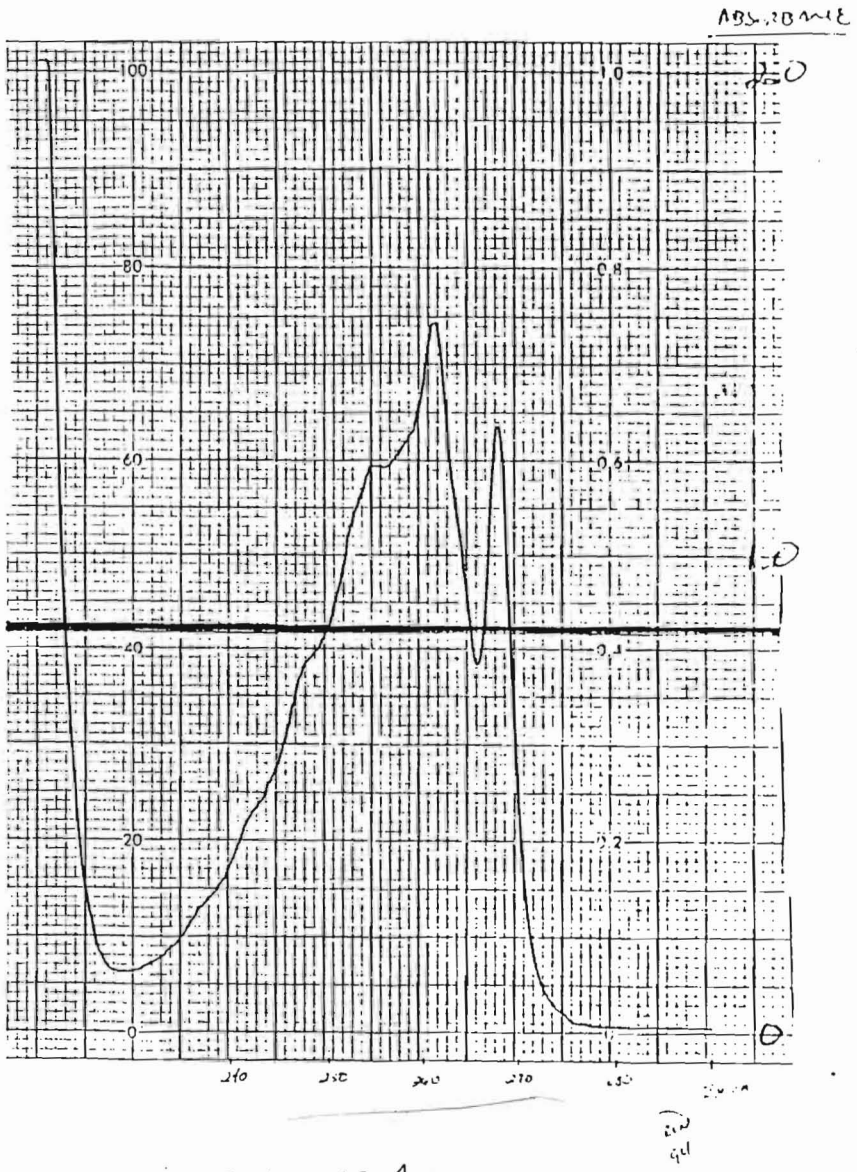

8.1 x 10^{-4} M toluene

FIGURE 7a

FIGURE 7b

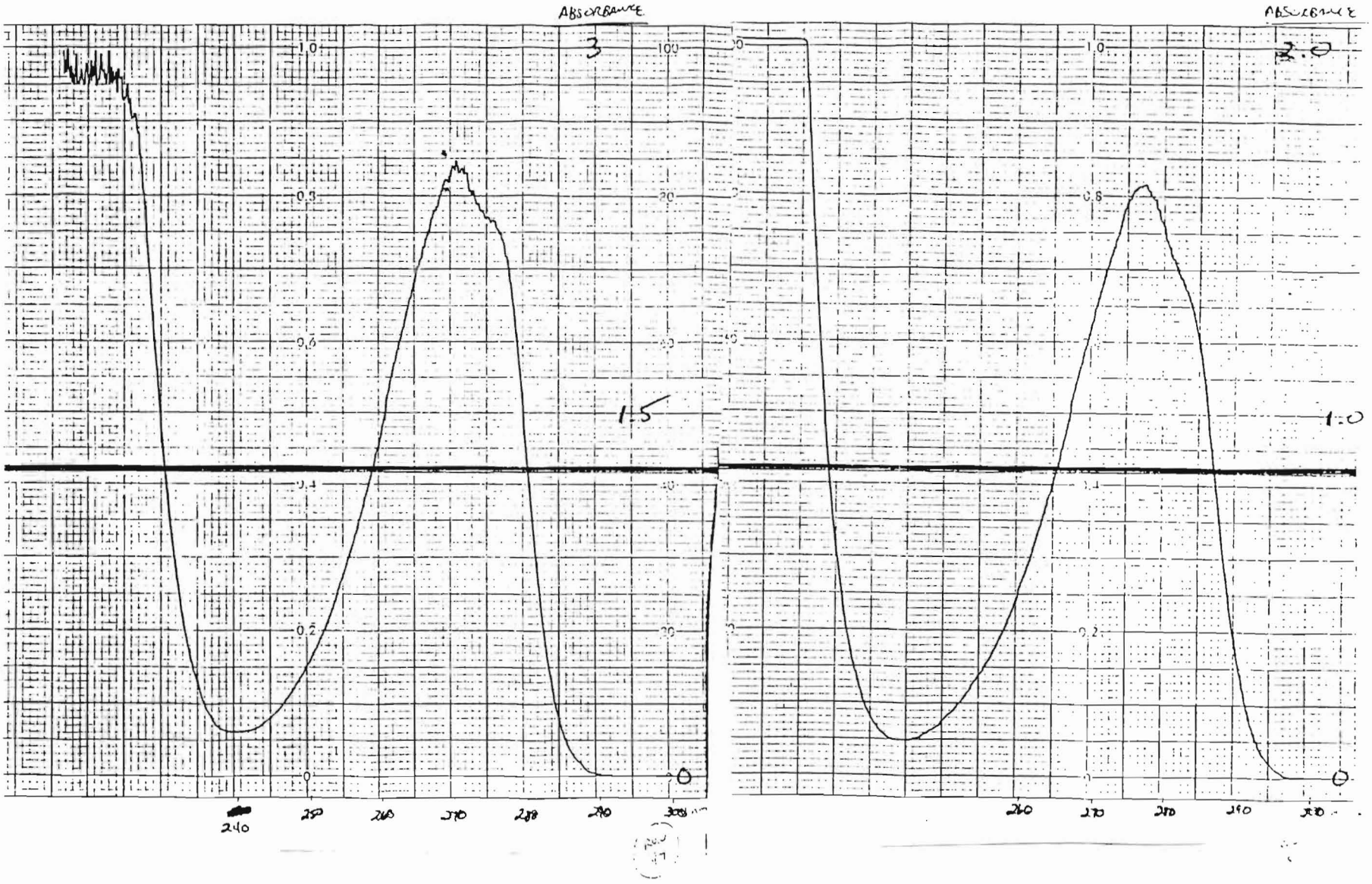

1.74 x 10^{-3} M p-cresol

1.06 x 10^{-3} M p-cresol

PART I.

32

FIGURE 8a

FIGURE 8b

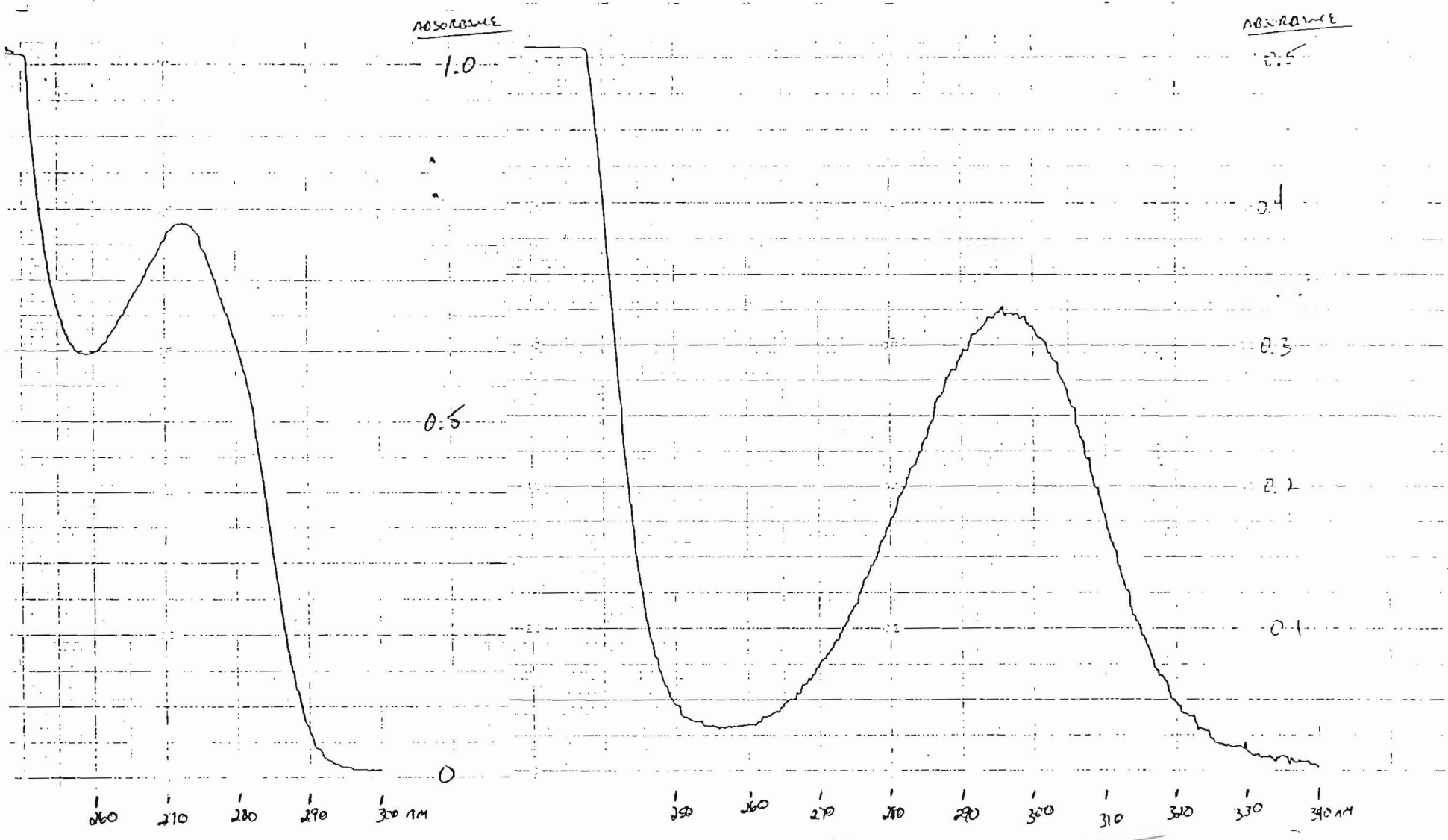

9.59 x 10^{-4} M benzoic acid

9.41 x 10^{-5} M salicylic acid

FIGURE 9a

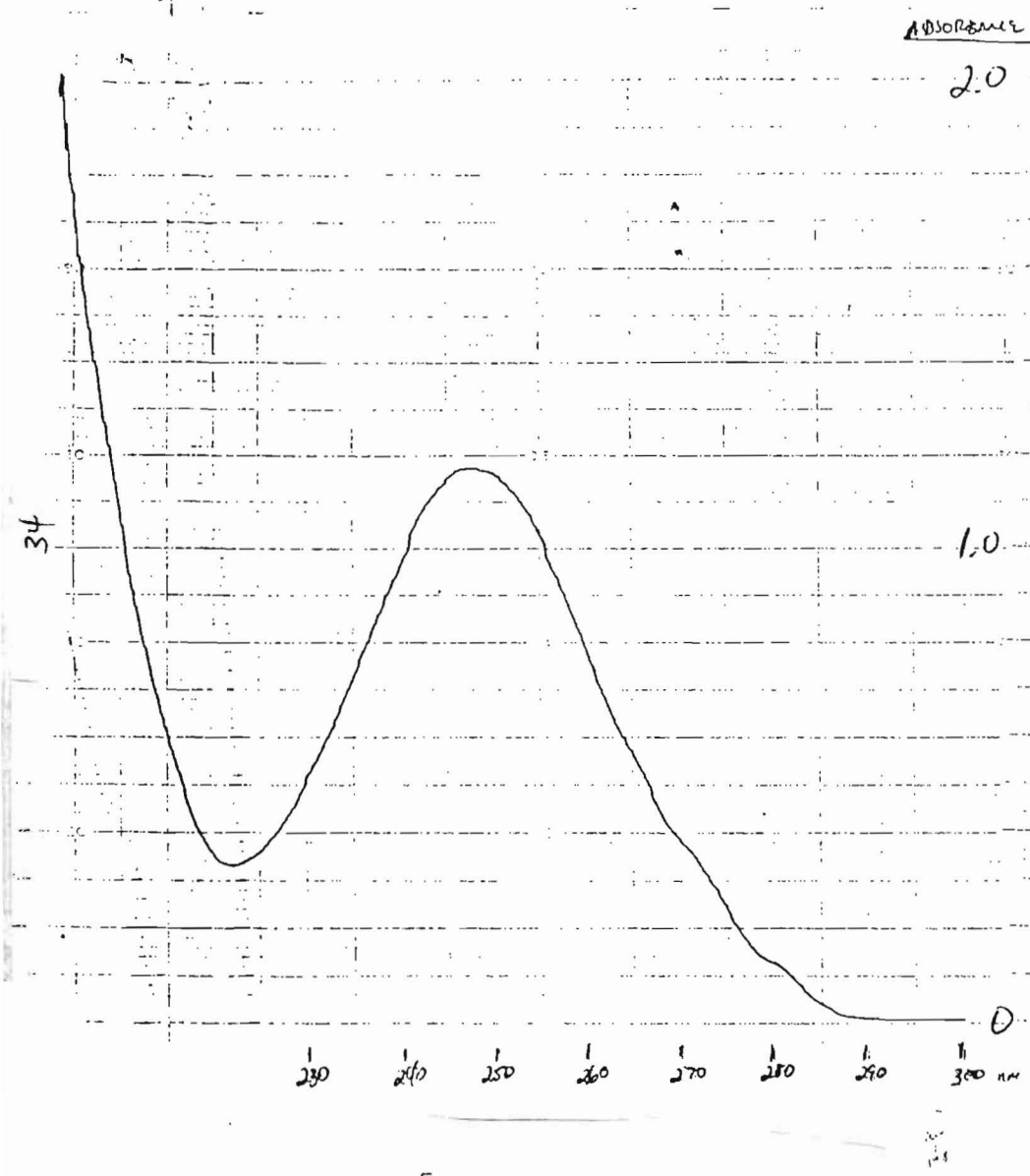

9.35 x 10^{-5} M p-hydroxybenzoic acid

FIGURE 9b

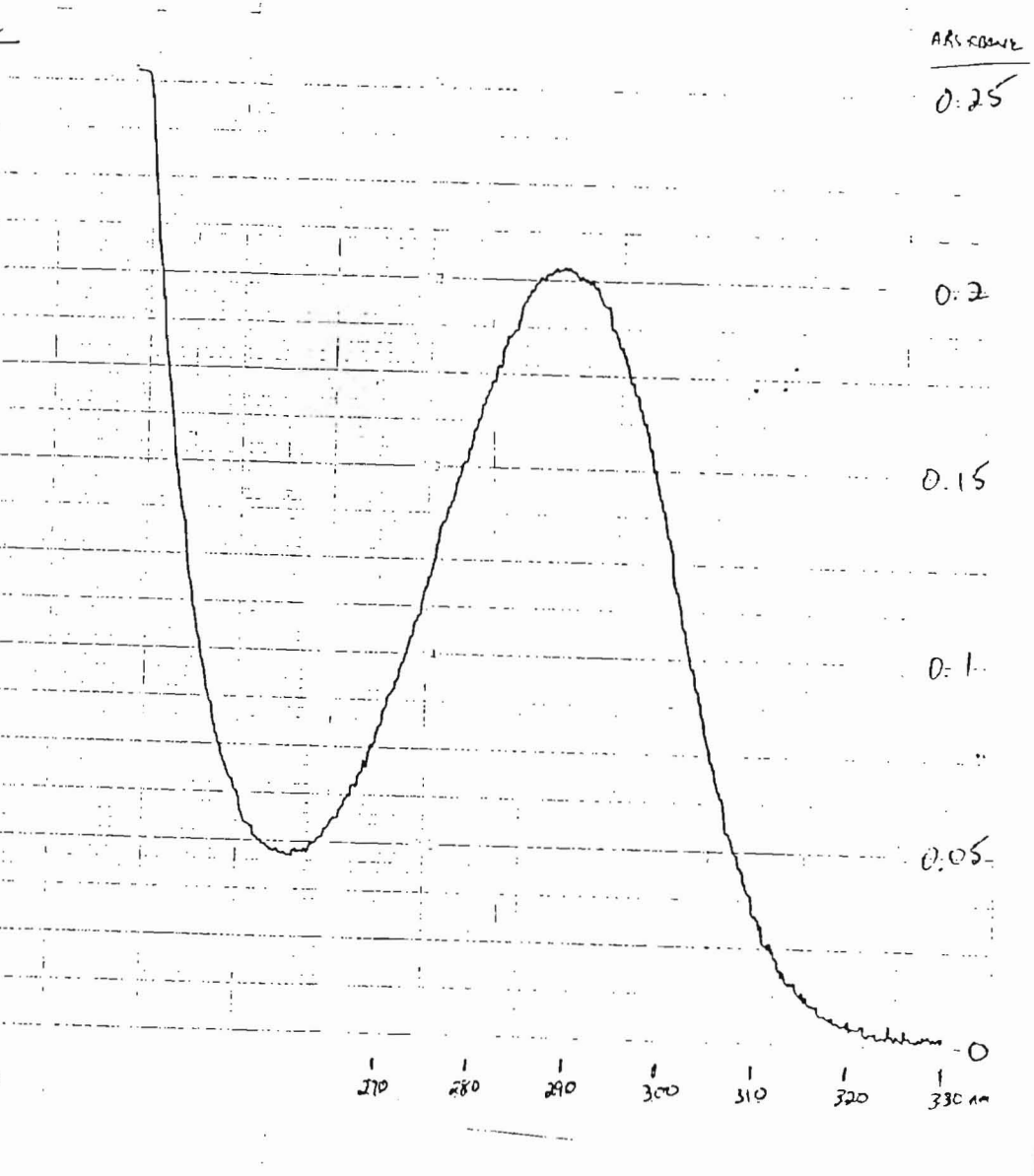

9.35 x 10^{-5} M m-hydroxybenzoic acid

FIGURE 10

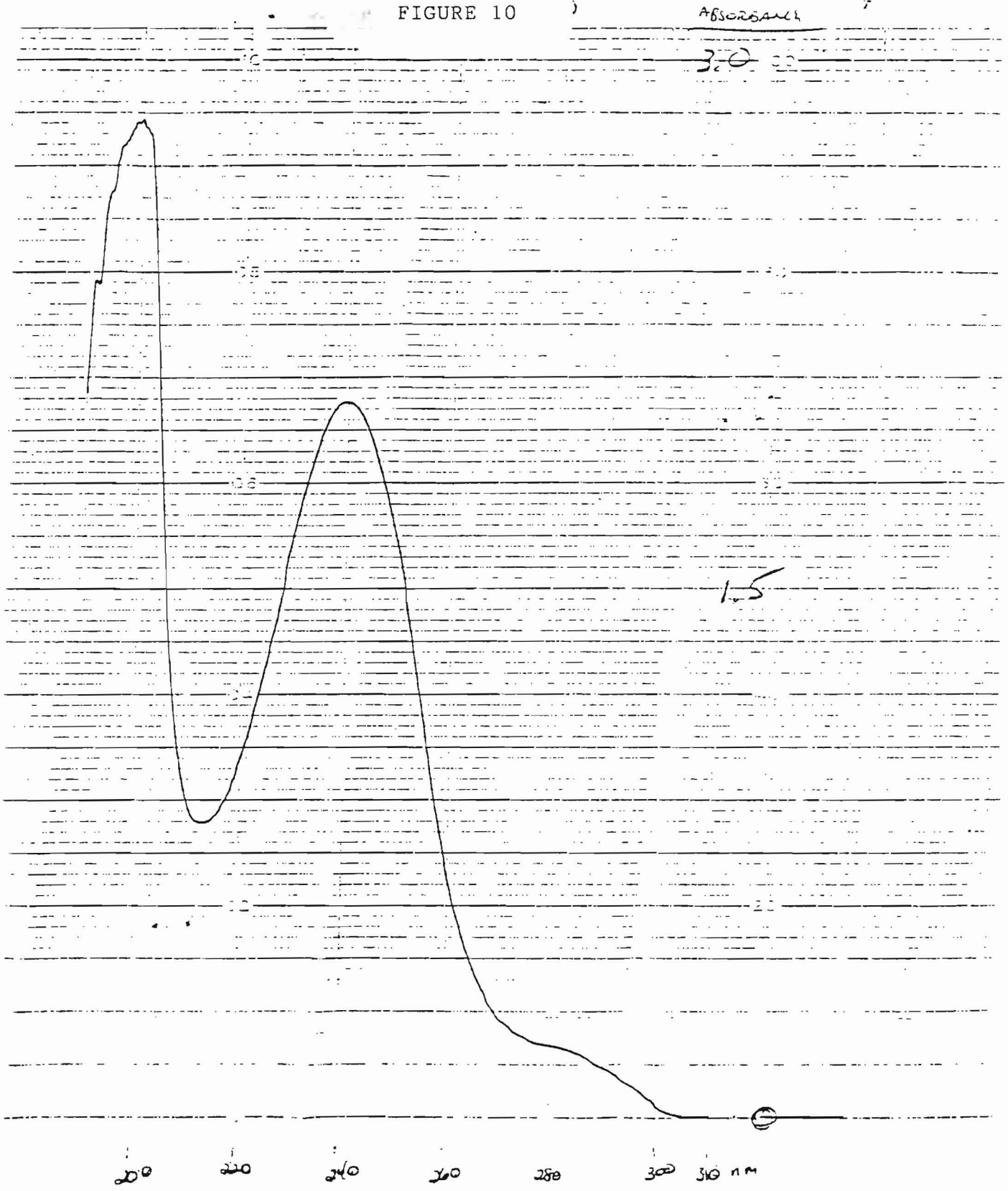

Saturated terephthalic acid (aq)

(approx. 1 x 10^{-4} M)

FIGURE 11a

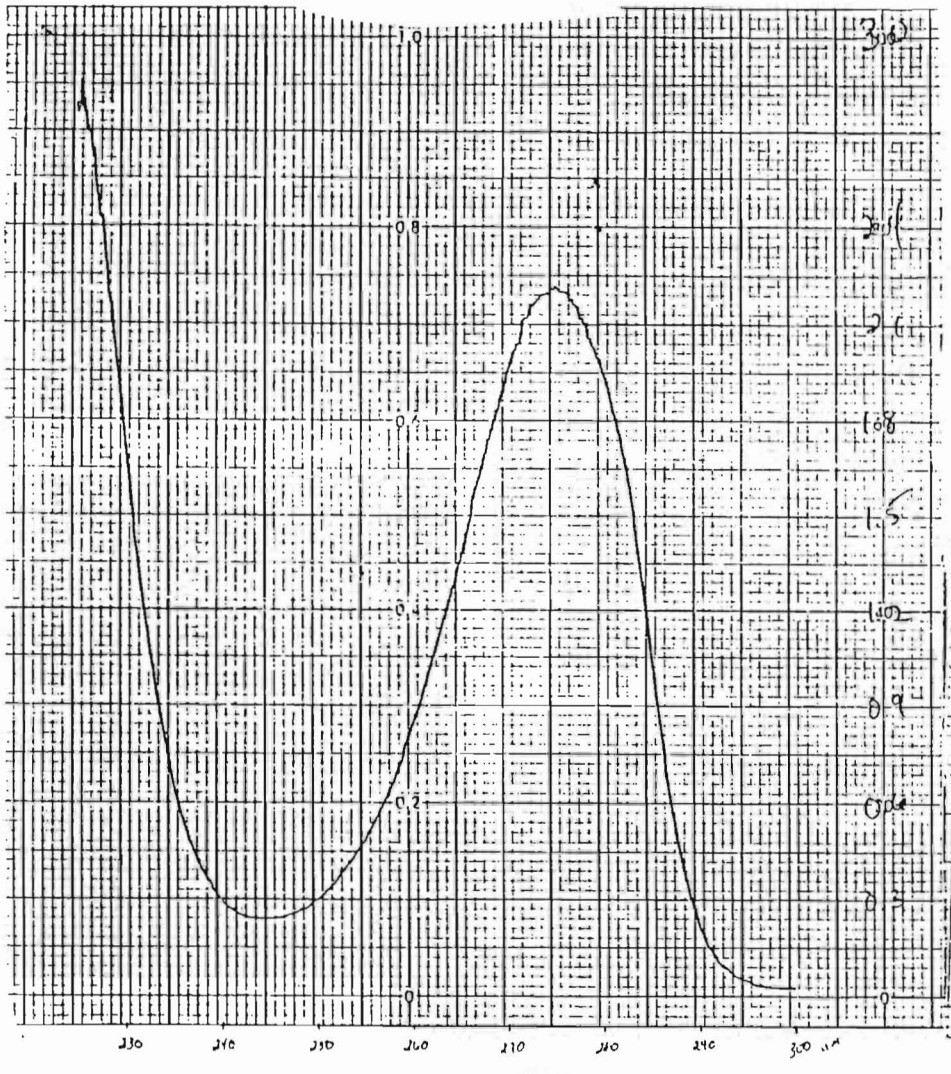

9.90 x 10^{-4} M catechol

FIGURE 11b

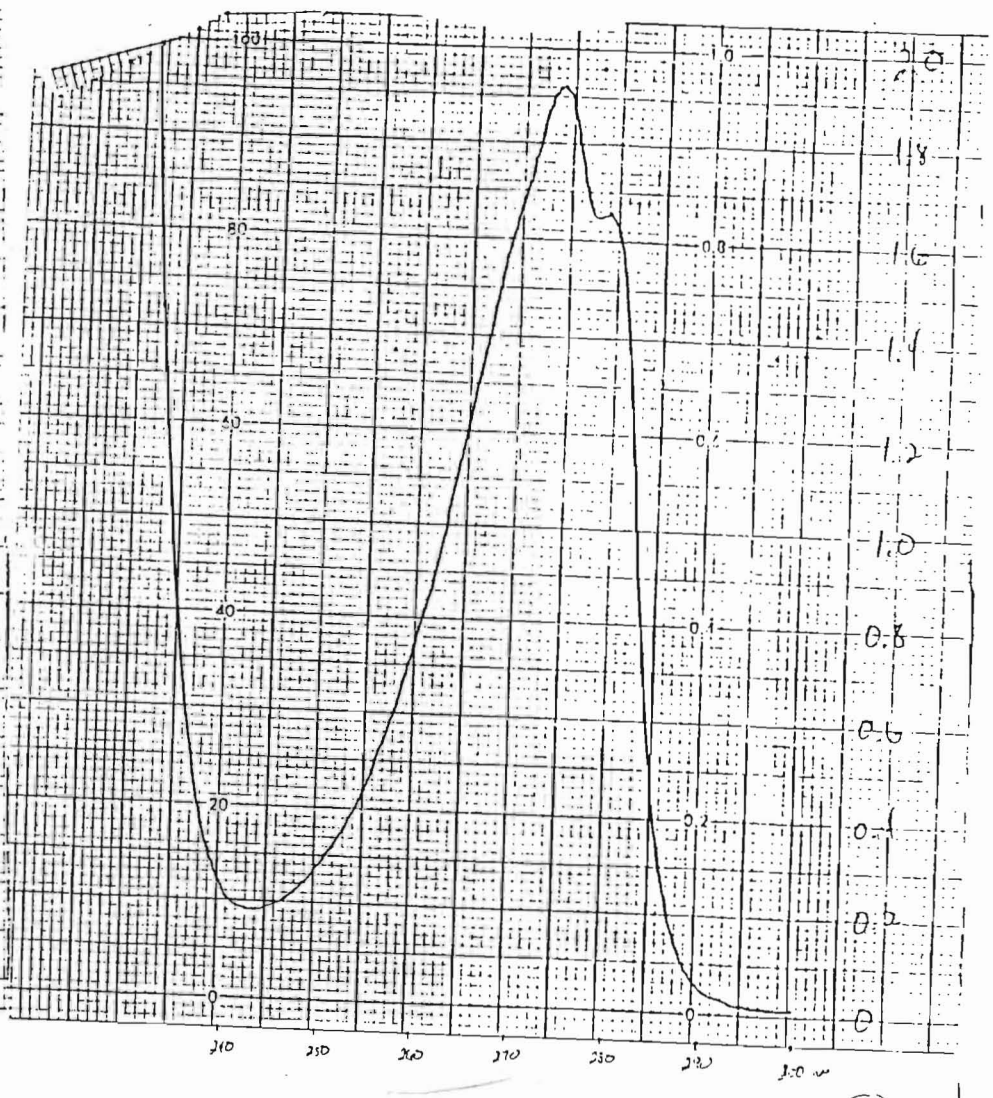

1.05 x 10^{-3} M resorcinol

FIGURE 12

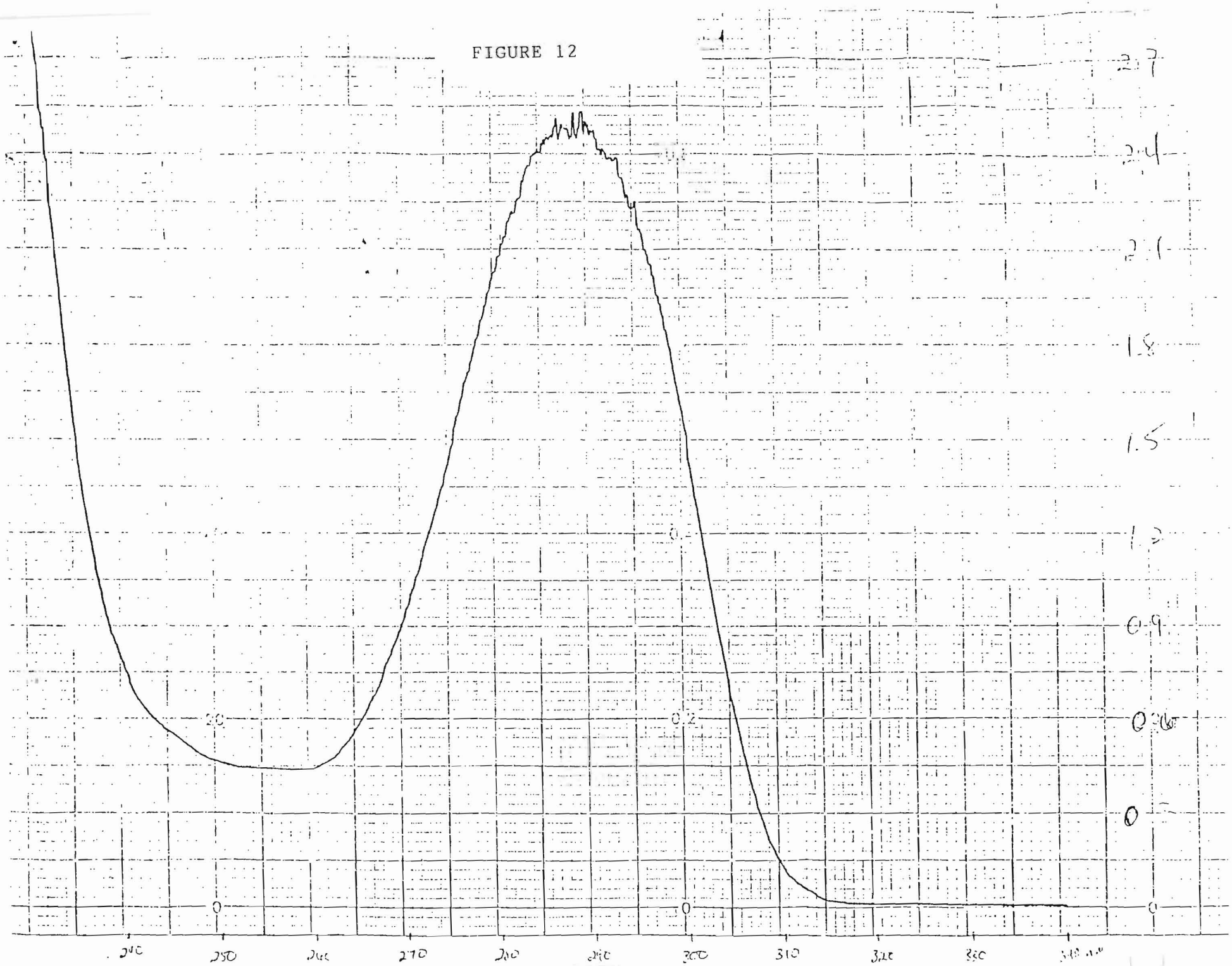

1.02 x 10^{-3} M hydroquino

HONO Thermolysis Results

The data for the HONO thermolysis reaction are presented in Tables (5-7) with corresponding Figures (13-15), respectively:

Table 5

HONO Concentrations in Thermolysis of 0.0566 M HONO

time (min.)	absorbance (371 nm)	[HONO], M
0		0.0566
7.50	2.82 ± 0.04	0.0562
58.83	2.73 ± 0.05	0.0544
121.00	2.63 ± 0.03	0.0524
167.58	2.55 ± 0.04	0.0508
234.67	2.38 ± 0.03	0.0474
284.50	2.31 ± 0.02	0.0460
355.50	2.15 ± 0.02	0.0428
404.00	2.04 ± 0.02	0.0406
495.33	1.83 ± 0.01	0.0365

Table 6

HONO Concentrations During Thermolysis of 0.0197 M HONO

time (min.)	absorbance (371 nm)	[HONO], M
0		0.0197
7.00	1.112 ± 0.005	0.0195
55.50	1.022 ± 0.005	0.0180
123.67	0.950 ± 0.003	0.0167
188.00	0.900 ± 0.002	0.0158
293.00	0.817 ± 0.003	0.0144
352.00	0.778 ± 0.003	0.0137

Table 7

HONO Concentrations During Thermolysis of 0.0101 M HONO

time (min.)	absorbance (371 nm)	[HONO], M
0		0.0101
18.0	0.544 ± 0.004	0.0100
44.5	0.523 ± 0.004	0.00960
73.5	0.485 ± 0.004	0.00890
98.0	0.478 ± 0.003	0.00877
166.5	0.438 ± 0.003	0.00804
201.5	0.404 ± 0.003	0.00741
243.5	0.381 ± 0.003	0.00699
272.5	0.370 ± 0.003	0.00679

In Table 8 are given the calculated kinetic orders (with respect to HONO) for HONO thermal decomposition using the fractional-life method:

Table 8

HONO Thermolysis Kinetic Orders (Fractional-Life Method)

initial [HONO], M	calc. order	rounded order
0.0566	−0.05 ± 0.1	0
0.0197	4.3 ± 2.5	4 ± 2.5
0.0101	−0.2 ± 0.1	0

Using the Method of Initial Rates, the kinetic order with respect to to HONO was calculated to be 0.5 ± 0.5.

FIGURE 13

[HONO] vs. Time for Thermolysis of 0.0566 M HONO

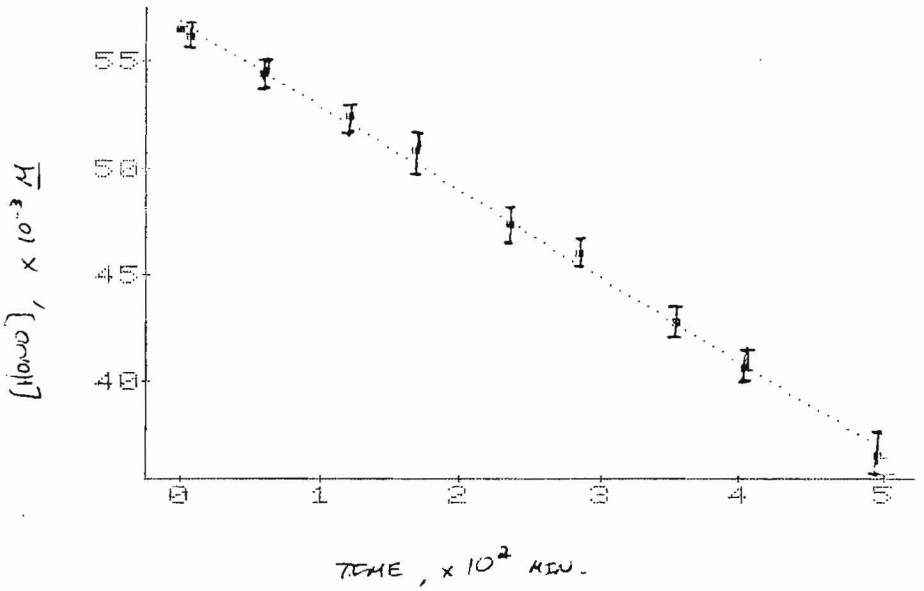

FIGURE 14

[HONO] vs. Time for Thermolysis of 0.0197 M HONO

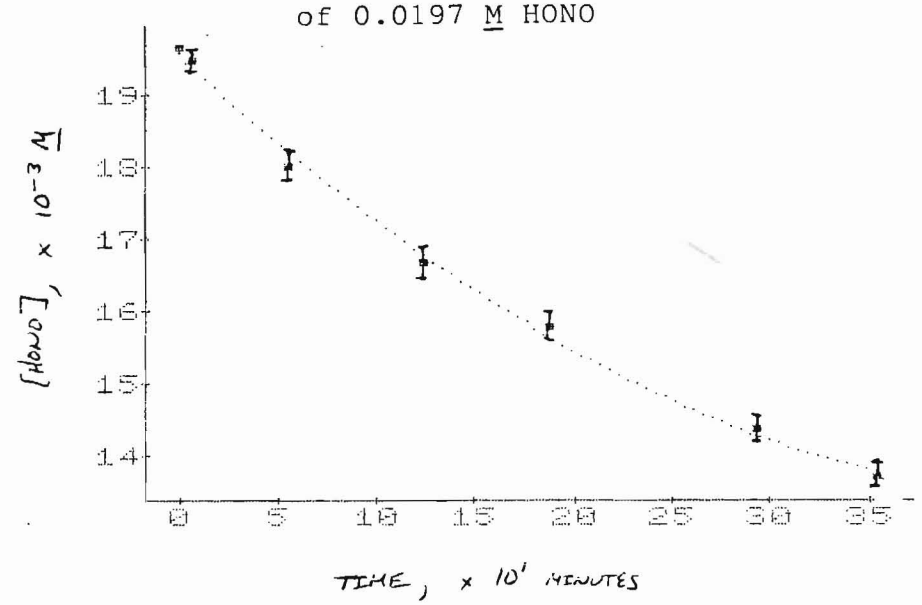

FIGURE 15

[HONO] vs. Time for Thermolysis of 0.0101 M HONO

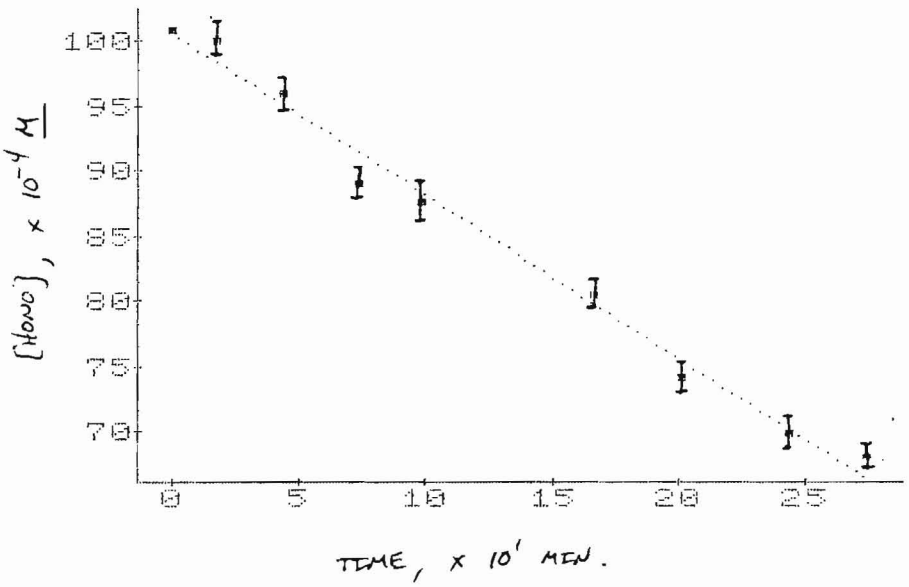

Results of HONO Photolysis in Absence of Scavenger

In Tables (9-11) and corresponding Figures (16-18), respectively, are given HONO concentrations as a function of time during photolyses:

Table 9

HONO Concentrations During Photolysis of 0.0145 M HONO in Absence of Scavenger

time (min.)	absorbance (371 nm)	[HONO], M
0	0.806 ± 0.002	0.0145 ± 0.001
38.91	0.770 ± 0.002	0.0138 ± 0.001
144.79	0.690 ± 0.002	0.0124 ± 0.001
235.42	0.590 ± 0.002	0.0106 ± 0.001
305.72	0.582 ± 0.002	0.0104 ± 0.001
365.53	0.541 ± 0.002	0.0097 ± 0.001

Table 10

HONO Concentrations During Photolysis of 0.0494 M HONO in Absence of Scavenger

time (min.)	absorbance (371 nm)	[HONO], M
0	2.70	0.0494 ± 0.0103
40.60	2.64	0.0483 ± 0.0101
84.28	2.58	0.0472 ± 0.0099
120.09	2.51	0.0459 ± 0.0096
338.90	2.02	0.0369 ± 0.0077
401.32	1.82	0.0332 ± 0.0069
465.00	1.72	0.0314 ± 0.0066

(all absorbances are ± 0.01)

Table II

HONO Concentrations During Photolysis of 0.0200 M HONO in Absence of Scavenger

time (min.)	absorbance (371 nm)	[HONO], M
0	1.096	0.0200
48.74	1.056	0.0193
112.73	0.974	0.0178
154.00	0.942	0.0172
240.00	0.826	0.0151
320.00	0.748	0.0136
370.00	0.693	0.0126
420.00	0.648	0.0118
461.18	0.604	0.0110

(absorbances are ± 0.002; [HONO] is ± 0.002)

FIGURE 16

[HONO] vs. Time for Photolysis of 0.0145 M HONO in Absence of Scavenger

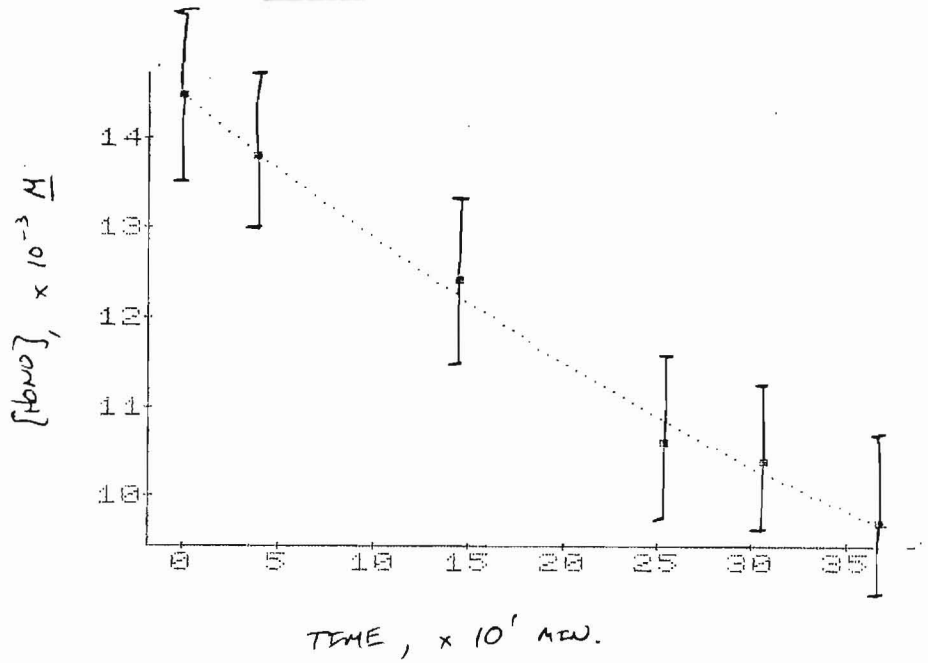

FIGURE 17

[HONO] vs. Time for Photolysis of 0.0494 M HONO in Absence of Scavenger

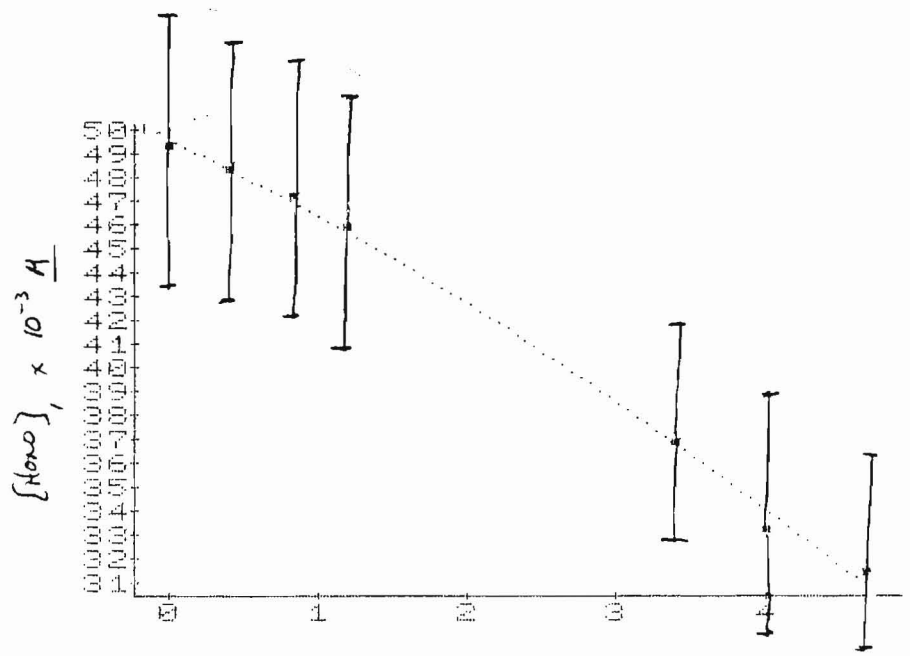

FIGURE 18

[HONO] vs. Time for Photolysis of 0.0200 M HONO in Absence of Scavenger

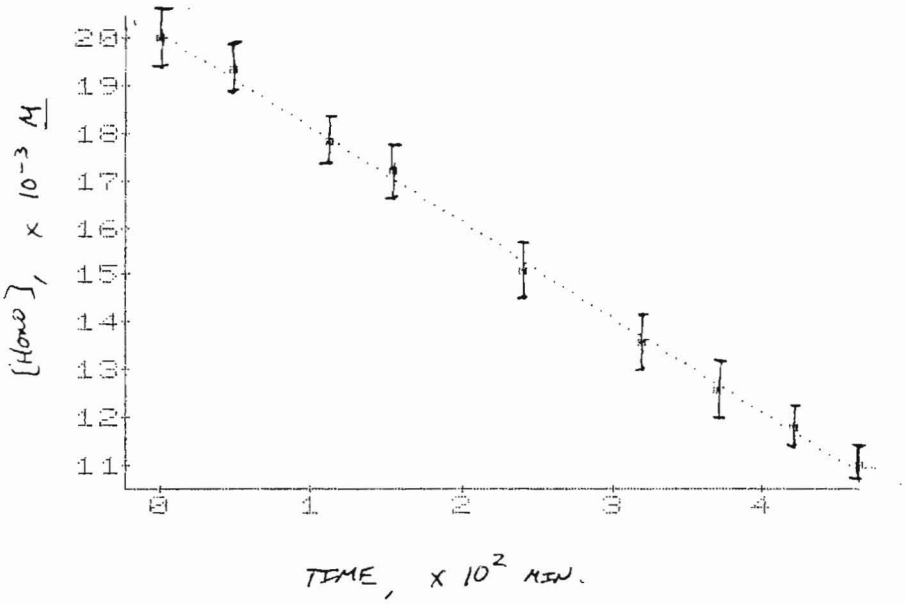

Photolysis of HONO in Presence of Benzene

Figure (19) shows a UV spectrum of a mixture of 0.0148 M HONO and 0.462 mM benzene after 155 minutes photolysis. Wavelength maxima corresponding to HONO are seen at 335, 346, 358, 371, and 386 nm. The broad peak with a maximum absorbance between 296-300 nm corresponds to p-nitrosophenol (PNP, see Fig.(5)). Tables (12-14) and corresponding Figures (20-25) show change in HONO and PNP concentrations during photolyses:

Table 12

HONO and PNP Concentration Changes During 0.0103 M HONO Photolysis

time(min.)	A (298 nm)	A (371 nm)	[HONO], M	[PNP], M
0	0.030	0.570	0.0103	0
18.39	0.138	0.552	0.00965	1.09×10^{-5}
54.71	0.362	0.541	0.00855	3.14×10^{-5}
105.09	0.530	0.520	0.00748	4.69×10^{-5}

(A = absorbance, $\pm$ 0.002; [HONO] is $\pm$ 10%; [PNP] is $\pm$ 30%)

Table 13

HONO and PNP Concentration Changes During 0.00998 M HONO Photolysis

time(min.)	A (298 nm)	A (371 nm)	[HONO], M	[PNP], M
0	0.001	0.535	0.00998	0
46.0	1.08	0.575	0.00634	9.7×10^{-5}
90.0	1.76	0.578	0.00362	1.6×10^{-4}
130.0	2.16	0.587	0.00216	2.0×10^{-4}
170.0	2.37	0.576	0.00109	2.15×10^{-4}
230.0	2.45	0.560	0.00047	2.23×10^{-4}

(abbreviations and uncertainties same as in Table 12)

Table 14

HONO and PNP Concentration Changes During 0.0148 M HONO Photoysis

time(min.)	A (298 nm)	A (371 nm)	[HONO], M	[PNP], M
0	0.040	0.825	0.0148	0
35.00	0.203	0.802	0.0140	1.6×10^{-5}
60.00	0.310	0.789	0.0133	2.6×10^{-5}
88.75	0.410	0.760	0.0124	3.5×10^{-5}
155.0	0.582	0.699	0.0106	5.1×10^{-5}
187.0	0.610	0.681	0.0101	5.4×10^{-5}
218.0	0.637	0.649	0.0094	5.6×10^{-5}

(abbreviations and uncertainties same as in Table 12)

Nitrite Photolysis in Presence of Benzene

In Figures (26-27) are given the UV absorption spectrum of a mixture of 0.02533 M NO_2^- and 0.04515 M benzene before and after 3 hours photolysis with 365 nm radiation. The wavelength maxima attributed to NO_2^- remains at 352 nm in both spectra, and there is no significant change in absorbance at 352 nm.

FIGURE 19

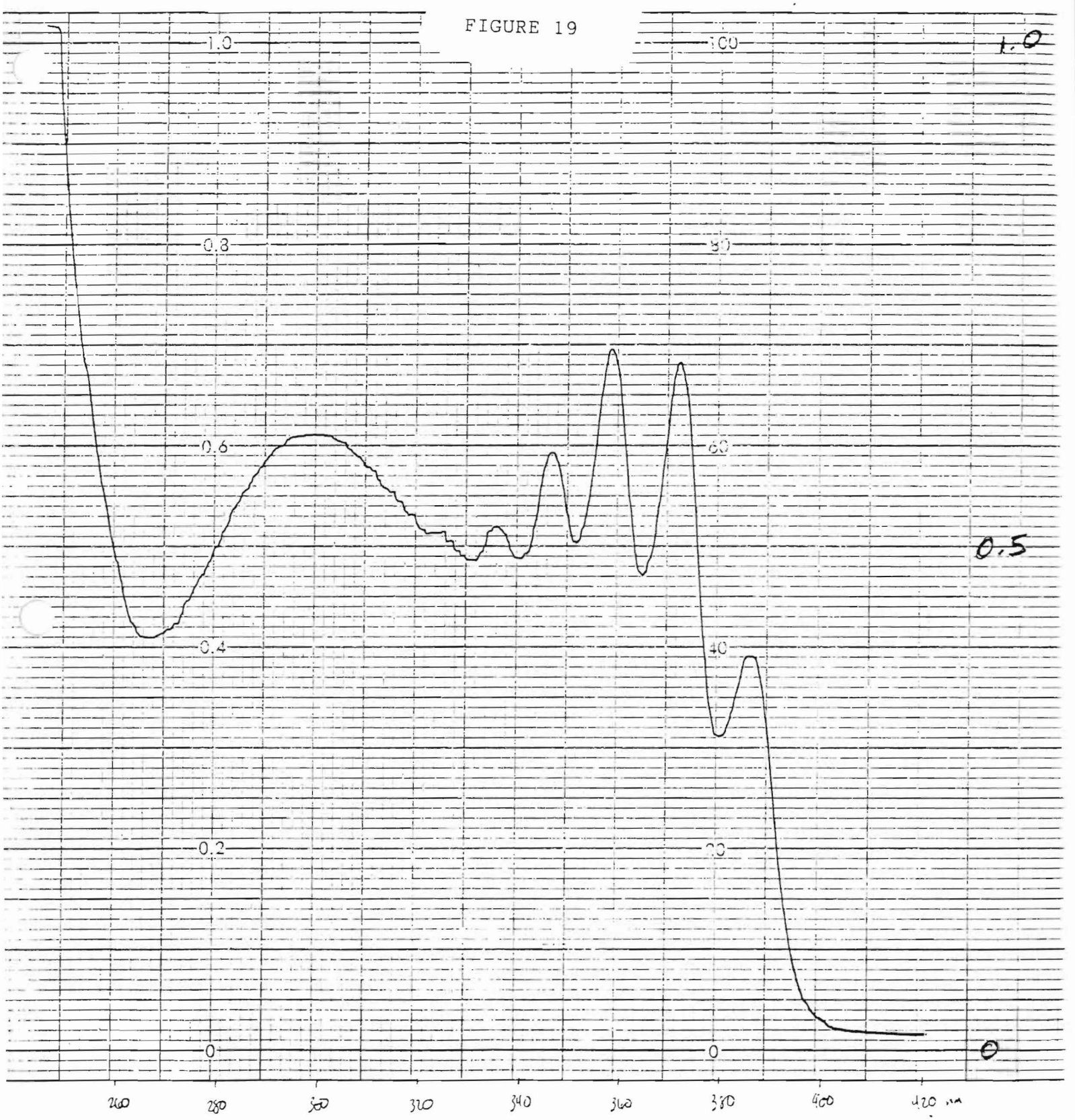

0.0148 M HONO and 4.62×10^{-4} M benzene

After 155 Minutes Photolysis

FIGURE 20

[HONO] vs. Time for Photolysis of 0.0103 M HONO in Presence of Benzene

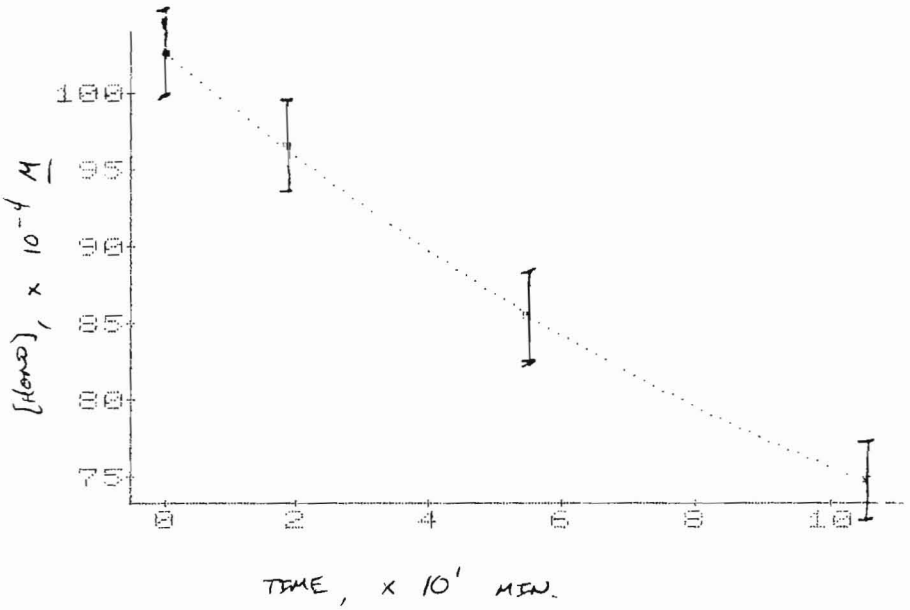

FIGURE 21

[PNP] vs. Time for Photolysis of 0.0103 M HONO in Presence of Benzene

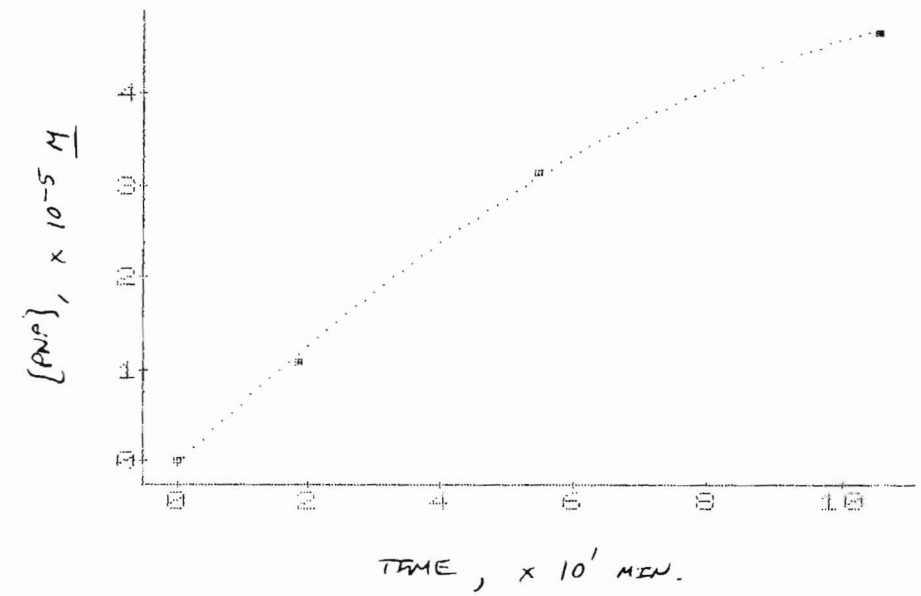

FIGURE 22

[HONO] vs. Time for Photolysis of 0.00998 M HONO in Presence of Benzene

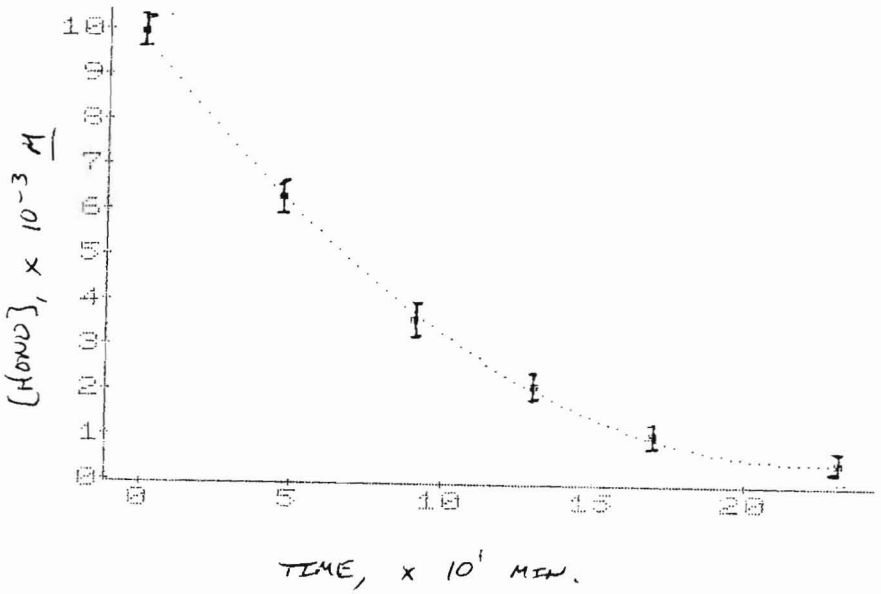

FIGURE 23

[PNP] vs. Time for Photolysis of 0.00998 M HONO in Presence of Benzene

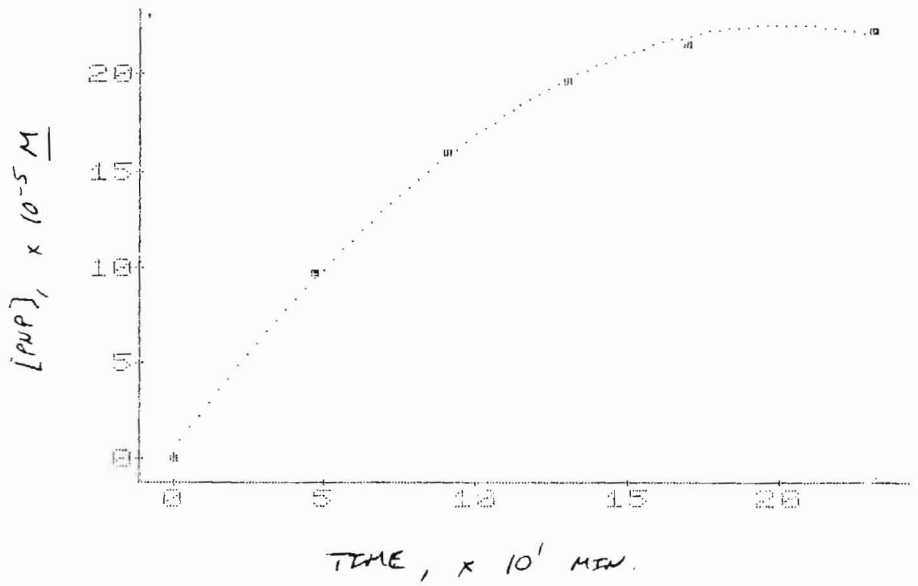

FIGURE 24

[HONO] vs. Time for Photolysis of 0.0148 M HONO in Presence of Benzene

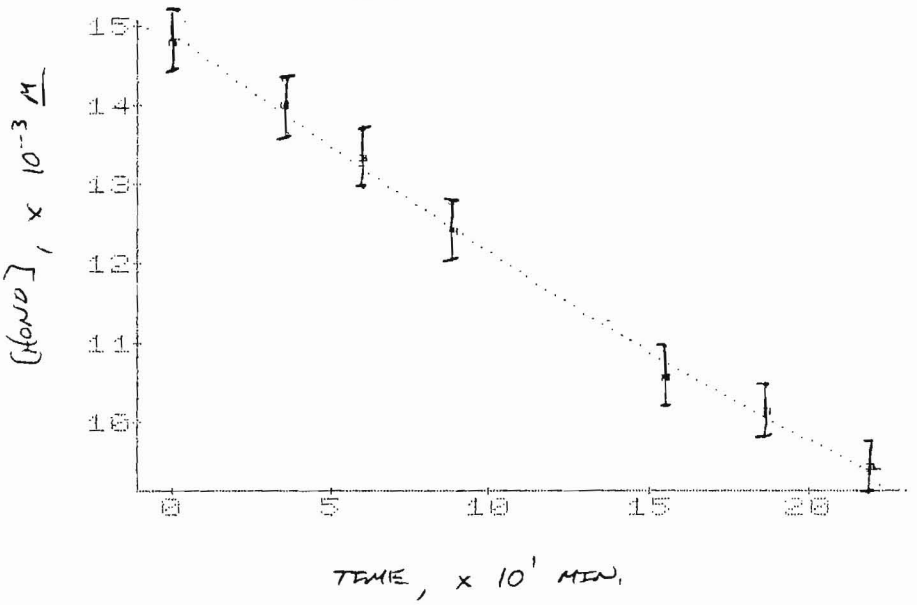

FIGURE 25

[PNP] vs. Time for Photolysis of 0.0148 M HONO in Presence of Benzene

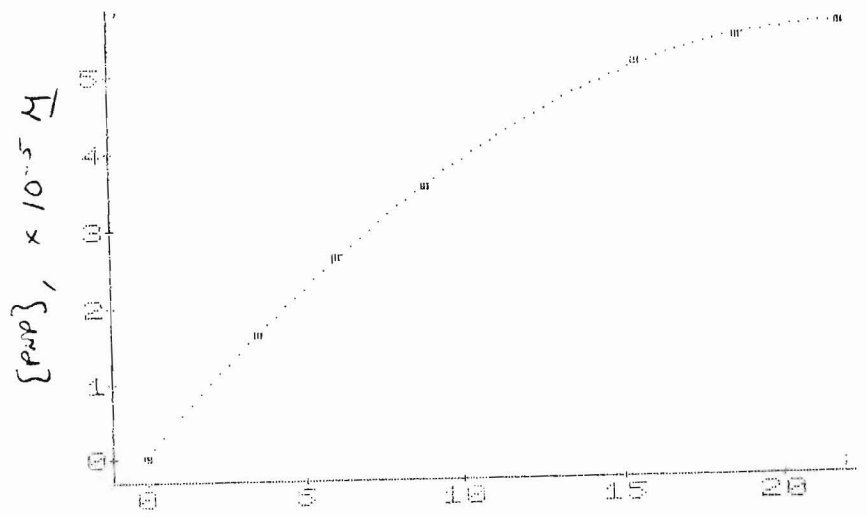

FIGURE 26

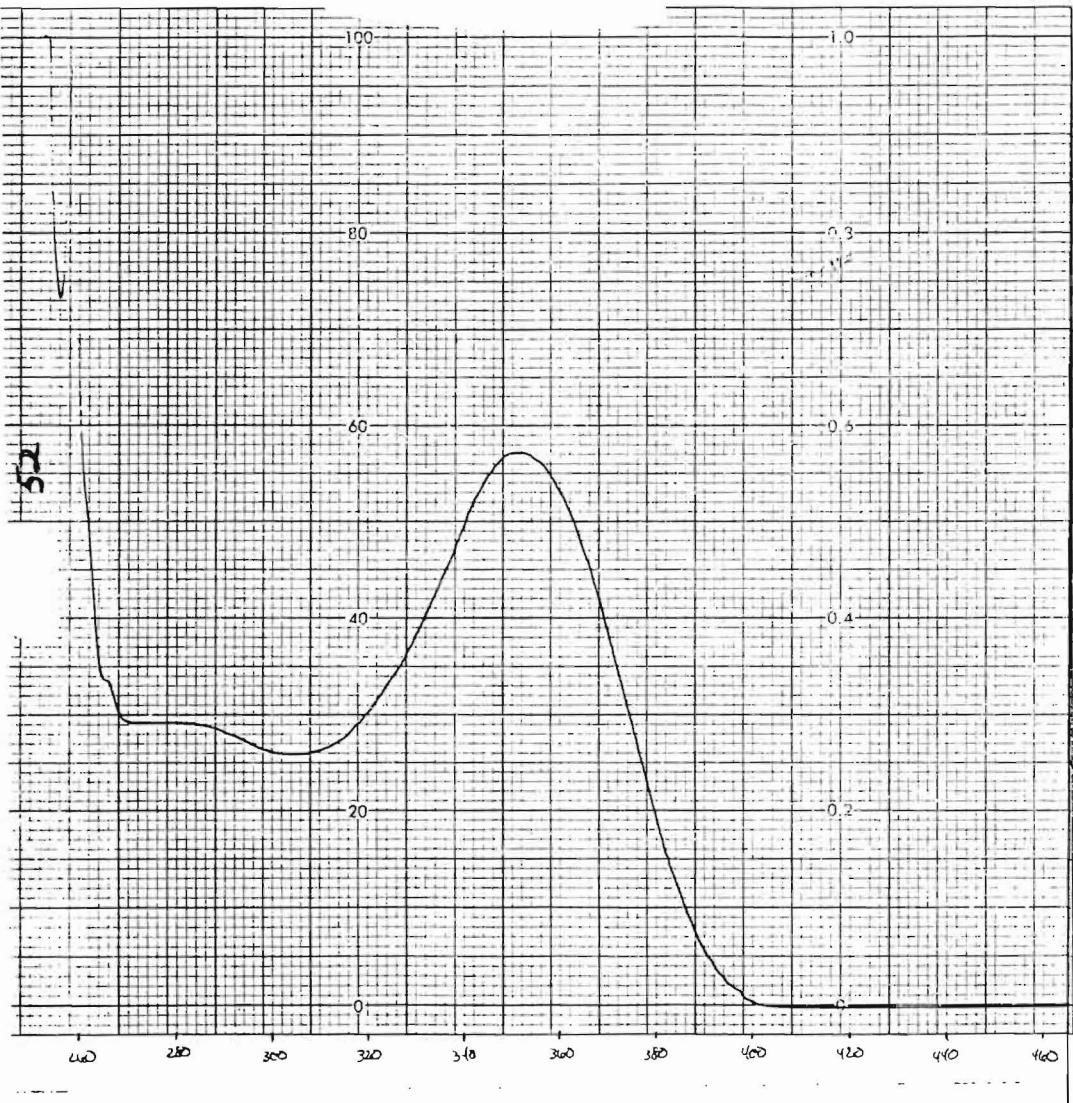

0.02354 M NO_2^- and 0.04575 M benzene

before photolysis

FIGURE 27

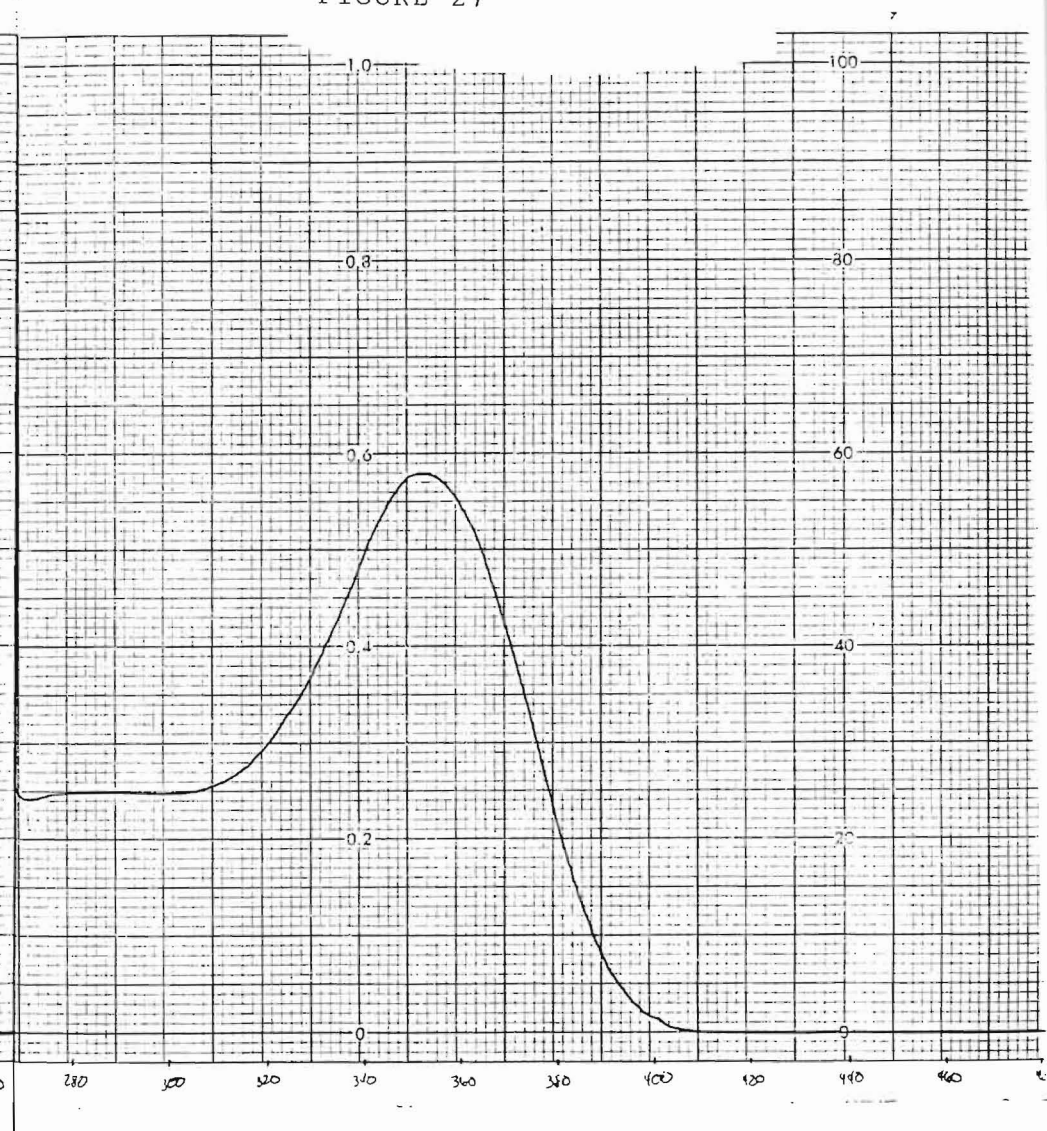

0.02354 M NO_2^- and 0.04575 M benzene

after 32 min., 20 s photolysis

HONO Photolysis in Presence of Toluene

UV/vis spectra of a mixture of 0.0101 M HONO and 1.55 mM toluene before and after 100 minutes photolysis are given in Figures (28-29). The resulting spectra are summarized in Table 15:

Table 15

UV Spectra of HONO/Toluene Photolysis Mixture

	Compound	Maxima (nm)
BEFORE PHOTOLYSIS	HONO	335,346,357,371,384
	toluene	261,268
AFTER PHOTOLYSIS	HONO	344,357,370,384
	toluene	268
	unknown product	304 (broad)

Photolysis of Nitrite in Presence of Toluene

UV/vis spectra of a mixture of 0.0255 M NO_2^- and 2.6 mM toluene before and after 110 minutes photolysis are given in Figures (30-31). The resulting spectra are summarized in Table 16:

Table 16

UV Spectra of NO_2^-/Toluene Photolysis Mixture

	Compound	Maxima (nm)	Absorbance
BEFORE PHOTOTLYSIS	NO_2^-	352	0.580
	toluene	261,268	0.625,0.578
AFTER PHOTOLYSIS	NO_2^-	352	0.580
	toluene	261,268	0.590,0.546

FIGURE 28

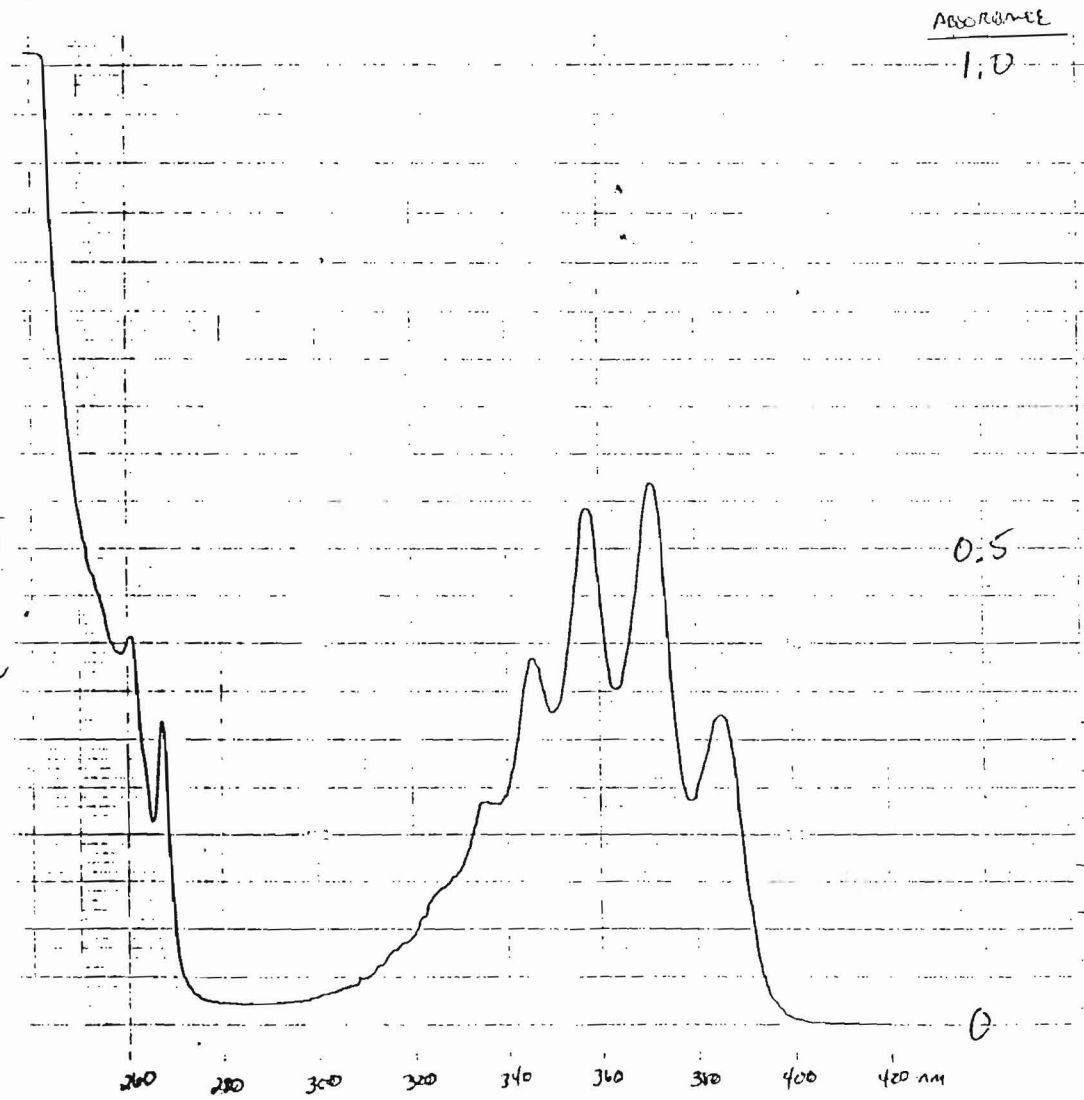

0.0101 M HONO and 1.55 x 10^{-3} M toluene

before photolysis

FIGURE 29

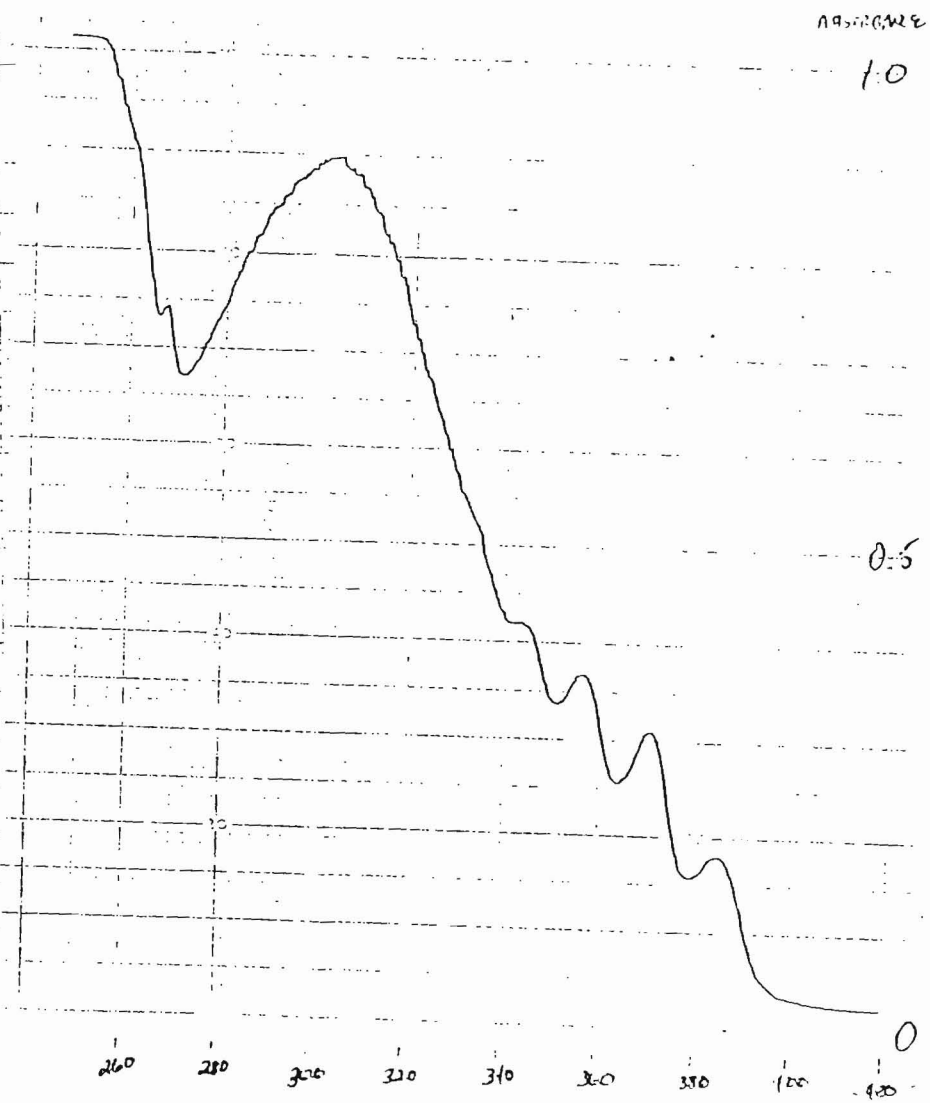

0.0101 M HONO and 1.55 x 10^{-3} M toluene

after 100 minutes photolysis

FIGURE 30

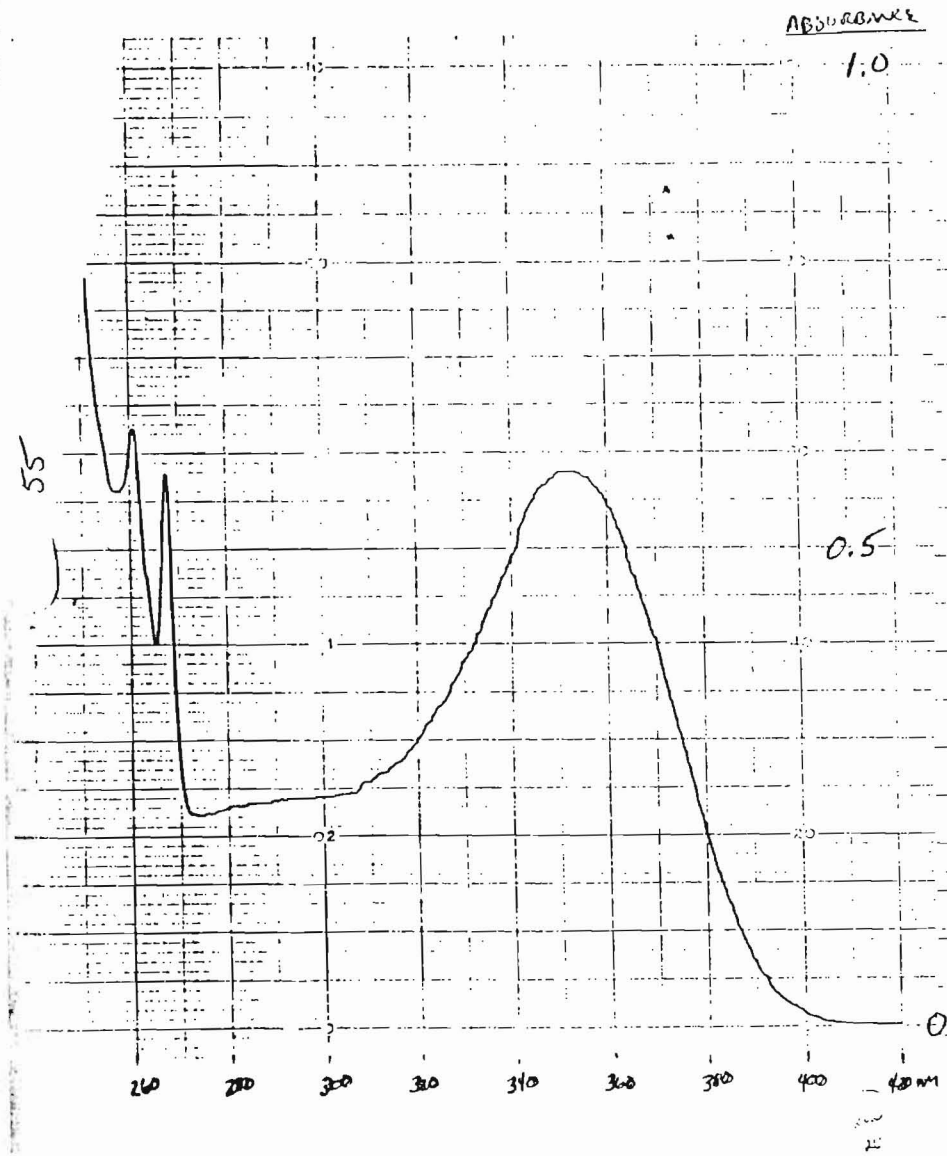

0.0255 M NO_2^- and 2.6 x 10^{-3} M toluene

before photolysis

FIGURE 31

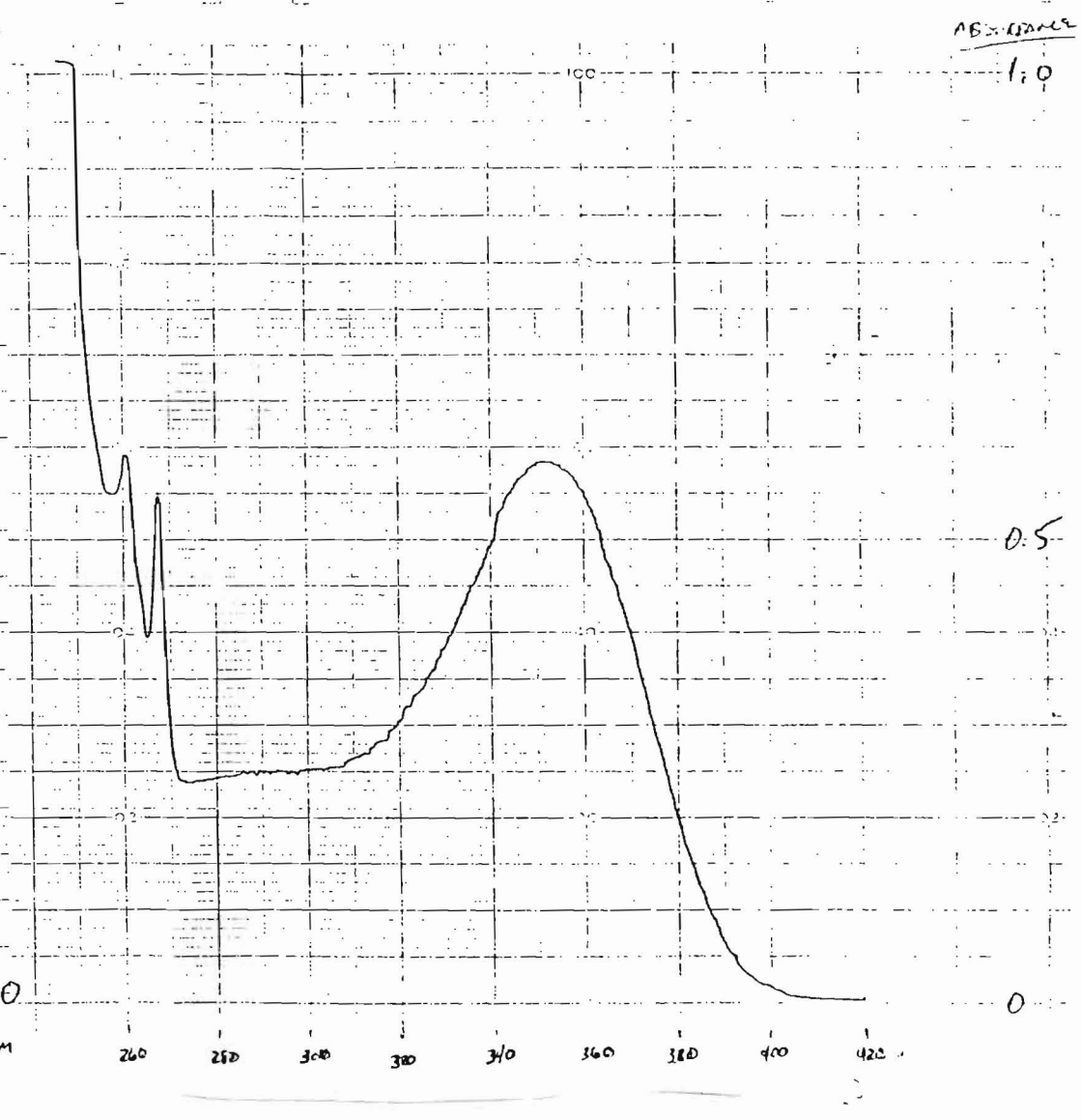

0.0255 M NO_2^- and 2.6 x 10^{-3} M toluene

after 110 minutes photolysis

HONO Photolysis in Presence of Benzoic Acid

UV/vis spectra of a mixture of 0.0101 M HONO and 1.9 mM benzoic acid before and after 30 minutes photolysis are given in Figures (32-33). The resulting spectra are summarized in Table 17:

Table 17

UV Spectra of HONO/Benzoic Acid Photolysis Mixture

	Compound	Maxima (nm)
BEFORE PHOTOLYSIS	HONO	335,346,357,371,385
	benzoic acid	273
AFTER PHOTOLYSIS	HONO	336,346,357,371,385
	benzoic acid	approx. 272
	unknown product	approx. 308

HONO Photolysis in Presence of Terephthalic Acid

UV/vis spectra of a mixture of 0.0151 M HONO and saturated (approximately 0.1 mM) terephthalic acid before and after 8 hours photolysis are given in Figures (34-35). The resulting spectra are summarized in Table 18:

Table 18

UV Spectra of HONO/Terephthalic Acid Photolysis Mixture

	Compound	Maxima (nm)
BEFORE PHOTOLYSIS	HONO	337,347,359,372,387
	terephthalic acid	289 (very small)
AFTER PHOTOLYSIS	HONO	337,347,359,372,386
	(HIGHER ABSORBANCE FROM 270-310 nm)	

FIGURE 32

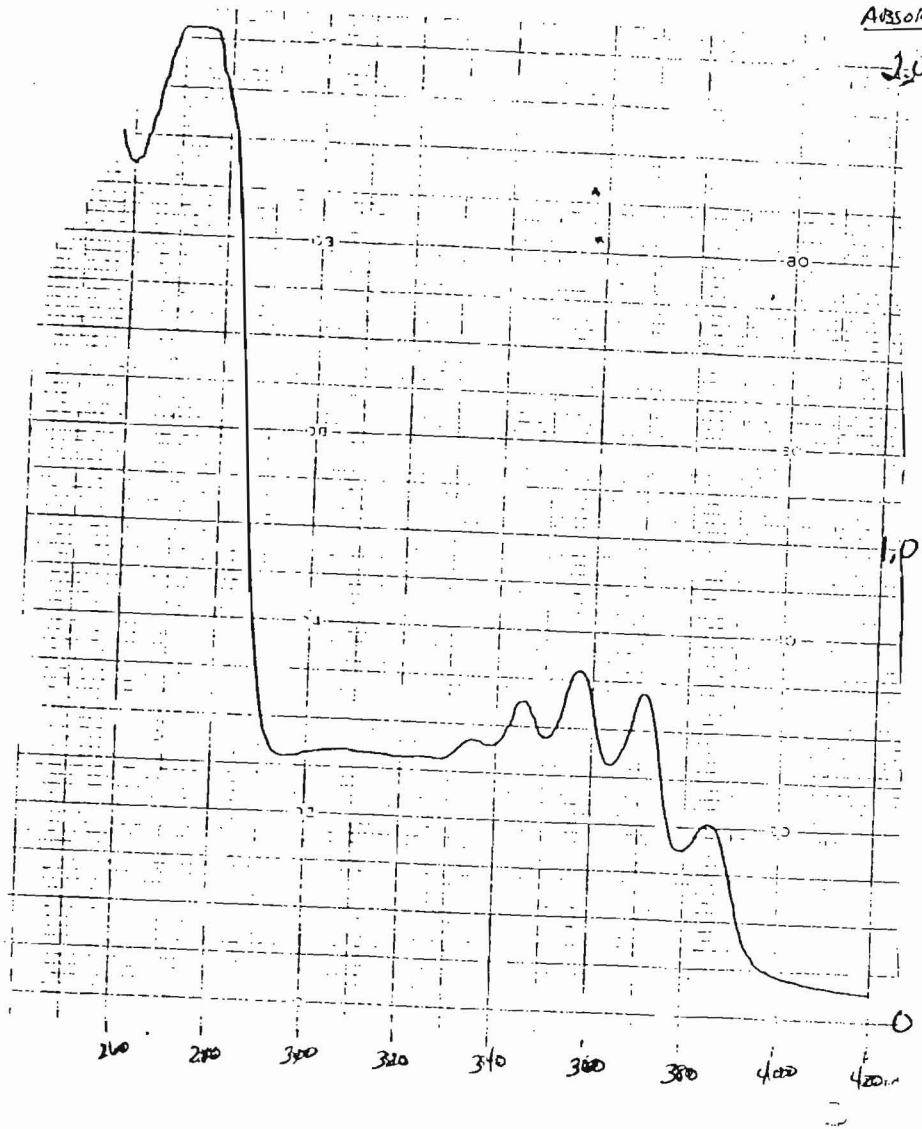

0.0101 M HONO and 1.9×10^{-3} M benzoic acid after 30 minutes photolysis

FIGURE 33

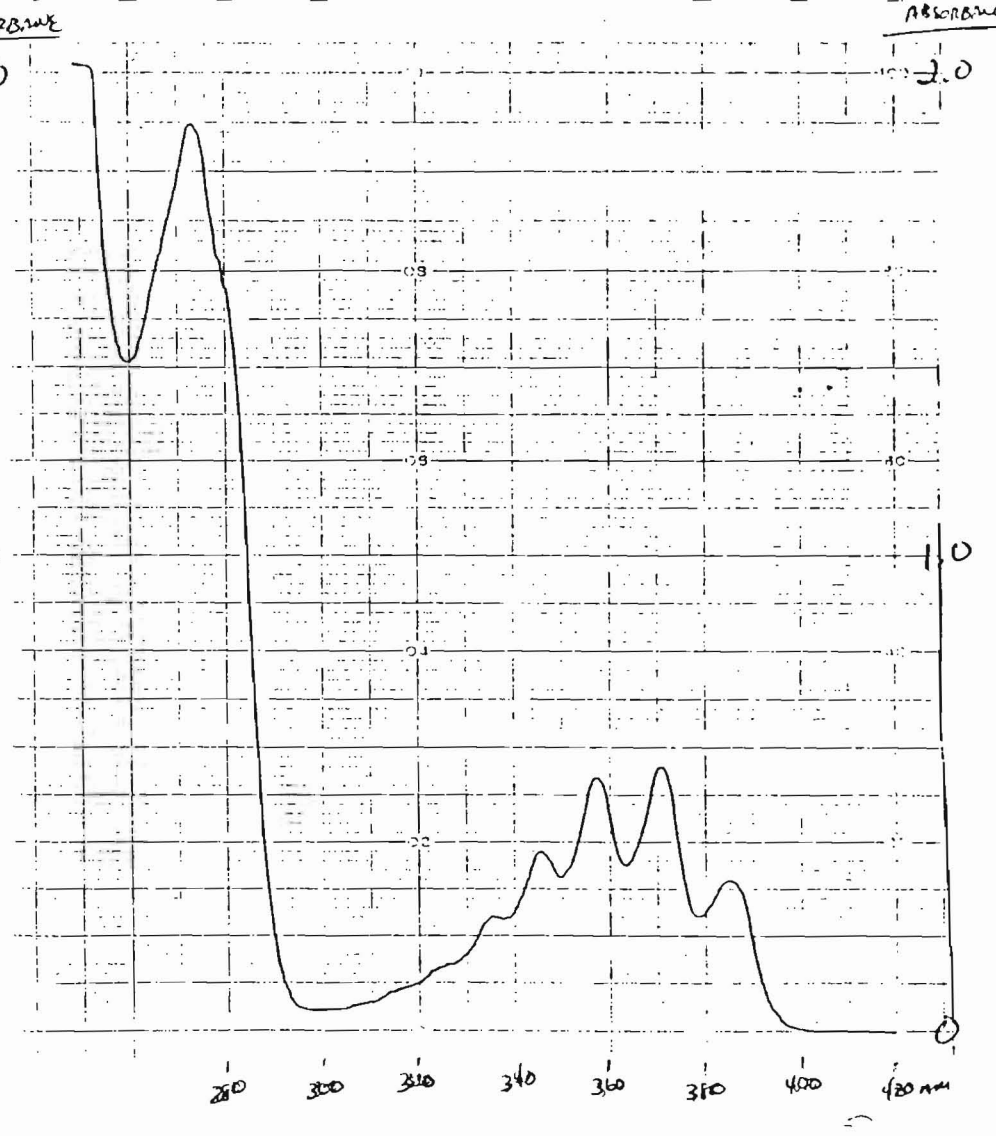

0.0101 M HONO and 1.9×10^{-3} M benzoic acid before photolysis

FIGURE 34

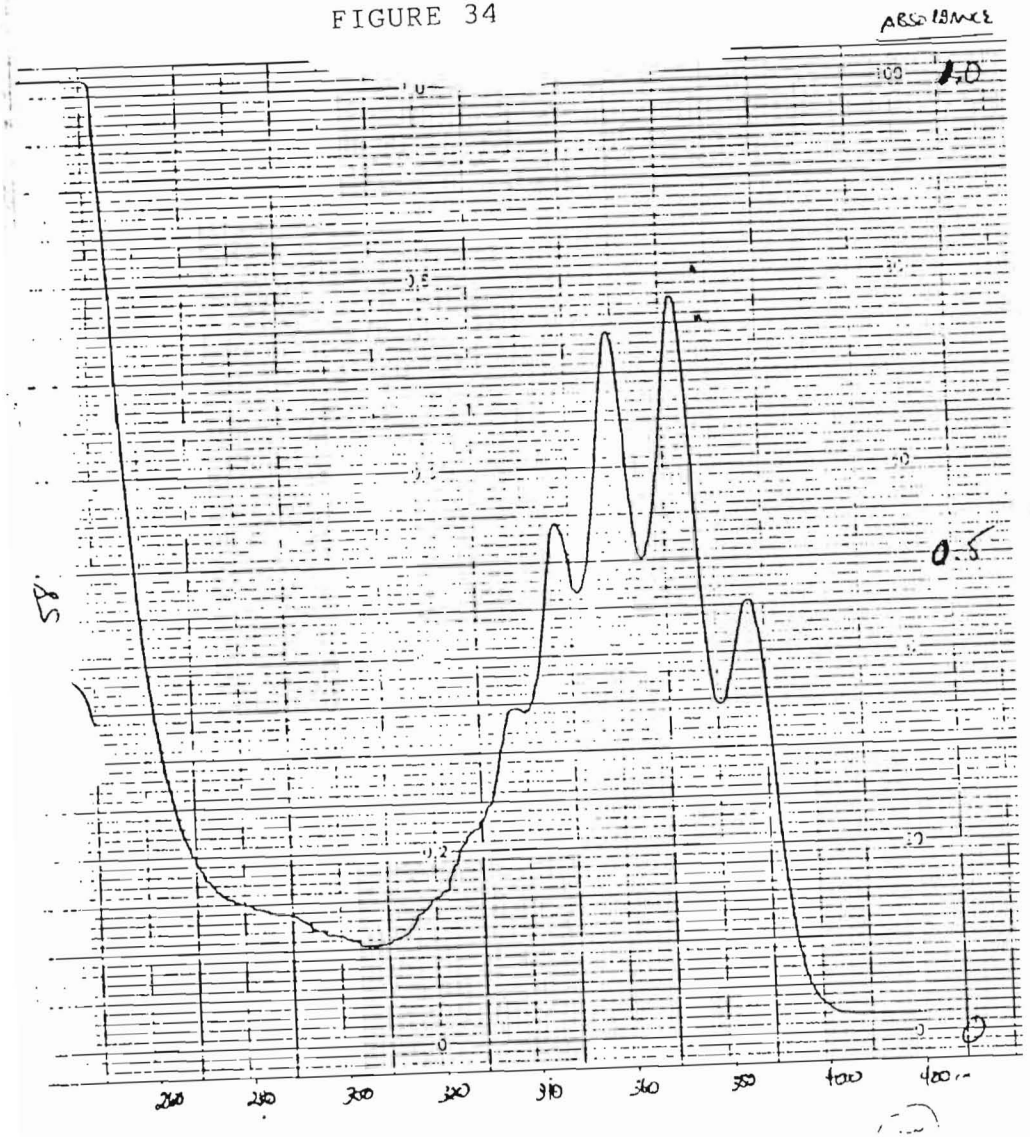

0.0151 M HONO and saturated terephthalic acid before photolysis

FIGURE 35

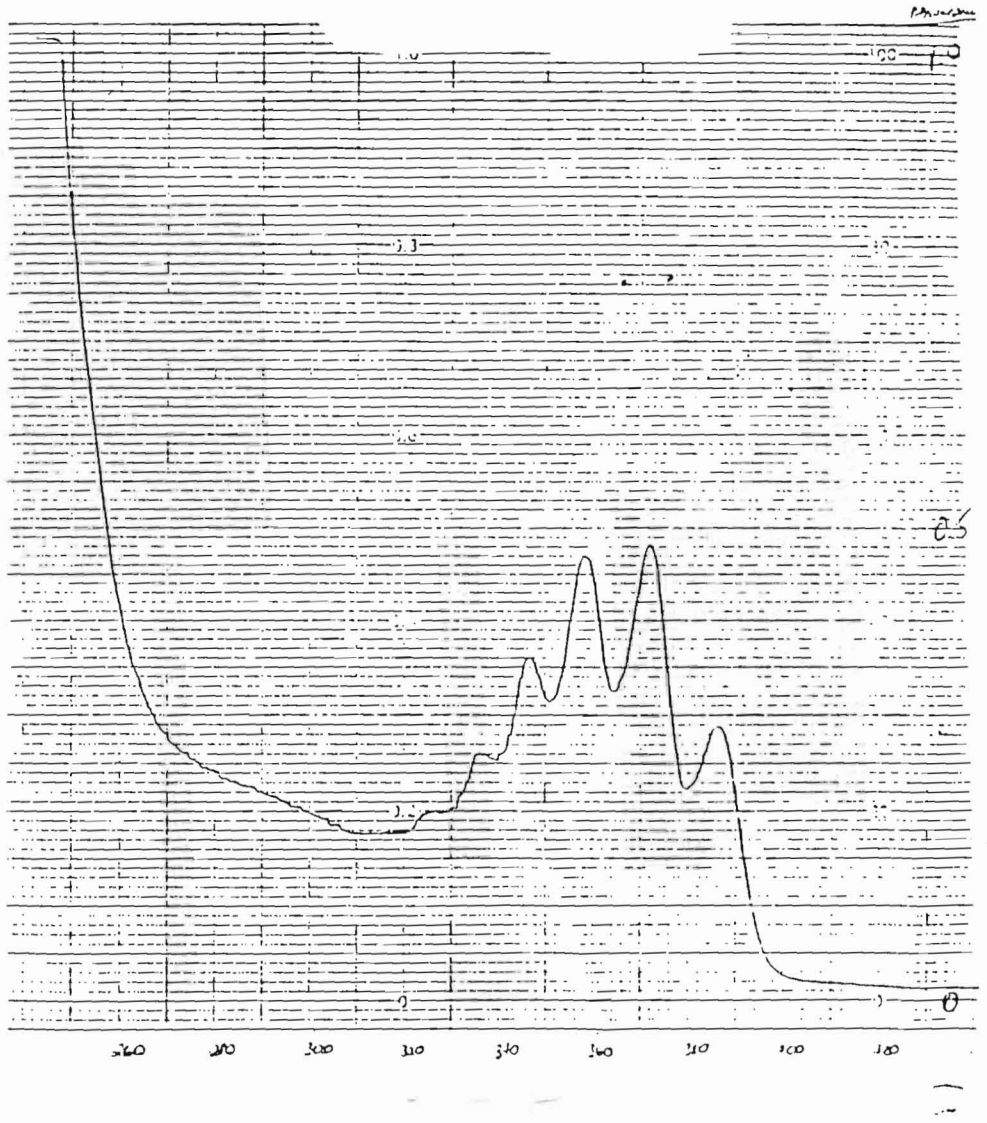

0.0151 M HONO and saturated terephthalic acid after 8 hours photolysis

Thermal Reaction of HONO with m-Cresol and Mixed Cresols

UV/vis spectra of the following reaction mixtures are presented: 0.0101 M HONO with 0.0424 mM p-cresol, 0.0416 mM m-cresol, 0.0348 mM o-cresol (Figure 36, after 235 minutes thermolysis); 0.0101 M HONO with 0.0624 mM m-cresol (Figure 37, after 220 minutes thermolysis); and 0.0101 M HONO with 0.673 mM phenol (Figure 38, after 160 minutes thermolysis). The resulting spectra are summarized in Table 19:

Table 19

UV Spectra of HONO/Cresols and HONO/Phenol Mixtures

HONO Reaction With	Compound	Maxima (nm)
Mixed Cresols	HONO	346,358,371,385
	unknown product	304
m-cresol	HONO	334,346,357,371,386
	unknown product	300
phenol	HONO	342,358,371,385
	unknown product	298-302

Photolysis of H_2O_2 in Presence of Benzene

Figure 38 shows the UV absorption spectrum of a mixture of 9 M H_2O_2 and 0.07 M benzene before photolysis. Figures 39-41 show the UV absorption spectra of mixtures of 9 M H_2O_2 and 0.07 M benzene initially at pH 0.1, 3.0, and 8.9, respectively, after 10 minutes photolysis and acidification to remove excess H_2O_2.

FIGURE 36

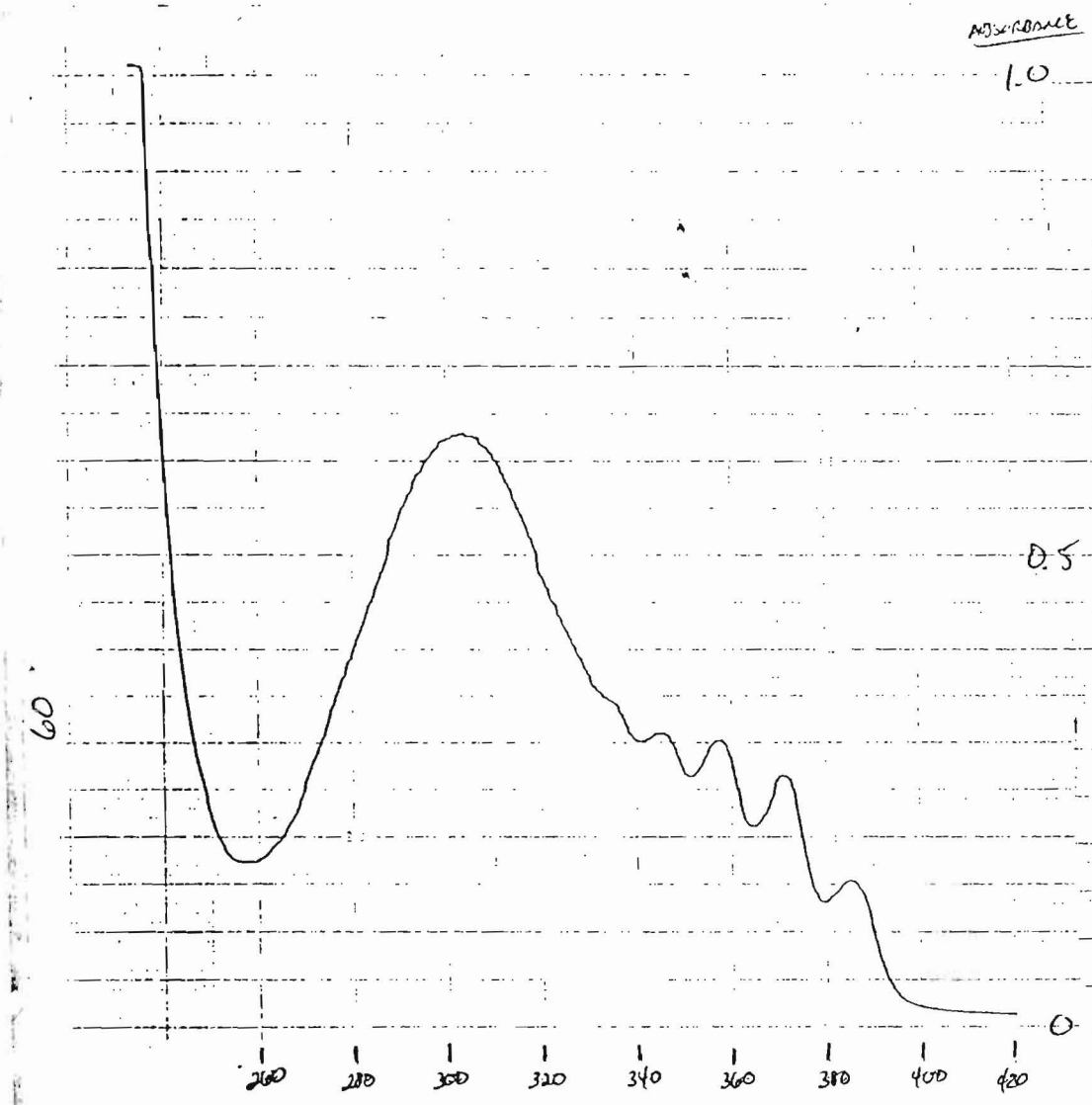

0.0101 M HONO, 4.24 x 10^{-5} M p-cresol,
4.16 x 10^{-5} M m-cresol, 3.48 x 10^{-5} M o-cresol
(total [cresols] = 1.19 x 10^{-4})
after 235 minutes thermolysis (1 °C)

FIGURE 37

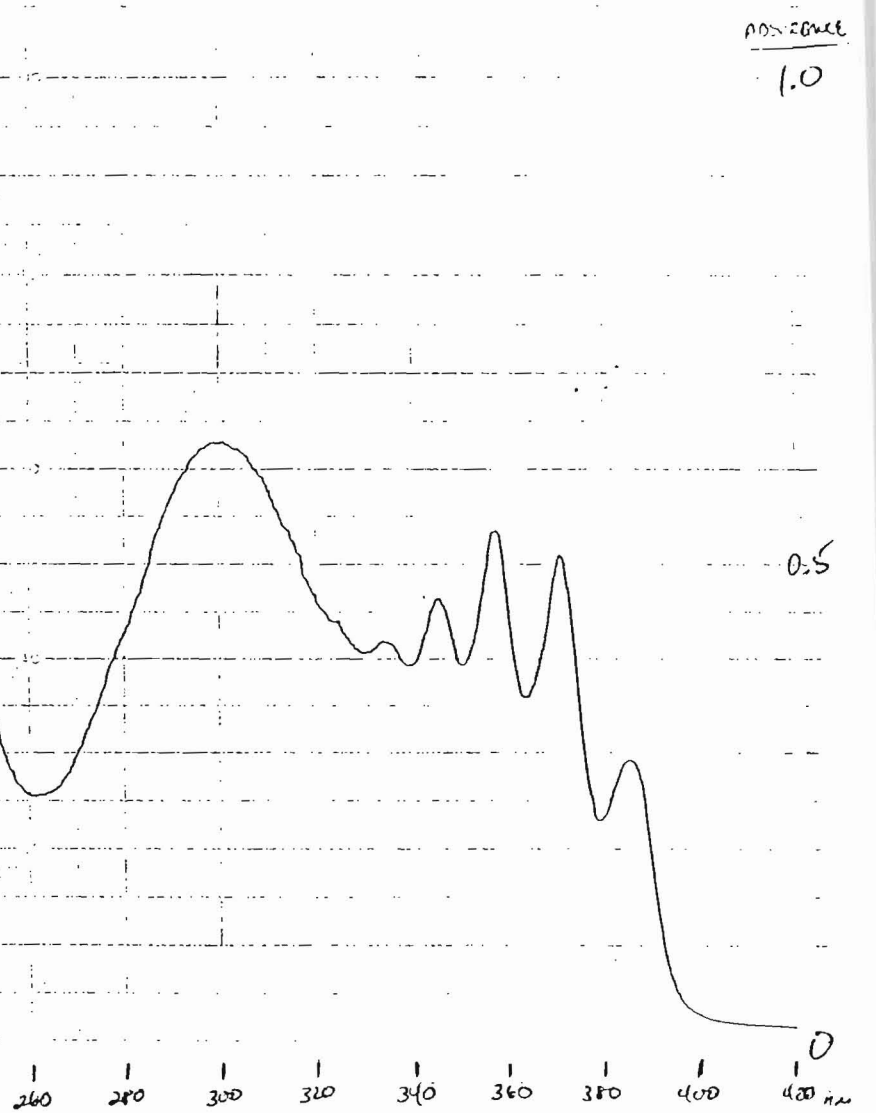

0.0101 M HONO and 6.24 x 10^{-5} M m-cresol
after 220 minutes thermolysis (1 °C)

FIGURE 38

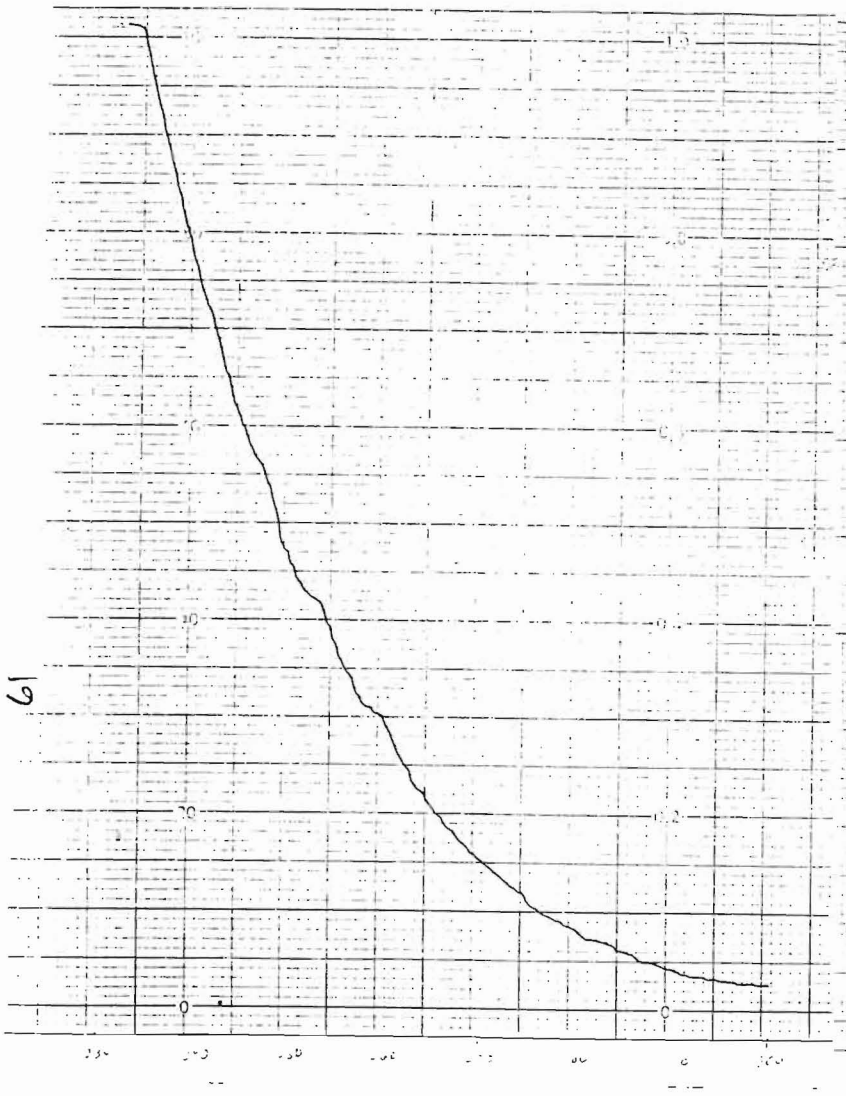

9 M H_2O_2 and 0.07 M benzene

before photolysis

FIGURE 39

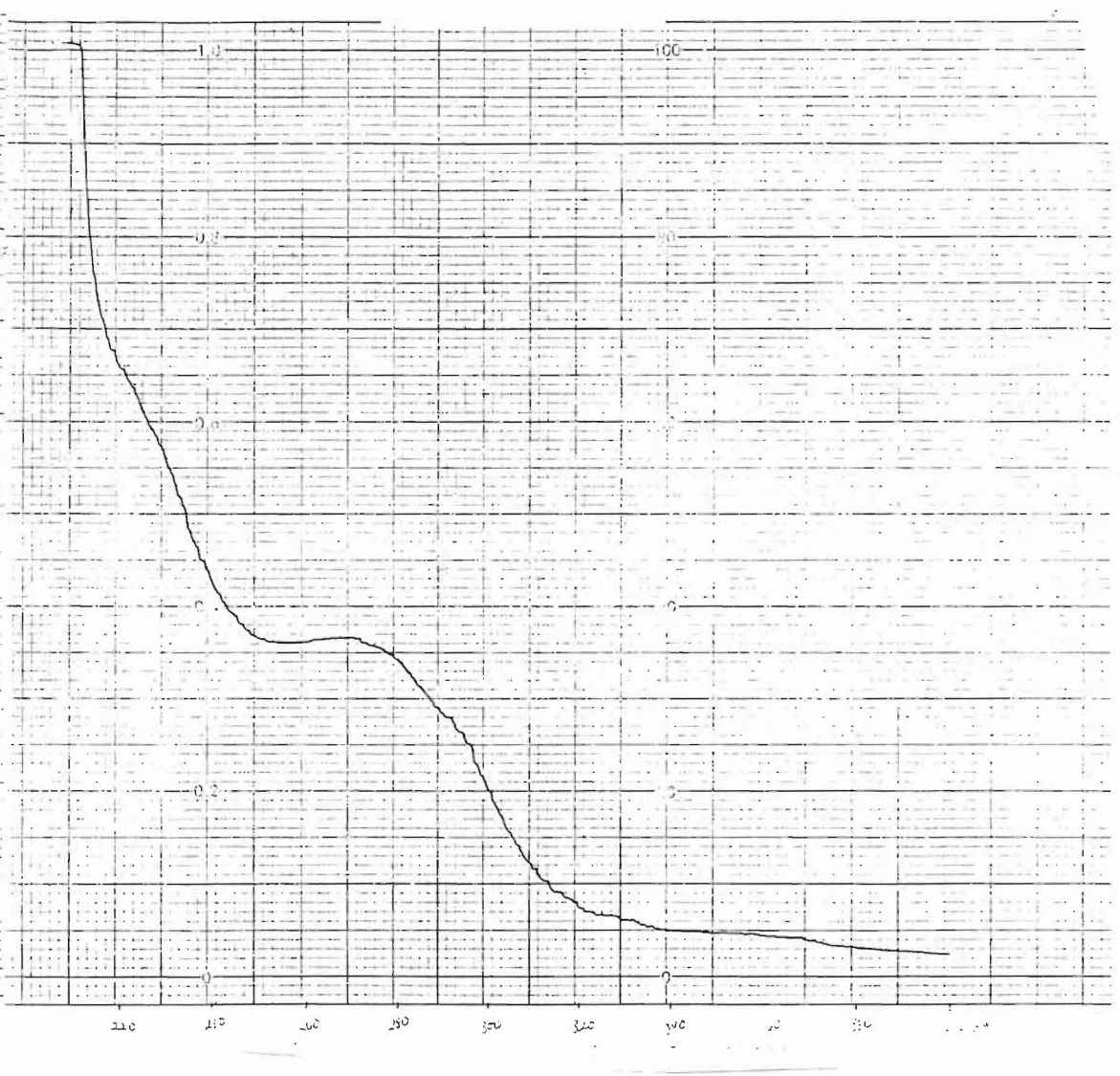

9 M H_2O_2 and 0.07 M benzene (pH = 3.0)

after 10 minutes photolysis

FIGURE 40

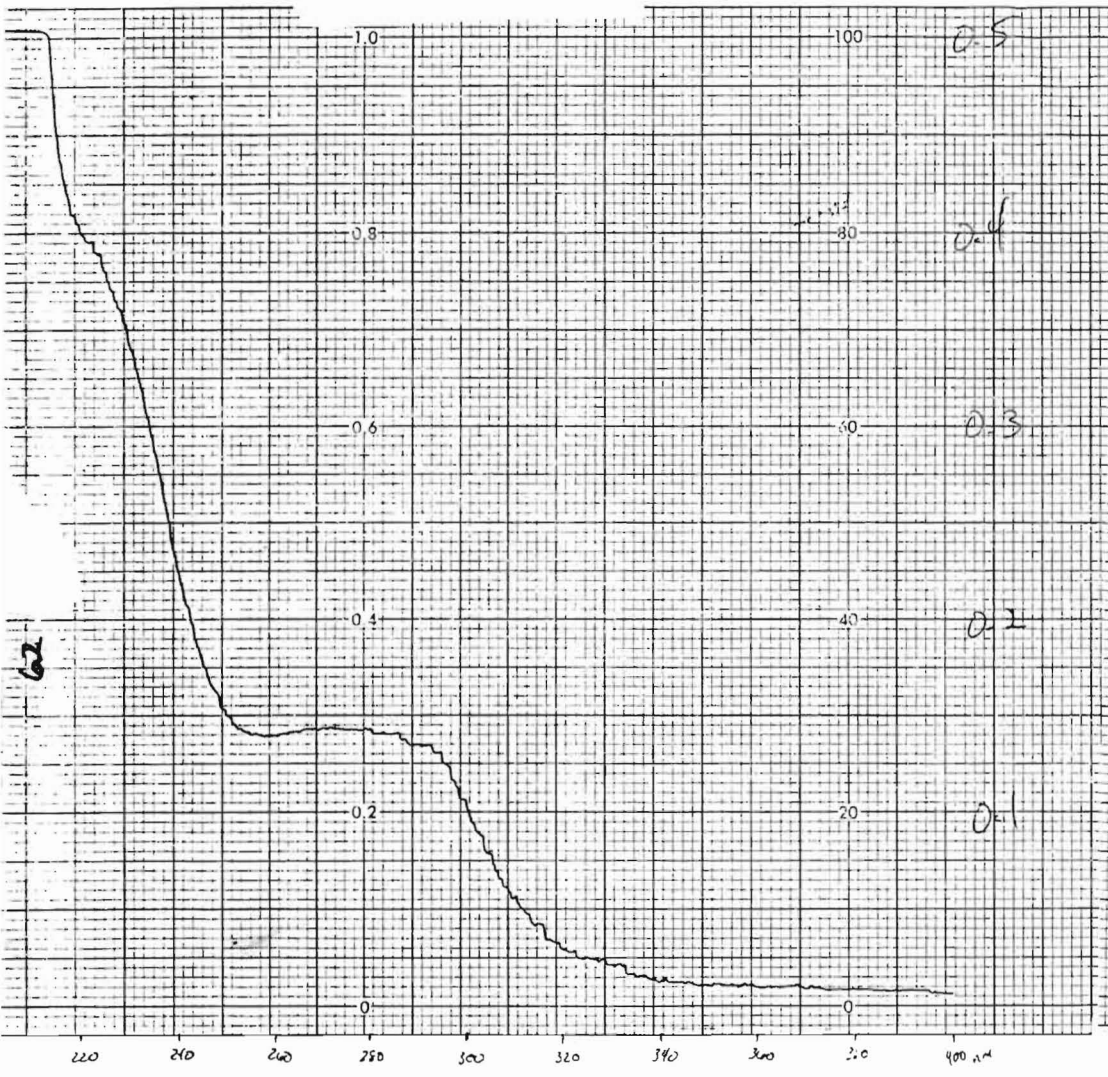

9 M H_2O_2 and 0.07 M benzene (pH = 0.1)

after 10 minutes photolysis

FIGURE 41

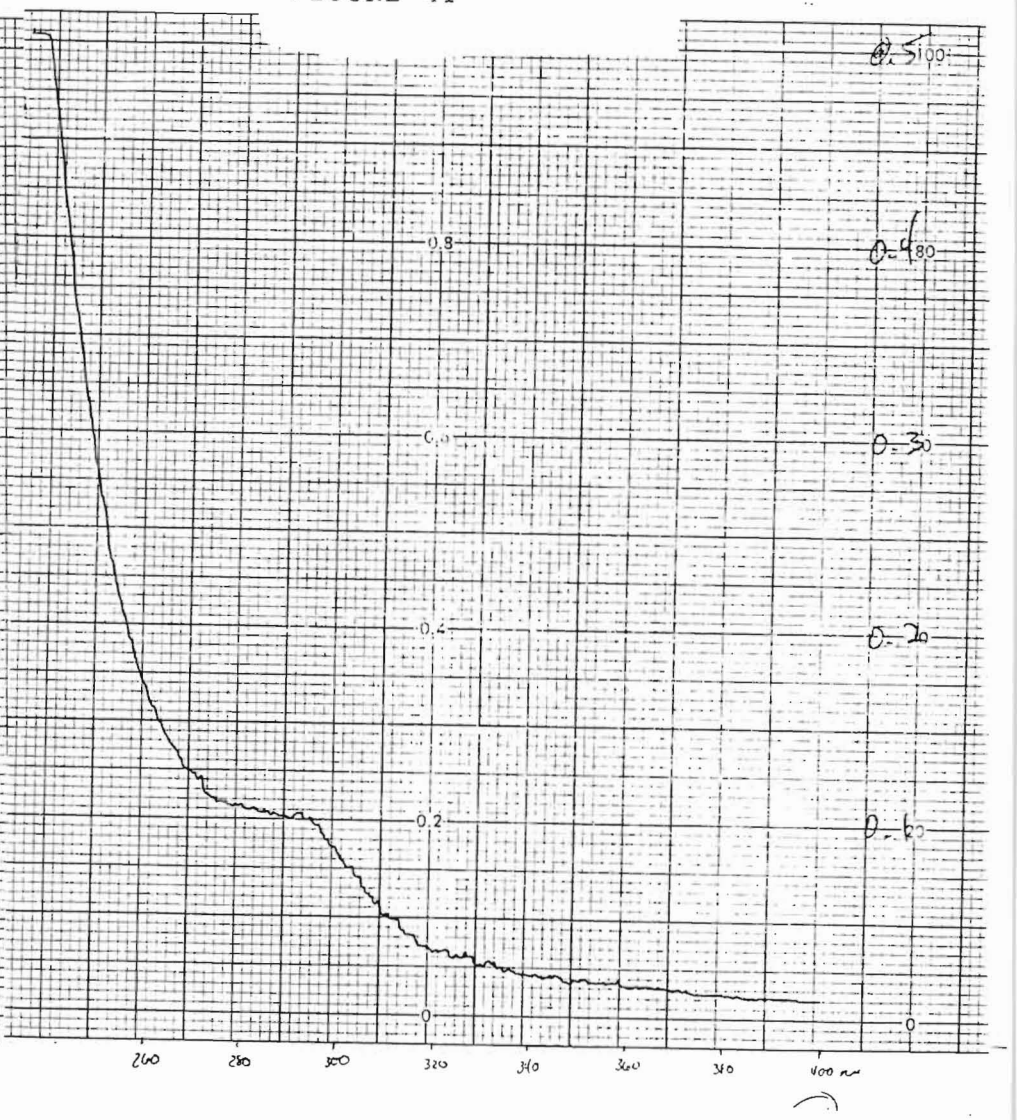

9 M H_2O_2 and 0.07 M benzene (pH = 8.9)

after 10 minutes photolysis

DISCUSSION

Qualitatively, the results of this work provide evidence that HONO does undergo photolytic dissociation, yielding OH, and NO_2^- does not undergo net photolysis.

Spectroscopic evidence indicates that p-nitrosophenol (PNP) is produced in HONO/benzene photolysis. The absorbance maximum at 298 nm in Figure (19) corresponds to that for known PNP (see Figure (5)). PNP is known to form in the thermal reaction between phenol and HONO [38,39], and in Figure (38) the 298 nm maximum absorbance by the product formed in the HONO/phenol thermal reaction corresponds to that found in Figure (19), the HONO/benzene photolysis. The overall reaction is given in equation (82):

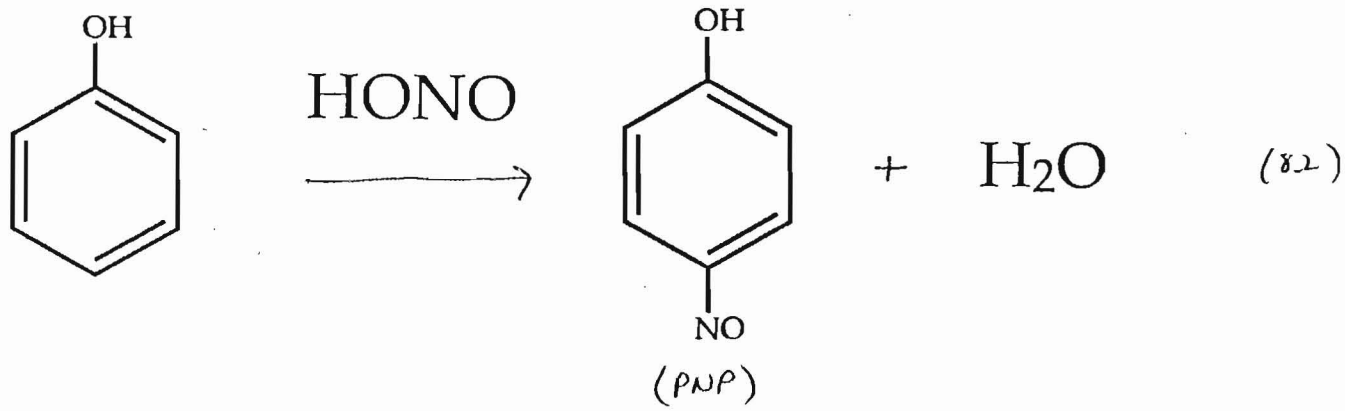

Product separation and isolation was not performed because of the extremely small amounts of PNP produced in each reaction and because of the potential explosiveness of dry PNP [50]. It is expected that product separation and isolation would reveal a mixture of o- and p-nitrosophenol, since -OH is an aromatic ring-activating, ortho/para directing substituent in the thermal nitrosation of phenol [51].

It may be deduced that PNP is formed from phenol, which must

have been formed from benzene and OH, which was formed upon HONO photolytic dissociation. However, experimental data indicates a difference in the HONO/phenol reaction kinetics between the thermal reaction and the HONO/benzene photolysis. In Figure (19), there is spectroscopic indication of HONO (334-384 nm) and PNP (280-320 nm) presence, but there is no indication of a phenol intermediate. In Figure (38), presence of phenol is seen at 270 nm after 155 minutes thermolysis of phenol and HONO. PNP formation is dependent on concentrations of both phenol and HONO [47,48]; thus, it would be expected that PNP formation in the HONO/benzene photolysis would be extremely slow because of the small amounts of phenol produced (approx. 1 mmol). Therefore, in the HONO/benzene photolysis, the presence of phenol should be detected because the radical addition of OH to benzene is very fast compared to the thermal nitrosation of phenol. Even though the absorptivity of PNP is 7.5 times greater than that of phenol, one would expect some sort of "bulge" in the UV spectra at around 270 nm.

It might be suggested that benzene reacts first with NO formed upon photolytic dissociation of HONO, yielding nitrosobenzene. To form PNP, the nitrosobenzene must react with OH via a radical mechanism because the NO substituent deactivates the benzene ring, rendering it inert to electrophilic substitution. If this is the case, then OH substitution would occur mostly on the meta and ortho sites of the nitrosobenzene. However, this possibility cannot be discounted because the UV spectra of o- and m-nitrosophenol were not investigated.

In the photolysis of HONO in the presence of toluene, benzoic

acid, and terephthalic acid, the broad absorbance maxima due to products are between 295-310 nm, the same region in which the PNP peak appears. Thus, it is suggested that these products are hydroxy- and nitroso-substituted parent molecules because the absorbance maxima are shifted to slightly longer wavelengths than those for the hydroxylated scavenger compounds. The maxima for the three isomeric cresols appear between 270-277 nm, but the HONO/toluene photolysis product absorbance maximum appears at 304 nm (see Figure 29). The maxima for the three isomeric hydroxybenzoic acids appear between 248-296 nm, but the HONO/benzoic acid photolysis product absorbance maximum appears at 308 nm (see Figure 33). These wavelength shifts are similar to the absorbance maximum wavelength shift from 270 nm (phenol) to 298 nm (PNP) that results after nitrosation of phenol.

According to the mechanism of OH scavenging proposed by Eberhardt [38,39], a substituent on an aromatic ring does not affect the mechanism of OH scavenging. The proposed reactions for aromatic scavenging in the HONO/toluene, HONO/benzoic acid, and HONO/terephthalic acid are presented in equations (83-85):

$$\mathrm{HONO} \xrightarrow{\text{radiation.}} \mathrm{NO} + \mathrm{OH}$$

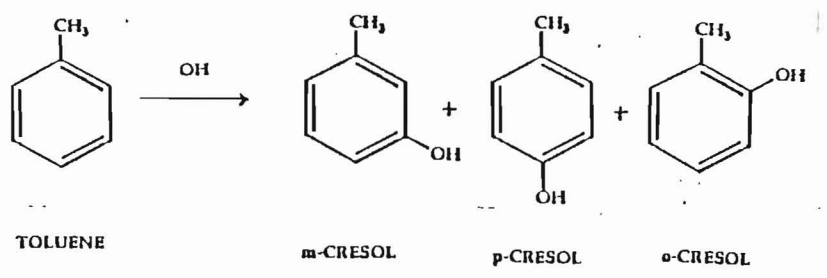

(83)

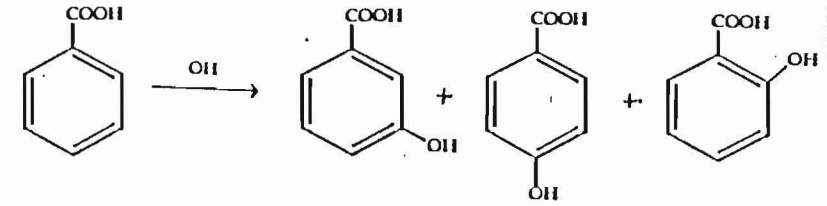

BENZOIC ACID

HYDROXYBENZOIC ACIDS

(84)

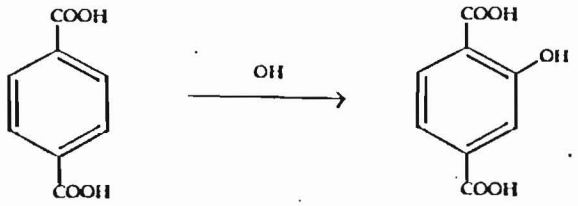

TEREPHTHALIC ACID

HYDROXYTEREPHTHALIC ACID

(85)

No change in nitrite concentration was observed upon photolysis in the presence of benzene or toluene. There is a decrease in toluene absorbance (see Figs. 28-29), but since there is no indication of another product formed, it is suggested that this is due to evaporation of the toluene out of aqueous solution to the walls of the flask or the rubber stopper and paraffin covering the flask. Even in aqueous solution, both benzene and toluene were observed to be volatile.

Experimental data indicate that nitrite undergoes no net photolysis, which contradicts reports of nitrite losses by Zafiriou [24-26]. He stated that nitrite undergoes radiation-induced dissociation to NO and O^- in seawater but not in distilled water, where NO_2^- is regenerated [26]. If nitrite undergoes radiation-induced dissociation due to direct radiation absorption in seawater, it should in distilled water as well. Likewise, if nitrite does not undergo radiation-induced dissociation due to direct radiation absorption in distilled water, it should not in seawater.

It seems more reasonable that one or more ions in seawater become promoted to an excited state upon absorption of UV radiation, and this excess energy is transferred to the NO_2^- upon collision with the excited ion. This mechanism has been suggested by Zafiriou but has generally been ignored as an area of investigation.

H_2O_2/benzene photolyses were performed to confirm the overall OH-scavenging reaction of benzene at acidic and basic pH. The small broad maxima in Figures 39-41 range from 270-300 nm, the same range in which maxima for phenol, catechol, resorcinol, and hydroquinone are observed. A product analysis by High-Performance Liquid Chromatography (HPLC) or Gas Chromatography (GC) may prove very helpful.

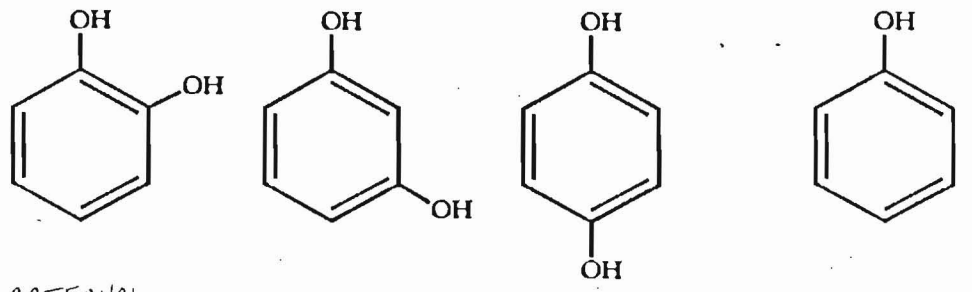

CATECHOL RESORCINOL HYDROQUINONE PHENOL

In order to determine the amount of HONO that decomposes due strictly to photochemical dissociation, the amount of HONO that decomposes thermally must be determined. Concentration of HONO is dependent on pH and its acid dissociation constant, K_a, which is dependent on ionic strength. According to Lumme, the dependence of pK_a on ionic strength may be calculated from the following equation [52,53]:

$$pK_a = pK_o - [2A(I)^{0.5}/(1 + 1.622(I)^{0.5})] + 0.0261(I) \quad (86)$$

where pK_o = pK_a of HONO at 0 °C and zero ionic strength = 3.423

I = ionic strength

A = Debye-Huckel Limiting Law Constant = 0.509

Once the K_a is determined, the concentration of HONO can be calculated from initial H^+ and NO_2^- concentrations and equation (1). Unfortunately, because many mathematical steps are involved in calculating [HONO], the relative uncertainty in [HONO] propagates to a very high level. For example, given 0.009357 $\pm$ 0.83% M H^+ and 0.00481 $\pm$ 0.88% M NO_2^-, the resulting uncertainty in [HONO] is 23%. The HONO uncertainties presented in the results do not account for this mathematical propagation but were simply standard deviations of average [HONO] values calculated through equation (86) and through molar absorptivity from UV/vis spectral data. Thus, the uncertainties presented in the results are very optimistic. Because equation (86) was also used to calculate the molar absorptivity of HONO, there is no mathematical way to avoid this large uncertainty.

In determination of kinetic orders of thermolysis, the method of initial rates is probably more accurate than the fractional-life method because the fraction-life used was only 0.1, and the thermolyses were run only to 0.3 to 0.5 times completion. Within experimental uncertainty, the determined order (0.5 $\pm$ 0.5) concurs with previously reported first-order results for low concentrations of HONO.

To determine quantum yields of OH formation from HONO

photolysis, it is necessary to determine the molar absorptivity of PNP. This may calculated from the UV/vis spectrum of PNP (see Fig. 5) or indirectly from the UV/vis spectra of the HONO/phenol thermal reaction. The PNP obtained from Aldrich was packed in approximately 40% water and had a "peat moss" texture. This substance was not readily soluble in water and had a tendency to clump together. Because the impurities in the PNP sample were unknown, the thermal reaction between HONO and phenol was used in an attempt to calculate the molar absorptivity of PNP.

Assuming that the only chemical species in solution which absorbed UV radiation were phenol, HONO, NO_2^-, and PNP, the Beer's Law Equation for absorbance by this system is given in equation (87):

$$\frac{A}{b} = \epsilon^{\phi\text{-}OH}[PHENOL] + \epsilon^{PNP}[PNP] + \epsilon^{HONO}[HONO] + \epsilon^{NO_2^-}[NO_2^-] \qquad (87)$$

where A = absorbance

b = cell path length, cm = 1.00 cm

$\epsilon^{\phi\text{-}OH}$ = molar absorptivity of phenol, $\underline{M}^{-1}$ cm^{-1}

ϵ^{PNP} = molar absorptivity of PNP, $\underline{M}^{-1}$ cm^{-1}

ϵ^{HONO} = molar absorptivity of HONO, $\underline{M}^{-1}$ cm^{-1}

$\epsilon^{NO_2^-}$ = molar abosrptivity of NO_2^-, $\underline{M}^{-1}$ cm^{-1}

[ ] = concentration, $\underline{M}$

The unknown variables in equation (87) were [phenol], ϵ^{PNP}, [PNP], [HONO], and $[NO_2^-]$. Since phenol reacts only with the HONO in aqueous solution, it may be assumed that one molecule of phenol is

lost for every molecule of PNP that is formed. [PNP] may then be expressed as the difference of initial [phenol] and [phenol] at a given time during the reaction:

$$\frac{A}{b} = \epsilon^{\phi\text{-OH}}[\text{PHENOL}]_t + \epsilon^{PNP}\left([\text{PHENOL}]_o - [\text{PHENOL}]_t\right) + \epsilon^{HONO}[HONO] + \epsilon^{NO_2^-}[NO_2^-] \qquad (88)$$

where $[\text{phenol}]_o$ = initial [phenol]

$[\text{phenol}]_t$ = [phenol] at time t

Another unknown variable may be eliminated by assuming that the ratio of $[NO_2^-]/[HONO]$ was constant at the initial ratio, which can be easily calculated in initial [HONO] determination. It was calculated that given 0.01 M HONO and 8×10^{-4} M NO_2^- initially, the $[NO_2^-]/[HONO]$ ratio remains constant within 3.5% through 75% total HONO decomposition. Thus, $[NO_2^-]$ may be expressed as $([NO_2^-]/[HONO])_o \cdot [HONO]$, reducing equation (88) to three unknown variables:

$$\frac{A}{b} = \epsilon^{\phi\text{-OH}}[\text{PHENOL}]_t + \epsilon^{PNP}\left([\text{PHENOL}]_o - [\text{PHENOL}]_t\right) + \epsilon^{HONO}[HONO] + \epsilon^{NO_2^-}\left(\frac{[NO_2^-]}{[HONO]}\right)_o [HONO] \qquad (89)$$

From this point, a three-equation system was solved using absorbances at 298 nm (max for PNP), 352 nm (max for NO_2^-), and 371 nm (max for HONO). The resulting PNP values were plotted against time of reaction and extrapolated to time = 0, the point where the constant $[NO_2^-]/[HONO]$ ratio assumption is most valid. The molar

absorptivity of PNP at this point was calculated to be 11700 $\underline{M}^{-1}$ cm^{-1} (to 2 significant figures).

A sample of the PNP was determined to contain 36.58% carbon, 7.30% nitrogen, and 6.36% hydrogen. If no impurities other than water were present, then the remaining 49.76% consisted of oxygen. After normalization with respect to carbon and nitrogen, the calculated PNP percentage in the sample of PNP was (62.49 $\pm$ 0.69)%. From this, the 10400 $\underline{M}^{-1}$ cm^{-1} molar absorptivity reported in Table 4 was calculated.

In the HONO/benzene photolyses, it was assumed that only PNP, HONO, and NO_2^- in the reaction mixture absorbed UV radiation. The Beer's Law absorbance equation is shown in equation (90):

$$\frac{A}{b} = \epsilon^{PNP}[PNP] + \epsilon^{HONO}[HONO] + \epsilon^{NO_2^-}[NO_2^-] \qquad (90)$$

The molar absorptivities in equation (90) were known, but all concentrations were unknown. By assuming a constant $[NO_2^-]/[HONO]$ ratio, equation (90) is reduced to two unknown variables:

$$\frac{A}{b} = \epsilon^{PNP}[PNP] + \epsilon^{HONO}[HONO] + \epsilon^{NO_2^-}\left(\frac{[NO_2^-]}{[HONO]}\right)_0[HONO] \qquad (91)$$

By using absorbances at 298 and 371 nm, [PNP] and [HONO] were calculated for the HONO/benzene photolyses.

Quantitative data from HONO photolyses were too inconsistent between trials to make reasonable comparisons to thermolyses. In

Tables 12 and 13, data from two 0.01 M HONO photolyses were presented. While initial HONO concentrations were the same, one HONO decomposition (see Table 13) proceeded approximately 2.5 times faster despite identical lamp and reaction vessel positions in each run.

Very few HONO decomposition mechanistic conclusions may be made from this work; however, formation of PNP upon photolysis of HONO in presence of benzene indicates that equation (92) is the primary process for HONO photolytic dissociation:

$$HONO(aq) + h\nu \longrightarrow OH(aq) + NO(aq) \qquad (92)$$

The rapid phenol to PNP reaction in HONO/benzene photolysis raises some interesting mechanistic questions. It is expected that hydration shells or a solvent cage of water molecules exist around species dissolved in aqueous solution. Because benzene and HONO are not formally charged species, these solvent cages are not expected to be as rigorously structured as those around ions. However, it may be possible that these cages inhibit OH transport to benzene molecules in the solution.

The mechanism of OH transport may be investigated using an isotope-labeling experiment. Using a water solvent containing ^{18}O, it may be determined if there is hydroxyl exchange between water molecules and OH formed upon HONO dissociation. If the HONO is prepared using unlabeled water, then the OH formed upon HONO dissociation will be unlabeled. If there is OH exchange with the solvent molecules, then the PNP product formed will contain ^{18}O. If the PNP product contains unlabeled oxygen, then it may be concluded

that after formation from HONO dissociation, the OH radical diffuses through the water solution until a benzene molecule is encountered.

Other Suggestions for Further Work

This work may lead to several avenues of research in the areas of physical and analytical chemistry. One important analytical aspect that was not undertaken was product separation and isolation. This could become a particularly interesting area of study in the cases of the toluene and benzoic acid scavenger reactions. Chromatographic separation could provide very useful information concerning isomeric distribution of the hydroxylated, nitrosated scavenger molecules, of which very little is known, and there are no reports of formation of these compounds in aqueous solution.

Benzoic acid and terephthalic acid were chosen as scavengers for potentially useful analytical reasons. Benzoic acid reacts with OH to yield a hydroxybenzoic acid. The ortho isomer, salicylic acid, complexes with Fe^{3+}, and this complex has a maximum absorbance at approximately 520 nm [40]. Even after nitrosation of salicylic acid, the resulting UV/vis absorption would lie well into the visible region (above 500 nm), away from the HONO peaks. Quantitative spectral analysis of the HONO photolysis system would be much easier because the overlap between HONO and Fe^{3+}-complex absorbances would be greatly reduced or eliminated. Unfortunately, the m- and p-hydroxybenzoic acid isomers do not complex with Fe^{3+}. Unless the isomeric distribution of the hydroxybenzoic acid products was known, quantum yields of OH production could not be calculated.

Terephthalic acid may be much more analytically useful as a

scavenger. The molecule contains two carboxylate groups in para positions. Thus, any site attacked by OH is an ortho site, and the resulting compound should complex with Fe^{3+} or other metal ions to form colored complexes. Unfortunately, terephthalic acid is much less water-soluble than benzoic acid because of intermolecular hydrogen bonding between terephthalic acid molecules. There are no reports concerning properties of terephthalic acid in water solution, and a study of such properties (e.g., solubility and acidities under varying pH and ionic strength conditions) would be very applicable to this research area.

Once the contribution of thermal decomposition with respect to HONO disappearance in photolysis is determined, HONO photolysis at varying temperatures may be studied to determine the activation energy for photolytic dissociation. This energy should correspond to the energy required to break the HO-NO bond. Determination of quantum yields of HONO destruction as a function of wavelength could be a closely related study, since HO-NO dissociation energy corresponds to a wavelength of radiation.

REFERENCES

1. Cox, R.A.; J. Photochem.; **1984**, 25, 43.

2. Jenkin, M.E.; Cox, R.A.; Chem. Phys. Lett.; **1987**, 137, 548.

3. Seinfeld, J.H.; Atmospheric Chemistry and Physics of Air Pollution; Wiley: New York, 1986; pp. 118-134, as cited in reference 10

4. Ray, P.C.; Dey, M.L.; Ghosh, J.C.; J. Chem. Soc.; **1917**, 111, 413.

5. Montemartini, C.; Acc. Lincei. Roma [IV]; **1890**, 6, II, 263, as cited in reference 9.

6. Mukerji, K.B.; Dhar, N.R.; Z. Elektrochem.; **1925**, 31, 255.

7. Usubillaga, A.N.; Ph.D. Thesis, University of Illinois, Urbana, Illinois, 1962.

8. Abel, E.; Schmid, H.; Z. Phys. Chem.; **1928**, 132, 55.

9. Rettich, T.R.; Ph.D. Thesis, Case Western Reserve University, Cleveland, Ohio, 1978.

10. Park, Y.-J.; Lee, Y.-N.; J. Phys. Chem.; **1988**, 92, 6294.

11. Thie, J.; J. Phys. Chem.; **1947**, 51, 540.

12. Cox, R.A.; Derwent, J.; J. Photochem.; **1976/77**, 6, 23.

13. Cox, R.A.; Atkins, D.H.; U.K. At. Energy Res. Establ., Rep. 1973, AERE-R7615, as cited in reference 9.

14. Cox, R.A.; J. Photochem.; **1974**, 3, 175.

15. Mitchell, R.C.; Simons, J.P.; Discuss. Faraday Soc.; **1967**, 44, 208.

16. Nash, T.; Tellus; **1974**, 26, 1, as cited in reference 9.

17. Vasudev, R.; Zare, R.N.; Dixon, R.N.; Chem. Phys. Lett.; **1983**, 96, 399.

18. Kenner, R.D.; Rohrer, F.; Stuhl, F.; J. Phys. Chem.; **1986**, 90, 2635.

19. Murty, K.S.; Dhar, N.R.; J. Indian Chem. Soc.; **1930**, 7, 985, as cited in reference 9.

20. Holmes, M.; J. Chem. Soc.; **1926**, 1898.

21. Hamilton, R.D.; Limnol. Oceanogr.; 1964, 9, 107.

22. Treinin, A.; Hayon, E.; J. Am. Chem. Soc.; 1970, 92, 5821.

23. Knight, R.J.; Sutton, H.C.; Trans. Faraday Soc.; 1967, 63, 2623.

24. Zafiriou, O.C.; J. Geophys Res.; 1974, 79, 4491.

25. Zafiriou, O.C.; True, M.B.; Mar. Chem.; 1979, 8, 9.

26. Zafiriou, O.C.; Bonneau, R.; Photochem. Photobiol.; 1987, 45, 723.

27. Gusten, H.; Filby, W.G.; Schoof, S.; Atmos. Environ.; 1981, 15, 1763.

28. Davis, D.D.; Bollinger, W.; Fischer, S.; J. Phys. Chem.; 1975, 79, 293.

29. Sloane, T.M.; Chem. Phys. Lett.; 1978, 54, 269.

30. Tully, F.P.; Ravishankara, A.R.; Thompson, R.L.; Nicovich, J.M.; Shah, R.C.; Kreutter, N.M.; Wine, P.H.; J. Phys. Chem.; 1981, 85, 2262.

31. Perry, R.A.; Atkinson, R.; Pitts, J.N.; J. Phys. Chem.; 1977, 81, 296.

32. Shepson, P.B.; Edney, E.O.; Corse, E.W.; J. Phys. Chem.; 1984, 88, 4122.

33. Atkinson, R.; Arey, J.; Zielinska, B.; Aschmann, S.M.; Environ. Sci. Technol.; 1987, 21, 1014.

34. Ahmad, M.; Clay, P.G.; Chem. Comm.; 1969, 61.

35. Jacob, N.; Balakrishnan, I.; Reddy, M.P.; J. Phys. Chem.; 1977, 81, 17.

36. Gowenlock, B.G.; J. Chem. Soc.; 1954, 3174.

37. Kabasakalian, P.; Townley, E.R.; Yudis, M.D.; J. Am. Chem. Soc.; 1962, 84, 2718.

38. Eberhardt, M.K.; J. Phys. Chem.; 1981, 85, 1085.

39. Eberhardt, M.K.; Yoshida, M.; J. Phys. Chem.; 1973, 77, 589.

40. Petrucci, R.; General Chemistry, 4th ed.; MacMillian: New York, 1984.

41. Abel, E.; Montash.; 1952, 83, 422, as cited in Chem. Abstr.; 1952, 46, 10182g.

42. Hunt, J.P.; Taube, H.; J. Am. Chem. Soc.; **1952**, 74, 5999.

43. Ohta, T.; Ohyama, T.; Bull. Chem. Soc. Japan; **1985**, 58, 3029.

44. Dainton, F.S.; J. Am. Chem. Soc.; **1956**, 78, 1278.

45. Collinson, E.; Dainton, F.S.; McNaughton, G.S.; J. Chim. Phys.; **1955**, 52, 556.

46. Rutenberg, H.; Taube, H.; J. Am. Chem. Soc.; **1950**, 72, 5561.

47. Challis, B.C.; Higgins, R.J.; Lawson, A.J.; Chem. Comm.; **1970**, 1223.

48. Challis, B.C.; Lawson, A.J.; J. Chem. Soc. (B); **1971**, 770.

49. Morrison, D.A.; Turney, T.A.; J. Chem. Soc.; **1960**, 4827.

50. Windholz, M.; The Merck Index; Merck: Rahlow, NJ, 1983.

51. McMurry, J.; Organic Chemistry; Brooks/Cole: New York, 1986.

52. Lumme, P.; Lahermo, P.; Tummavuori, J.; Acta Chem. Scand.; **1965**, 19, 2175.

53. Lumme, P.; Tummavuori, J.; Acta. Chem. Scand.; **1965**, 19, 617.